THE FATIGUE BEHAVIOUR OF WELDED AND BOLTED SHEAR CONNECTORS IN COMPOSITE HIGHWAY BRIDGES

by
Matthew Sjaarda

A thesis
presented to the University of Waterloo
in fulfilment of the
thesis requirement for the degree of
Doctor of Philosophy
in
Civil Engineering

Waterloo, Ontario, Canada, 2018

EXAMINING COMMITTEE MEMBERSHIP

The following served on the Examining Committee for this thesis. The decision of the Examining Committee is by majority vote.

External Examiner	Dr. Michael Bartlett Professor, University of Western Ontario
Co-Supervisor	Dr. Jeffrey S. West Adjunct Professor, Civil and Environmental Engineering
Co-Supervisor	Dr. Scott Walbridge Associate Professor, Civil and Environmental Engineering
Internal-external Member	Dr. Adrian Gerlich Associate Professor, Mechanical and Mechatronics Engineering
Internal Member	Dr. Adil Al-Mayah Assistant Professor, Civil and Environmental Engineering
Internal Member	Dr. Mahesh Pandey Professor, Civil and Environmental Engineering

AUTHOR'S DECLARATION

This thesis consists of material all of which I authored or co-authored: see Statement of Contributions included in the thesis. This is a true copy of the thesis, including any required final revisions, as accepted by my examiners.

I understand that my thesis may be made electronically available to the public.

STATEMENT OF CONTRIBUTIONS

The work of Taylor Porter (2016) and Kyle Balkos (2018) was conducted in parallel with the work presented in this thesis, with full sharing of experimental test design and results. This collaboration is confined to Chapters 3 and 4 of this thesis. The primary experimental test design was initiated by the author and thesis supervisors (Profs. Walbridge and West) in 2013. Fabrication, instrumentation, testing, and the gathering of results from the stud-connected specimens was completed collaboratively by Taylor Porter and the author. These same tasks were completed entirely by Kyle Balkos for the through-bolt specimens, and entirely by the author for the embedded bolt specimens. Further finite element analyses and reliability analysis, included in Chapters 5 and 6 of this thesis, were completed entirely by the author.

All writing within this thesis was completed entirely by the author. The following is a list of all co-authored publications resulting from the work in this thesis, along with the full names of the MASc theses of both Taylor Porter (2016) and Kyle Balkos (2018).

Balkos, K. D. (2018). *The Static and Fatigue Behaviour of Through-Bolt Shear Connectors in Steel-Precast Composite Bridge Girders.* (Unpublished Master of Applied Science in Civil Engineering). University of Waterloo.

Balkos, K.D., Sjaarda, M., West, J. S., & Walbridge, S. (2018). Static and fatigue tests of steel-precast composite beam specimens with through-bolt shear connectors. *Journal of Bridge Engineering (Submitted)*.

Porter, T. K. (2016). *The Fatigue Resistance of Headed Shear Stud Connectors in Steel-Precast Composite Girders.* (Unpublished Master of Applied Science in Civil Engineering). University of Waterloo.

Sjaarda, M., Porter, T., West, J. S., & Walbridge, S. (2016). Fatigue of Stud Shear Connectors in Steel-Precast Composite Bridges. *CSCE Conference Proceedings.* London, ON, CAN.

Sjaarda, M., Porter, T., West, J. S., & Walbridge, S. (2017). Fatigue Behavior of Welded Shear Studs in Precast Composite Beams. *Journal of Bridge Engineering, 22(11)*, 04017089.

ABSTRACT

At present, many Canadian bridges are overdue for rehabilitation or replacement. In the case of steel-concrete composite bridges, the shear connection between the concrete deck and the steel girders is a vital element of the bridge system, and has significant impacts on construction time, cost, structural integrity, and durability. The general performance of the shear connectors in these bridges is becoming an increasingly important issue, as existing bridges are used past their intended design lives, and new bridges are being designed with accelerated construction and longer service lives in mind.

Welded shear studs are the standard method of shear connection in composite bridge construction, either cast-in-place or concentrated in grouted “shear pockets” in the case of steel-precast applications. The primary disadvantage of using welded shear studs in structures subjected to repeated loading is that they are believed to perform poorly from a fatigue perspective. As a result, design standards in North America require most bridges to have more than double the number of studs needed for ultimate strength purposes. This leads to construction challenges including arduous deck reinforcement placing, and it reduces the economy gained through steel-precast construction by requiring excessive numbers of shear pockets. It is possible that an enhanced understanding of the performance of welded shear studs in composite beams, including system effects, may allow for relaxed design provisions. High strength bolt shear connectors may be a viable alternative to shear studs in some cases, providing greater fatigue resistance due to the absence of welds, and having a higher material strength than conventional welded studs.

The work presented herein is aimed at increasing the state-of-understanding of the fatigue behaviour and reliability of welded shear studs in both cast-in-place and precast concrete composite bridge applications, while also presenting the benefits and drawbacks of two alternative high strength bolt shear connection concepts. A laboratory research program carried out at the University of Waterloo featured the testing of eighteen large-scale beam specimens over a period of two years. In addition to the laboratory work completed by the research team, the author used finite element and reliability analysis methods to augment the test results and extend their applicability to full-scale medium span highway bridges.

Over sixty stud fatigue failures and four bolt fatigue failures were observed over the course of this study, greatly adding to a dearth of existing test results, and allowing the construction of a statistically meaningful fatigue design curve of the stud detail from beam tests for the first time. System effects of multiple stud failures were studied in a finite element model of a typical highway bridge girder and revealed that the current design rules are overly conservative for all bridge classes in the Canadian Highway Bridge Design Code, and for all bridge configurations except for short spans. The results support the proposed new fatigue category dedicated to welded shear studs, recognizing the unique redundant and uninspectable nature of the detail, and suggest a fatigue endurance limit of 36 MPa (one and a half times the current limit). It is proposed that the embedded high strength bolt detail be viewed as a viable alternative to studs, given greatly increased fatigue performance and exceptional ease of deconstruction. The benefits of such a connection would be particularly useful in combination with precast deck panels.

ACKNOWLEDGEMENTS

I would like to thank the Steel Structures Education Foundation, the Canadian Institute of Steel Construction, the Ministry of Transportation of Ontario, and the National Sciences and Engineering Research Council for providing research funding, as well as Hogg Ready Mix Ltd. and KPM Industries Ltd. for the generous donation of concrete and grout. Most importantly, I would like to thank my supervisors Dr. Jeffrey S. West and Dr. Scott Walbridge for their continued guidance and support, as well as research colleagues Taylor Porter, Ben Dow, and Kyle Balkos, and lab technicians Richard Morrison, Douglas Hirst, and Peter Volcic.

A special thanks to all the members of my Thesis Examination Committee:

Dr. Scott Walbridge (Co-Supervisor);
Dr. Jeffrey West (Co-Supervisor);
Dr. Adil Al-Mayah;
Dr. Mahesh Pandey;
Dr. Adrian Gerlich;
and *Dr. Michael Bartlett* of the University of Western Ontario.

DEDICATION

I dedicate my work to my family and my Saviour, Jesus Christ.

"*Whatever you do, work at it with all your heart, as working for the Lord, not for men." Colossians 3:23*

TABLE OF CONTENTS

LIST OF FIGURES

LIST OF TABLES

LIST OF ABBREVIATIONS

AASHTO	American Association of State Highway and Transportation Officials
ABC	Accelerated bridge construction
ADTT	Average daily truck traffic
API	Application programming interface
ASTM	American Society for Testing and Materials (formerly)
CA	Constant amplitude
CAFL	Constant amplitude fatigue limit
CHBDC	Canadian Highway Bridge Design Code
CIP	Cast-in-place
COV	Coefficient of variation
CS	Cast-in-place specimen with welded stud shear connectors
CSB	Load-slip curve from CS beam specimens
CSP	Load-slip curve from CS push test specimens
DLA	Dynamic load allowance
DTI	Direct Tension Indicator
EB	Precast specimen with high strength bolts embedded in grouted shear pockets
EBB	Load-slip curve from EB beam specimens
FE	Finite element
FLS	Fatigue limit state
FS	Factor of safety
HAZ	Heat affected zone
HSTB	High strength through-bolt
HSB	High strength bolt
IIW	International Institute of Welding
LVDT	Linear variable displacement transducer
MTO	Ministry of Transportation of Ontario
MLA	Moving load analysis
MLE	Maximum likelihood estimation
NCHRP	National Cooperative Highway Research Program
PFS	Post-failure stiffness
PS	Precast specimen with welded stud shear connectors in grouted shear pockets
PVC	Polyvinyl chloride
LRFD	Load and resistance factor design
RV	Random variable
TB	Precast specimen with high strength through-bolts
TBB	Load-slip curve from TB beam specimens
TBP	Load-slip curve from TB push test specimens
ULS	Ultimate limit state
USA	United States of America
UW	University of Waterloo
VA	Variable amplitude
VAFL	Variable amplitude fatigue limit

1 INTRODUCTION AND BACKGROUND

It is a well-known fact that many transportation structures around the world are in dire need of maintenance or reconstruction, and this is especially true in North America. It is estimated that 30 bridges reach their design life every day in the United States, with 9% of all bridges reported to be structurally deficient by the American Society of Civil Engineers (Federal Highway Administration, 2017). Canada faces the same dilemma, with the 2016 Canadian Infrastructure Report indicating that current reinvestment levels will result in a decline of the already poor condition of bridges over time (The Federation of Canadian Municipalities, 2016). As a consequence of high building activity levels in the 1950s and 1970s, the country is entering a period of unprecedented infrastructure replacement obligations (Mirza, 2007). There exists a definitive need for bridge replacement systems that are efficient by way of cost and construction, and that have minimal impact on the existing flow of transportation. Furthermore, engineers require better tools for assessing existing bridges to make intelligent decisions about the prioritization of overextended assets.

This thesis presents work undertaken at the University of Waterloo (UW) to improve the state-of-understanding and design of traditional welded stud shear connectors in composite bridges, and to introduce new test results and analysis pertaining to high strength bolt shear connection concepts that may be used as an alternative to conventional welded studs. The application of this work is in both traditional cast-in-place (CIP) composite construction, as well as steel-precast composite bridges. The latter application will be discussed in detail as it was the initial motivation for the work. Steel-precast composite bridges have gained popularity in recent years by answering the call for a superstructure system that enables accelerated, low impact construction and long-term durability. The shear connection between the steel girders and the precast concrete deck in this bridge system will be shown to be a critical element, which stands to be improved upon in terms of fatigue performance, evaluation, and design.

1.1 Background and Motivation

1.1.1 Accelerated Bridge Construction

Maintaining and replacing bridges is a challenge because they are natural bottlenecks for traffic. Accelerated bridge construction (ABC) techniques can minimize traffic delays during a project overall, with a high impact disruption over a short duration (Burak & Seraderian, 2010). Lost opportunity costs of motorists, late deliveries, wasted fuel, increased air pollution, and increased collision frequency are all direct consequences of traffic congestion due to lanes closed for bridge work. It has been estimated that delays on many urban projects cost road users over $50,000 per day in lost time and late deliveries alone, without considering the high cost of traffic control itself nor the reduced construction productivity due to the close proximity of motor vehicles (FOCUS, 1999). Not only are long delays more costly, but surveys indicate that road users prefer a significant short term impact in favour of a moderate long term impact (Burak & Seraderian, 2010).

There are two distinct ABC approaches that are being utilized today. The first, rapid bridge replacement, involves the use of modern bridge movement technology to rapidly move completed bridges into alignment after the removal of an existing bridge, and the second is the use of prefabricated systems to drastically reduce construction time. Several projects in Ontario have used the former method in the last number of years, most notably in the nation's capital where eight projects of this type have taken place. The Carling Avenue bridge on Highway 417 was replaced in July of 2013 in only 17 hours (Figure 1-1), and on another project, the Province of Ontario estimated savings of $2.4 million in construction fees due to the avoidance of long term lane closures (MTO, 2013). Typically, these rapid replacements are only executed on high-volume freeways where significant traffic control and user delay-related cost savings can be realized. Furthermore, the provision of a well paved road beneath the overpass and adequate construction space adjacent to the site are imperative for the successful implementation of this approach.

Figure 1-1: Rapid bridge replacement in Ottawa, Ontario.

The second method of accelerated bridge construction includes reducing or eliminating formwork, beam erection, rebar tying, and concrete curing on site through the use of prefabricated components (Transportation Research Board Strategic Highway Research Program, 2013). This approach has fewer constraints in terms of its application, and can be achieved with less dependence on specialized equipment and expertise. Precast bridge decks are the primary source of reduced construction time on such projects, having the advantage of significant time savings over traditional CIP bridge decks, which require considerable construction time to install formwork and deck reinforcement, as well as concrete placement and curing. With ABC in mind, composite modular bridge systems consisting of precast concrete deck panels connected to steel girders are becoming increasingly popular in Canada, the US, France, Korea, and Japan (Bowser, Walbridge, & West, 2012).

1.1.2 Steel-Precast Composite Bridges

The use of precast concrete bridge decks began in the 1960s in North America, with regulatory authorities recognizing the benefits of reduced construction time compared to CIP construction (Issa, Patton, Abdalla, & Yousif, 2003). Aside from its use as a key piece in ABC, it is sometimes the only option in remote locations

where ready-mix concrete is not available or where CIP procedures are not possible. The original use of precast decks was in non-composite systems where the deck was used simply as a road surface and to transmit loads transversely to the bridge girders. It was soon realized that a very efficient means of resisting longitudinal moments is through the use of the composite system, where the deck and girders resist moment in combination.

Today almost all concrete bridge decks, both CIP and precast, are shear connected to girders to take advantage of composite action. A composite cross-section is ideally suited to resist positive moments; resistance is provided through a force couple consisting of a compressive force in the concrete, and a tensile force in the steel. A shear connection for a CIP bridge is commonly made by casting the concrete around the connectors, which are welded to the top flange of the steel; precast panels are not able to be affixed in this way. The precast connection is made by leaving full depth voids in the panels (termed “shear pockets”) and placing the pockets around groups of studs. The pockets are then grouted to complete the connection. A typical CIP section is shown in Figure 1-2 and a precast bridge with shear pockets is shown in Figure 1-3.

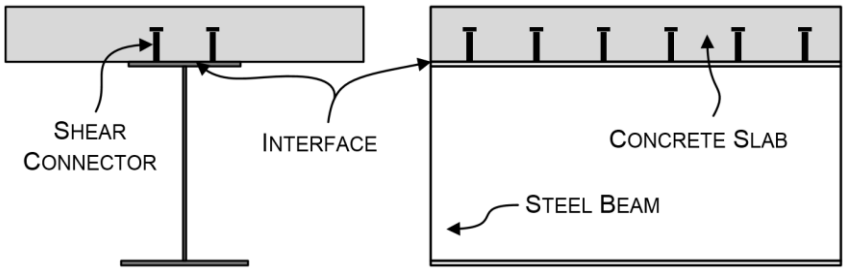

Figure 1-2: CIP section and basic features.

Despite being used almost exclusively in new bridge construction, the pocketed shear connection has some significant drawbacks including the need for a large number of connectors / pockets to achieve satisfactory fatigue performance with the typically employed welded shear connectors, and the introduction of a vertical cold joint in the bridge deck, which may lead to durability issues. Several other connector types, including bolted shear connectors, have been proposed and even implemented with some success (Dorton, Holowka, & King, 1977). In the next section, welded stud shear connectors and other connection types are presented and their properties compared with those of an ideal shear connection.

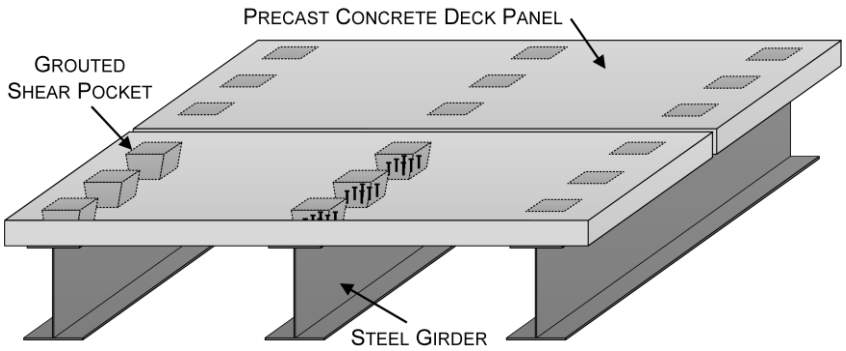

Figure 1-3: Precast bridge deck on girders with welded stud groups.

1.1.3 Shear Connectors for Precast Deck Panels on Steel Girders

Table 1-1 lists the attributes of an ideal shear connection for steel-precast composite bridges.

Table 1-1: Attributes of the ideal shear connection.

Attribute	Rationale
Grout-Free	Grouting requires time and temperature conditions to cure and is labour intensive. Durability and maintenance issues arise if the grout shrinks or is installed poorly.
Large Tolerances	Connections with small tolerances can be time consuming to install and time and material may be wasted if fit is not initially achieved.
Top Access Install	Access to the underside of the structure is not always possible and is rarely convenient. Levelling of the panels and proportioning of a haunch must also be considered.
Easily Disassembled	The deck design life is normally shorter than that of the bridge superstructure, so it must be designed to be replaced during the bridge service life.
Fatigue Resistant	More connectors will have to be used if the design is governed by fatigue rather than ultimate strength. This is especially important when connectors cannot be inspected or replaced during the life of the bridge.
Durable	The presence of holes or vertical joints in the deck can lead to water damage, specifically corrosion both of the deck itself, and the girders beneath.
Stiff and Ductile	The stiffness of the connection reduces slip at the interface and allows for more composite action, while ductility is important for redistribution of forces at failure.
Low Cost	Consideration should be given to costs of material, labour, installation, equipment, speed of construction, and inconvenience to motorists.

There are two ways that shear can be resisted at the interface of the steel and concrete. The vast majority of connections work by mechanical resistance and these require some slip for shear transfer to occur. The second type resists chemically through some type of adherence (glued connections) or bond, and is very stiff. This stiffness allows for high levels of composite interaction, approaching the fully composite condition. Although chemical adherence-based connections can have exceptional stiffness, they are not easily assembled or disassembled, and they commonly lack ductility.

Mechanical shear connectors are embedded in the case of CIP construction, taking the form of various shapes welded to the top flange of the steel section. These shapes include headed and hooked studs, channels, angles, spirals, or hoops. Headed studs have become the standard over the years, in large part because of the stud welding gun, which makes shear connector installation rapid either in the fabrication facility or on-site. The headed stud is also the standard for precast panel shear connections with the use of grouted shear pockets (see Figure 1-3), but other possible precast panel connections include high strength

bolt configurations, panel-end connections (Bowser et al., 2012), or post-installed connections (using studs or bolts in drilled deck holes) as shown in Figure 1-5.

The primary disadvantage of welded studs is that the fatigue limit state (FLS) governs over the ultimate limit state (ULS), often requiring more than two times the number of studs. Studs are expensive both in material and installation, and for CIP construction the presence of large numbers of them can make the task of placing deck reinforcement difficult (see Figure 1-4). In precast applications, high numbers of studs require more grouted shear pockets. In both CIP and precast applications, it is important to be able to predict the fatigue behaviour of headed studs, because bridges are often used past their design service lives and condition assessment of embedded studs is generally not possible apart from during deck replacement events.

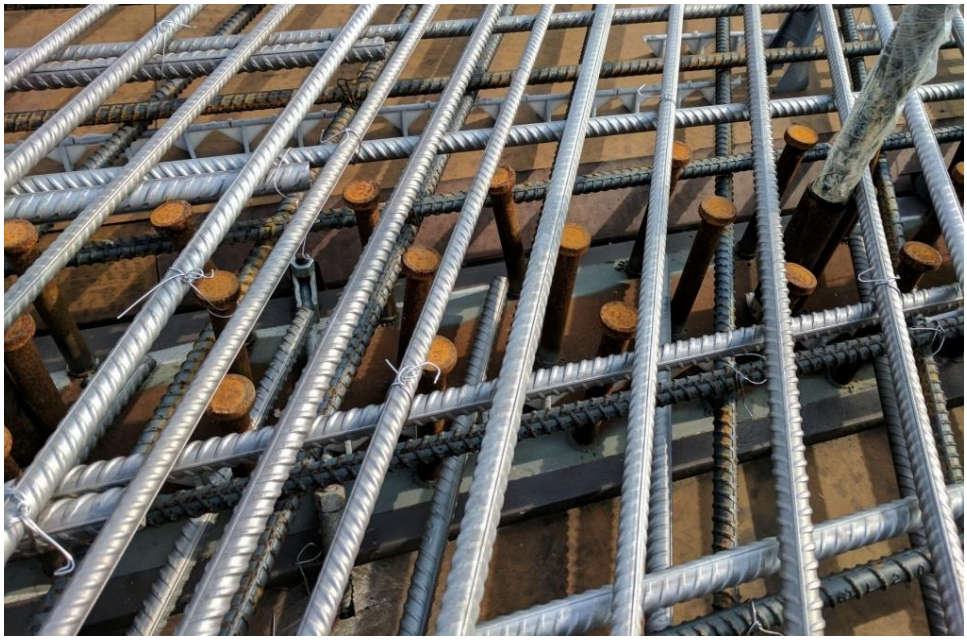

Figure 1-4: High numbers of studs lead to difficult deck reinforcement placing.

Embedded stud construction has the advantages of requiring top access only, having large tolerances, and being relatively stiff and extremely ductile. Relatively poor fatigue behaviour and difficult disassembly are the main drawbacks of welded studs, and the need to grout shear pockets is an added disadvantage in the case of precast panel construction. Through-bolts have the disadvantage of requiring access to the underside of a bridge during assembly and disassembly but have the potential to provide a connection that is free of grout, whereas the high strength bolts in grouted shear pockets only require top access for installation (provided the bolts are mounted prior to girder erection). Another benefit of high strength bolts in grouted shear pockets over the through-bolts is that only a small part of each bolt is put into tension and friction is resisted by steel on steel contact, rather than concrete on steel contact. These connections will be discussed in greater detail in the literature review section of this thesis. The panel end connection, shown in Figure 1-5 (bottom), involves connecting girders to precast panels at the panel end points only. This connection is unique and has only been demonstrated in theory to date (Bower et al., 2012).

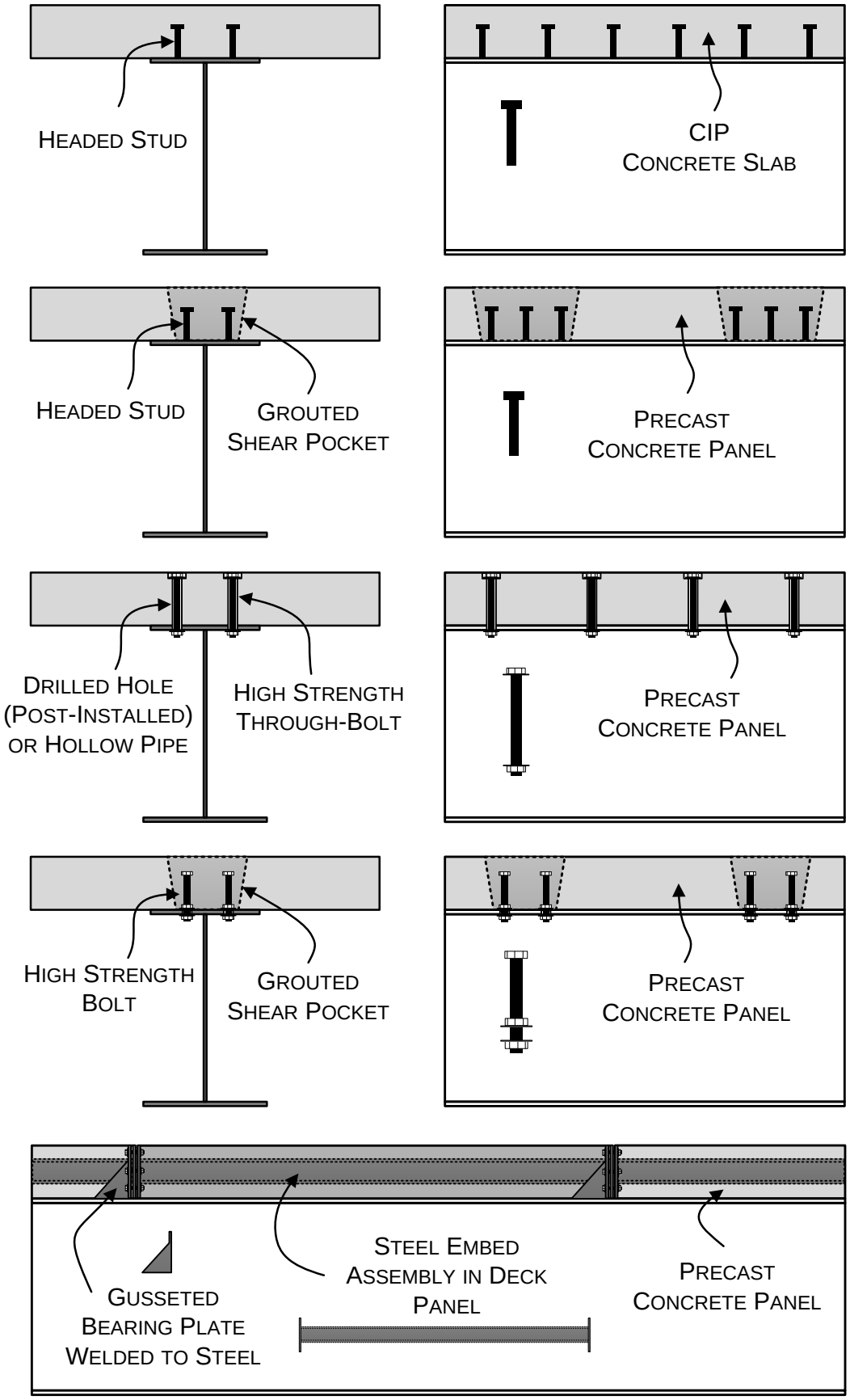

Figure 1-5: Conventional and innovative precast panel shear connections.

1.2 Statement of Research Problem

Although widely used today, welded shear studs are prone to structural fatigue at relatively low stresses, and grouted pockets in steel-precast applications present durability concerns. The fatigue failure mode and accompanied uncertainty can lead to high numbers of studs, congested reinforcement layouts, and time-consuming grouting. *There exists a strong need for enhanced, updated understanding of the fatigue behaviour of welded shear studs in CIP and precast bridge decks. Additionally, there is a need to develop alternative shear connection methods that have the ideal qualities of being rapidly constructible, highly fatigue resistant, and having a low overall life-cycle cost.* Although bridge design codes do not currently permit partial shear connection, it remains necessary to explore the impact of this approach on the strength and failure mode of a composite beam. Current code provisions for shear connections in bridges may be overly conservative, and economy may be gained through the allowance of partial shear connections, the recognition of reduced shear flow due to partial interaction, and the reliability associated with system effects. This economy would take the form of a reduced number of shear studs and pockets, or a viable alternative shear connection, made possible using enhanced design procedures.

1.3 Objectives and Research Approach

Despite a substantial number of investigations performed on the fatigue of shear stud connectors, there is still a surprising lack of beam tests with connector failures reported in the literature. This is demonstrated by the fact that bridge codes in Canada and the United States still use push test results to establish the stud fatigue design curves (AASHTO, 2014 and CSA S6, 2014). This inconsistency is demonstrated in that all other fatigue details are designed using provisions based on tests from the actual detail and establishing a design curve two standard deviations conservative to the mean. For studs, the design criteria are based directly on the mean test results from push tests, and it is assumed that these tests are inherently conservative (without a clear indication of how conservative they are). Investigations concerning studs in grouted pockets for precast panel construction have mainly focussed on affirming the applicability of CIP design rules rather than discerning what effect the different construction method might have on fatigue life. Concrete shrinkage and interfacial friction are two variables that are changed from one method to the other, and the effects of these variables on the fatigue behaviour of studs has not been thoroughly studied or quantified.

High strength bolts (either embedded bolts or post-tensioned through-bolts) have been used sparingly as an alternative for shear studs in composite construction, but there is no clear indication of how bolt slip might affect fatigue performance and system stiffness. Load reversals causing shifts in bolt bearing surface is a subject that has received very little attention. Despite field implementation in several pilot projects (Dorton et al., 1977) (Issa et al., 1995), there are still no design procedures available to substitute studs for bolts, partly due to questions of constructability and uncertainty related to how the bolted shear connection systems will behave on a large-scale over a long period of time.

While a great number of fatigue push tests have been performed on individual stud and bolt connectors, comparably very few have been tested until failure in beams with the goal of observing the consequences of such failures. Furthermore, there are no studies known to the author that have taken push test and beam test failure results and applied them in full-scale bridge analyses to observe overall system effects. The consequence of a single shear connector failure on a bridge is not known, because no failures have been observed in the field and simulation models have not been developed. It is not known if connector force redistribution will result in rapid subsequent stud failures, or whether this process occurs very gradually, perhaps even to the point that the overall system is insensitive to several connector failures.

It has been shown, and the literature review herein bears out, that there is a definitive need for growth in the body of knowledge surrounding the fatigue behaviour of stud and bolt shear connectors. In response to this need, the current research program has the following objectives:

1. *to obtain S-N fatigue data for stud shear connectors in beams;*
2. *to investigate the fatigue behaviour of studs in precast slabs with grouted shear pockets;*
3. *to conduct fatigue tests on two high strength bolt connector types in beams;*
4. *to investigate bolted shear connector fatigue behaviour in beams and full bridges; and*
5. *to assess and calibrate the fatigue design of studs considering the risk of system failure.*

The approach used to accomplish these objectives has included a laboratory beam testing program (Objectives 1-4), finite element (FE) analysis extending the beam test results to full-scale bridge girders (Objective 4), and assessing the structural reliability and risk of connector failure using statistical methods in conjunction with the developed FE model (Objective 5). The laboratory beam testing program consisted of the fabrication and testing of twelve beam specimens with welded stud connectors and six with bolted shear connectors. FE models were built and executed in SAP2000 (Structural Analysis Program, 2014) to simulate both the fatigue tests and a full-scale bridge. The FE model was then used to perform probabilistic simulations to assess and calibrate the fatigue design provisions for shear studs.

1.4 Thesis Outline

This thesis is divided into seven chapters including the current one.

In Chapter 2 a literature review is presented, which reviews the current state-of-understanding of the behaviour of welded shear studs and several alternative shear connection systems used in composite construction. A review of the target reliability of fatigue components is also presented.

Chapters 3 and 4 include a description of the laboratory component of this work, including test specimens, setups, and procedures, along with a presentation of the test results and associated discussion. The laboratory work for this thesis was completed in collaboration with Taylor Porter (MASc) and Kyle Balkos (MASc). Their thesis reports are cited for further details, where appropriate.

Chapter 5 presents an FE composite beam model that was created to extend the results of the laboratory work and serve as a tool for the evaluation of new shear connection concepts. In Chapter 6 this model is modified to assess the reliability of stud shear connectors designed using current code provisions. Modified design procedures are presented, based on the reliability analysis results.

Chapter 7 is a synthesis of the work presented in the preceding chapters. The main conclusions of the thesis are presented, along with recommendations and suggested future work items.

2 LITERATURE REVIEW

The following chapter provides a review of the current body of knowledge pertaining to the fatigue behaviour of welded shear studs and high strength bolt shear connectors, as well as the reliability of fatigue details in general. The history and development of the current state-of-knowledge will be discussed, along with the evolution of the design process as it has responded to research findings over the decades. The first two subsections of this review will introduce several key terms and outline their importance.

2.1 Push Tests and Composite Beams

Mechanical shear connectors were first proposed for composite construction in the 1920s, but it was not until the 1960s that systematic testing began. King, Slutter, Johnson, Hallam, and Oehlers are names associated with early experimental studies of the composite behaviour induced by shear connectors, specifically the fatigue capacity of shear studs (Johnson, 2000), (Oehlers & Foley, 1985), (Slutter & Fisher, 1966). Fatigue was recognized as being a significant factor in the design, given the sudden change in geometry and imperfections (e.g. voids, inclusions, lack of fusion, and other geometric variations) introduced through the welding process. The use of push tests began early on as both an ultimate and fatigue strength measurement tool. A push test is a relatively inexpensive test used to study shear across an interface, often meant to replicate the longitudinal shear in a composite beam. A typical push test specimen is shown in Figure 2-1; note the doubly symmetric shape used to eliminate eccentricity.

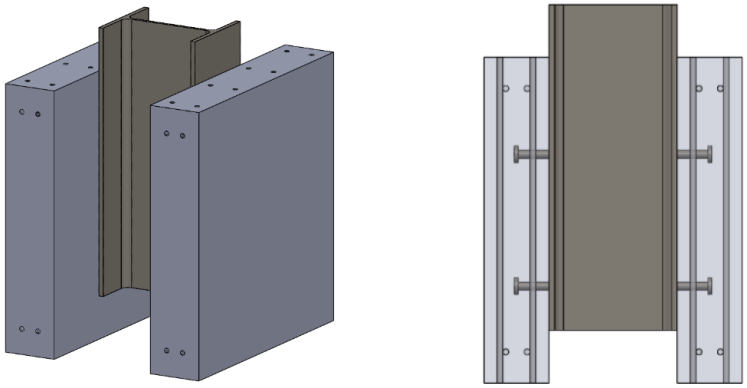

Figure 2-1: Push test specimen.

Push tests were the first experimental tests performed on shear connectors to determine their capacity to facilitate composite action, and they remain standard practice (see Eurocode 4 Annex B, CEN, 2005). Push tests have been found to be a reliable method for determining shear capacity by some (Issa, Patton, Abdalla, & Yousif, 2003) even though they do not perfectly simulate the shear behaviour in a beam. Some have shown that studs in beams have increased fatigue performance when compared to push tests (Johnson, 2000), (Slutter & Fisher, 1966). However, others are not convinced of the credibility of push test results due to the difference in the boundary conditions between beams and push test specimens (Gattesco & Giuriani,1996), (Oehlers & Foley, 1985).

In a push test, the shear forces on individual connectors remain constant relative to one another throughout the test. A beam test, on the other hand, features force redistribution; when one shear connector begins to crack and fail (in fatigue, for example), other neighbouring connectors compensate and attract increased shear force. The crack then grows more slowly because the cracked connector is more flexible and therefore attracts less force. The force being transferred to the slab does not remain constant, as the connectors begin to plastically deform. Furthermore, a beam test engages friction at the slab-beam interface, which lessens the force transferred through the shear connectors.

It is worth comparing the strain profile of the composite section in the push test and beam test cases and discussing the interfacial slip. The key difference between beams and push tests is in the way the connector shear forces arise. In the beam, the externally applied load causes a strain gradient with a discontinuity at the interface (also called “slip strain”), and connectors are subjected to shear force to resist the accumulation of slip due to the strain discontinuity along the length of the beam. In a push test, however, connectors resist shear force because they are part of the load path between the applied load and the balancing reaction at the base of the specimen. A push test is determinate (in that average connector forces can be computed using equations of equilibrium), while the beam is not (information about geometry and material properties is necessary). Figure 2-2 shows conceptual illustrations of the typical strain profiles and final deformed shapes in each case. A push test is useful for generating load-slip curves for shear connectors. These curves give information about connector strength, stiffness, and ductility. The drawback of the load-slip curve is that it does not give a quantitative indication of the composite action that may result from the presence of a connector in a beam. Since the induction of composite action is the primary function of a shear connector, it is clear that the push test fails to evaluate connectors on this basis.

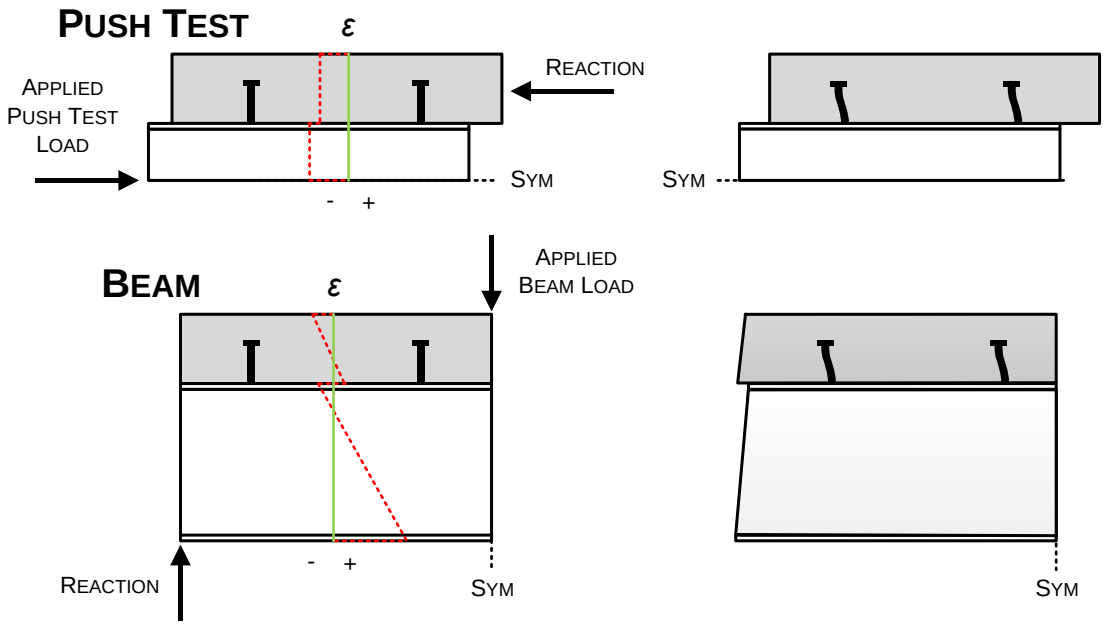

Figure 2-2: Strain profiles (left) and deformed shapes (right) in push tests and composite beams.

2.2 Shear Connection and Composite Interaction

2.2.1 Definitions

It is necessary to review the basics of shear connection and interaction to better understand the forces that shear connectors are subjected to, and to define two terms that will be used frequently in the current thesis to describe shear connector behaviour: the degree of shear connection and the degree of composite interaction. The degree of shear connection refers to the equilibrium of forces in a composite beam at the ultimate limit state (ULS), while the degree of interaction refers to the compatibility of displacements and more specifically the shape of the strain profile through the depth of a given section (Oehlers, Nguyen, Ahmed, & Bradford, 1997). The degree of shear connection, η, is shown in Equation 2-1 and is defined as the ratio of the ultimate shear strength of the interface in a shear span, F_i, to the minimum strength necessary for the section to develop its full flexural capacity at the end of the shear span, F_f. This connection can be full, partial, or there can be no connection at all. Figure 2-3 shows the longitudinal equilibrium of forces at the ULS for a full shear connection ($\eta = 1$), partial shear connection ($0 < \eta < 1$), and no shear connection ($\eta = 0$). In design codes, the shear strength of the interface is calculated using the ultimate strength of all shear connectors in the shear span ($A_{sc}f_u$), neglecting friction and bond. The section can reach its full flexural capacity when F_i is equal to F_f, which is the lesser of the steel beam area multiplied by the yield strength of the material (A_sf_y) and the product of the stress block factor α_1, the concrete area A_c, and the 28-day compressive strength of concrete, f'_c. It should be noted that the shear span is determined using a moment envelope for moving loads, and it is independent of the load at any given time. As a result, a beam or girder can be described as having a constant degree of shear connection.

Equation 2-1
$$\eta = \frac{F_i}{F_f}$$

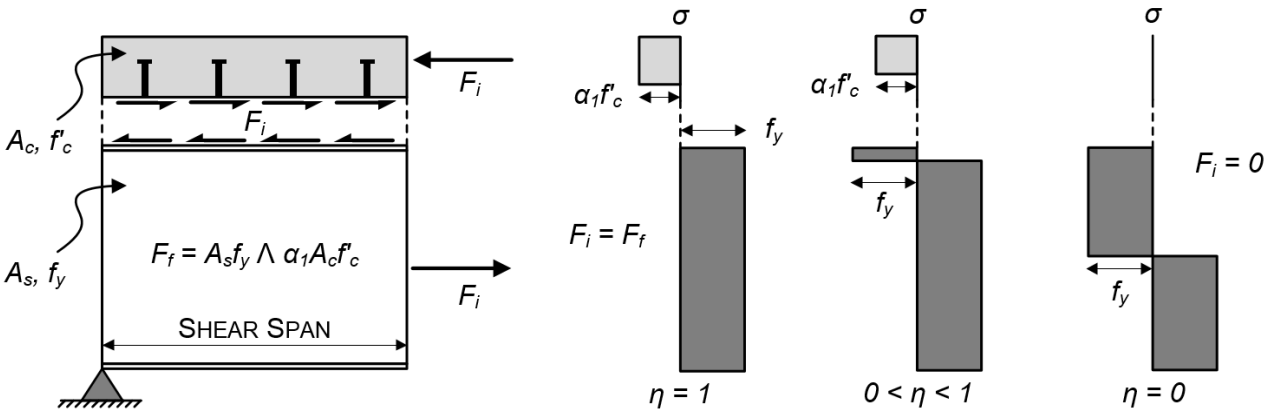

Figure 2-3: Degree of shear connection.

The degree of composite interaction, φ, is difficult to completely define without the use of differential calculus and complicated compatibility equations. In 1951 Newmark, Siess, and Viest published a classic paper on linear elastic partial-interaction theory, which was later extended and simplified by Oehlers et al. (1997). A

simplified definition for the degree of interaction is given in Equation 2-2 and is based on the ratio of the neutral axis separation, h, to the maximum neutral axis separation, h_0. This maximum neutral axis separation is the distance between the steel and concrete neutral axes in the case of non-composite behaviour. Figure 2-4 shows three beam strain profiles illustrating full, or complete interaction ($\varphi = 1$), partial interaction ($0 < \varphi < 1$), and no interaction ($\varphi = 0$). As stated earlier, mechanical shear connectors require slip to transmit shear, so full interaction is only possible through a very stiff chemical bond. Equation 2-2 is valid for shored construction only (but could be modified for the unshored construction case).

Equation 2-2
$$\varphi = 1 - \frac{h}{h_0}$$

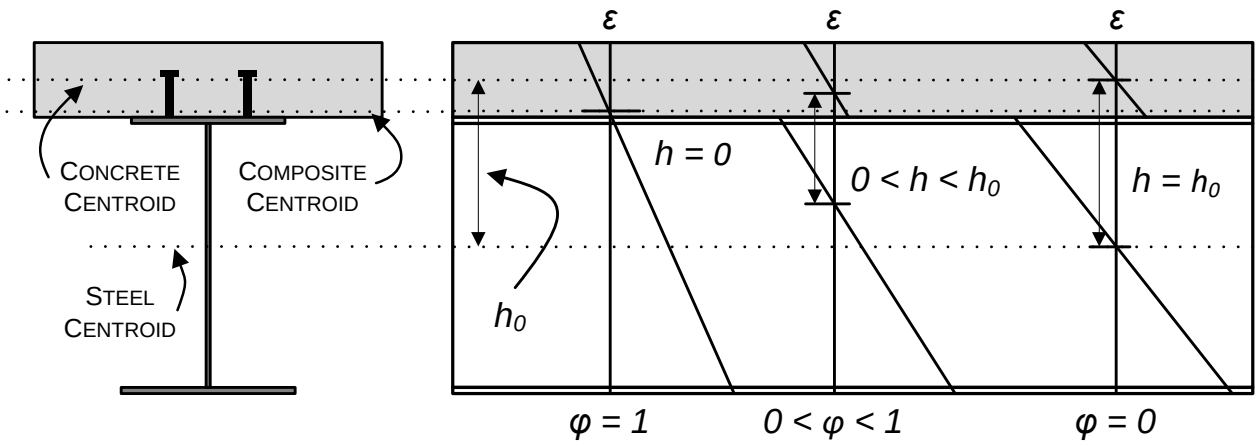

Figure 2-4: Degree of composite interaction.

Unlike the degree of shear connection, the degree of composite interaction is not defined at a particular section along a composite beam, nor is it defined under a particular loading condition. As a result, a beam or girder cannot be described as having a constant degree of composite interaction. In fact, the degree of interaction changes with loading, over the length of the beam, and even over the life of a beam; it has been shown that the stiffness of a composite beam decreases when subjected to repeated loading (Yura, Methvin, & Engelhardt, 2008). In contrast to the degree of shear connection, the degree of composite interaction is difficult to calculate, resulting in a reduction in usefulness to the practicing engineer.

2.2.2 Degree of Shear Connection in Design Codes

To simplify the design and analysis of composite beams, the degree of composite interaction is often assumed to be full or perfect, particularly in design codes. Newmark et al. stated that this assumption is reasonable for a properly designed beam (Newmark et al., 1951). The steel design code for buildings in Canada places a limit of 40% on the degree of shear connection that must be provided, stating that below 40% shear connection, composite action cannot be assured (CSA S16, 2014), (CISC, 2014). Additional to the assumption of full interaction, design codes neglect the helpful effects of friction along the steel-concrete interface, instead assuming that shear is carried by the mechanical connectors only.

In contrast to the codes for steel buildings, the Canadian (CSA S6, 2014) and American (AASHTO, 2014) bridge codes do not permit partial shear connection by stating that the full capacity of a section must be developed through shear connection regardless of the loading conditions. In a technical report written for the Federal Highway Administration of the United States, Yura, Methvin, and Engelhardt contend that current bridge code design rules may require an excessive number of shear studs, to the point where it can be difficult to fit them all on the girder top flange (2008). Interestingly, they point out that some editions of the AASHTO code have included provisions allowing composite beam bending strength to be computed based on the number of shear studs provided; these provisions were removed at one point, citing that partial composite action is not permitted by the code, so the provision was not useful (AASHTO, 2014). This instance suggests that composite action is (or was) not fully understood by the code makers. In the conclusions of their report, they recommend that partial composite action be considered for bridges, so that shear connection design is based on required strength and not on cross-section properties, and that the lower limit for shear connection should be placed at 50% (Yura et al., 2008).

2.2.3 Impact of Partial Shear Connection on Strength

A partial shear connection theoretically forces the ultimate failure mode of a composite beam to be failure of the shear connectors. Additionally, as the number of shear connectors decreases, the degree of composite interaction also decreases and interfacial slip increases; concerns regarding cyclic interfacial slip may be the primary motivation for requiring a full shear connection in bridges. According to Yura et al., partial shear connection construction has been used in the building industry since 1969, and the majority of composite beams designed today use a partial connection (2008). The reason behind this is that a partially shear connected beam is very efficient; it can be shown that a beam with 50% shear connection will have approximately 75% to 85% of the moment capacity compared to the same beam with 100% shear connection.

It may be argued that having a full shear connection is necessary to prevent interfacial slip. However, from the definitions laid out previously, slip depends on the stiffness of the connection, not on the strength. As a result, there is no transition in the way a composite beam behaves as the level of shear connection reaches the “full” value. The only change that occurs is in the overall failure mode of the beam; with a partial shear connection the failure mode is no longer controlled by the cross-section, but is instead initiated in the shear connection itself. This itself is dubious, since the magnitude of interfacial slip required to fail a shear connector (under static loading) is not likely to occur; the failure of a stud shear connector has been shown to be very ductile (see Figure 2-5). One final note that shall be kept in mind when considering the reasons why bridge design codes do not permit partial shear connections is that in many bridges the number of shear connectors provided is governed by the FLS, and this often means that more studs are required for fatigue than for a full shear connection.

Figure 2-5: Shear connectors exhibit ductile behaviour in bend tests.

2.2.4 Impact of Partial Composite Interaction on Fatigue Life

The assumption of full or perfect interaction in composite beams is conservative from a fatigue perspective (Oehlers, & Seracino, 2002). Full interaction assumes that the shear connectors are perfectly rigid, and therefore attract or develop more connector shear force than they actually do. The elastic calculation of shear flow with a full interaction assumption leads to overestimated connector design shear forces. Despite not being accounted for, it is known that partial interaction is inevitable under service loads when mechanical shear connectors are used, and although the interfacial slip only has a small effect on strength, it can have a significant influence on the fatigue life of a composite beam or girder.

In the past, rigorous hand calculations would have needed to be performed to calculate the beneficial effects of partial interaction and interfacial friction. At present, however, commercially available finite element (FE) analysis packages enable modelling that will take partial interaction into account based on known (input) connector stiffness or load-slip response. This stiffness data can be in the form of a single number (termed the “modulus of shear connectors” by Newark et al.), or a full load-slip curve obtained from shear connector push tests (1951). Furthermore, Oehlers and Seracino devised a simplified method to incorporate partial interaction into design or analysis, by using linear segments to approximate the shear flow force range envelope obtained from computer simulation and partial interaction theory (2002).

Oehlers and Seracino present a tiered approach to fatigue assessment that provides increasing levels of complexity and accuracy as necessary. This method is a valuable tool, particularly for maximizing the service life of existing structures. The approach begins by assuming full interaction, just like current bridge design codes. This is the most conservative and least complicated approach. Following this, friction is taken into account by altering the well-known shear flow equation, as shown in Equation 2-3.

Equation 2-3 $$q = V\left(\frac{Q}{I} - \frac{\mu}{\ell}\right)$$

In Equation 2-3, *VQ/I* is the well-known shear flow equation, μ is the coefficient of friction at the interface, and ℓ is the length of the shear span. After friction is taken into account, partial interaction shear flow can also be accounted for to realize the maximum fatigue life. The equation used to do this is not described here for brevity, but can be found in the manuscript by Oehlers and Seracino (2002). Even small reductions on the connector design force manifest themselves in significant extensions of fatigue life.

2.3 Welded Shear Stud Connectors

2.3.1 Fatigue Behaviour

The current understanding of the fatigue behaviour of welded shear studs has its roots in the seminal work of Slutter and Fisher, performed at Lehigh University in Pennsylvania around 1965. Prior to that time, fatigue provisions for design were based on over-conservative approximations from static test results. With the goal of overhauling the shear connector design procedure, Slutter and Fisher performed 44 constant amplitude (CA) fatigue tests on push test specimens with 19 mm (3/4") and 22.2 mm (7/8") stud connectors (1966). Tests were performed using 30 MPa concrete at a loading rate of approximately 6 Hz. They found that the stress range during cycling is the most important variable in the fatigue life of a stud, which is in agreement with general fatigue principles. In addition, they found that they could relate stress range to the number of fatigue cycles until failure for a stud using Equation 2-4.

Equation 2-4 $$\log N = A - B(\Delta\tau)$$

In Equation 2-4, *N* is the number of cycles experienced by a shear connector until failure, $\Delta\tau$ is the range of shear stress, and *A* and *B* are constants (obtained by regression analysis). The stress range was recommended to be calculated using elastic theory given by Equation 2-5.

Equation 2-5 $$\Delta\tau = \frac{\Delta V \cdot Q \cdot s}{I \cdot A_{sc}}$$

In Equation 2-5, *V* is the transverse shear at a section, *Q* is the statical moment of area of the shear connected geometry, *I* is the moment of inertia of the composite section, *s* is the stud spacing, and *A* is the area of a stud. The relationship they used to relate stress range and fatigue life was semi-logarithmic. The justification of using push tests instead of beam tests was based on cost, convenience, and their assertion that push test results represent a lower bound for shear connector failure. King, Slutter, and Driscoll were conducting beam tests in the same facility that year, so the decision to use push tests was based on firsthand experience, rather than speculation. Further to their proposed *S-N* design relationship (stress vs. number

of cycles to failure), they stated that connectors should be placed at a maximum spacing of 2' or 610 mm to prevent separation between the steel and the concrete.

Oehlers began his work in on the subject in 1981 at the University of Warwick, England, and continued later in the decade at the University College Cork in Ireland with several notable colleagues including Johnson and Foley. They performed a large number of push tests in the 1980s and provided a comprehensive summary of work completed up to that time on the fatigue strength of headed studs, which had become the convention by then. At one point they analyzed 129 push tests (their own work and the work of others) to make the following observations (Oehlers & Foley, 1985):

- The static strength of a stud decreases at the onset of cyclic loading.
- The slope (*m*) of the log-log *S-N* relationship is between 2.9 and 13.9.
- The crack growth rate and associated reduction in static strength is constant.
- Failure occurs when the peak load exceeds the capacity of the un-cracked stud area.
- Reverse cyclic loading is equivalent to uniaxial loading in two directions.
- A cumulative damage law can be applied to variable amplitude (VA) test results.

In 1999 Johnson summarized the available data at the time from the USA, UK, Australia, and Japan to obtain the most accurate values for *S-N* curve regression coefficients (Johnson, 2000). This time the form of the *S-N* relationship was chosen to be log-log, as given by Equation 2-6.

Equation 2-6 $$\log N = \log C - m\log(\Delta\tau)$$

In Equation 2-6, *C* is a constant obtained from regression analysis, and *m* is an exponent (when this equation is placed in common design form) that determines the slope of the *S-N* curve. Johnson suggested conservative design values of 5.5 for *m*, and 16.4 MPa for *log(C*). He noted, however, that the reliability for the fatigue design of stud connectors remained unclear and the lack of observed failures is due to inaccurate stress range estimates rather than soundness of design. Besides inaccurate loading estimation, complexities regarding interfacial slip and friction are the main sources of inaccurate stress range calculations; Equation 2-5 assumes full composite interaction. Figure 2-6 shows the fatigue data discussed so far including Slutter & Fisher's work (and regression), Johnson's regression, and beam test results from King, Slutter, and Driscoll (1965).

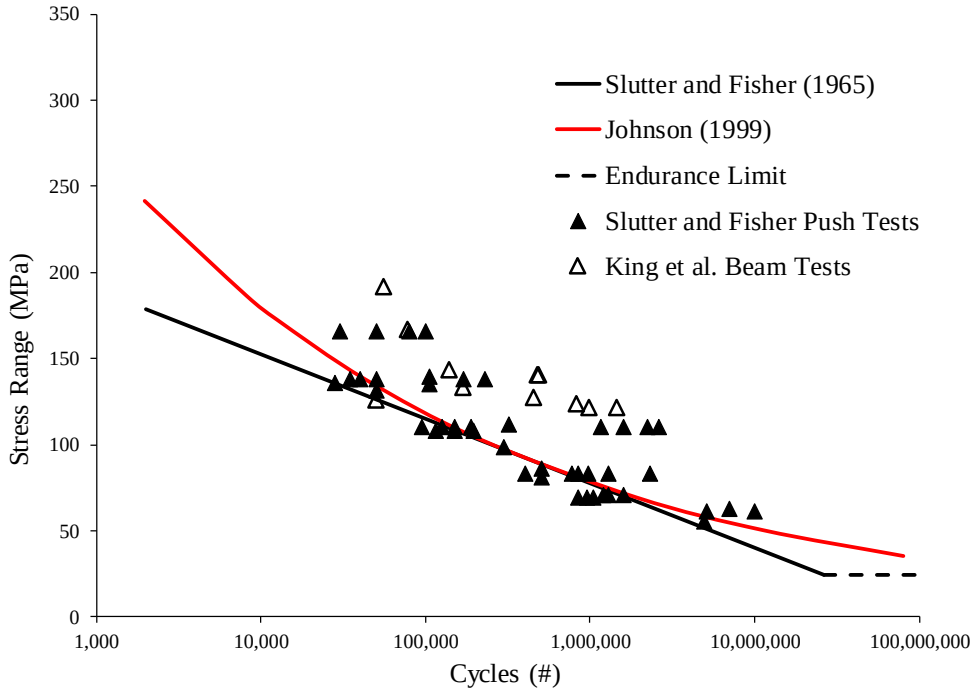

Figure 2-6: *S-N* data from Slutter & Fisher, Johnson, and King et al. for stud connectors.

The beam tests performed at Lehigh were important because they were the first meaningful ones of their kind; prior tests did not achieve fatigue failure in any studs. Several important observations were made in addition to the obvious result that the fatigue lives eclipsed those of their push test counterparts, as shown in Figure 2-6. King et al. tested 4 beams to start, in part to verify that fatigue failure of a stud was possible on a beam, and in part to experiment with instrumentation and testing conditions (1965). Following this, they tested 8 primary beams. The primary beams had a 1200 mm wide by 100 mm thick slab of 20 to 25 MPa concrete mounted onto a 12 x 27 wide flange beam (12 inches deep and 27 lb/ft) of A7 steel (F_y = 207 MPa). The span of the composite beams was 4.6 m long. The shear connection was made using 20 pairs of two 12.7 mm diameter shear connectors, welded at a local fabrication shop. The 40 connectors were enough to form a full shear connection, which is to say that the ultimate capacity of the composite cross-section could be developed. In the first four beams only a 58% shear connection was provided to ensure that failure would occur.

CA fatigue loading was applied at the centre of the beams at a rate of 4.2 Hz, with the ranges of shear connector stress shown in Figure 2-6, and a minimum load of approximately 10% of the maximum load (King et al., 1965). Specimens were loaded initially for several thousand cycles in order to break the bond between the concrete and the steel. Instrumentation took the form of 4 slip gauges along the length, a vertical deflection gauge, and numerous strain gauges. It was found that slip and deflection data were not as significant as strain gauge data in determining failure of the studs. Strain gauges mounted on the bottom of the steel flange opposite the location of studs were found to be particularly useful in identifying the occurrence of stud failure. These gauges captured local distortions in the flange due to stud engagement, and proved to be very accurate in determining when studs began to fail. The area of influence of this local

distortion was found to be about twice the diameter of the stud itself. In all, 141 studs were failed in 11 of the 12 beam specimens. A decision was made by King et al. to plot just one *S*-*N* data point from each beam, since redistribution made it difficult to determine the stress range applied to the studs once the first stud pair was cracked.

King et al. investigated the behaviour of a composite beam as the shear connectors failed. They found that the fatigue failure of studs was gradual and progressive in nature, with failure beginning at connectors near the ends of the member where stresses were approximately 25% higher than average (1965). Fatigue failure usually occurred in the base metal (steel flange) in the heat affected zone (HAZ) of the stud weld, and it was observed that composite behaviour remained effective long after the initial cracking of the studs. Figure 2-7 shows a fatigue failure of the outermost stud pair on one of the primary beams.

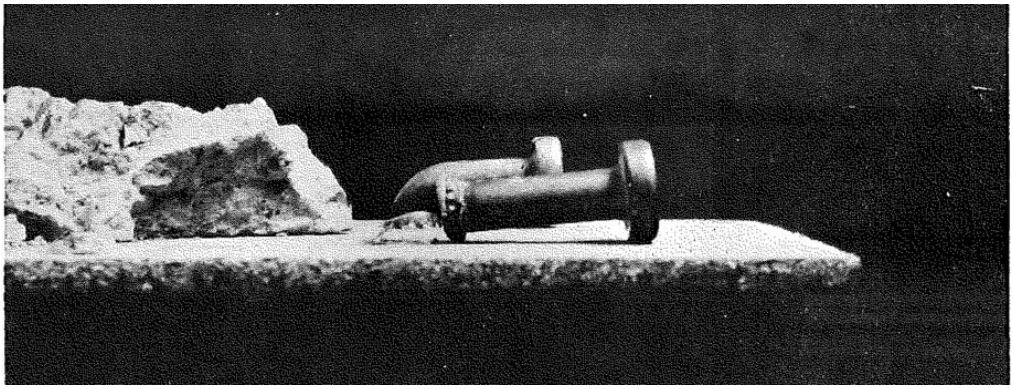

Figure 2-7: A failed and intact stud from King et al. (1965).

2.3.2 Fatigue Design Provisions

Prior to the introduction of the 2000 edition of the Canadian Highway Bridge Design Code (CHBDC, CSA S6-00), the applicable code in Ontario was the 1991 edition of the Ontario Highway Bridge Design Code. This code had a fatigue category specifically for welded shear studs, called “Stress Category y” (OHBDC, 1991). The category was based on the recommendations of Slutter and Fisher, although it was a log-log curve and included limiting stress range of 65 MPa. This limit was called the Constant Amplitude Fatigue Limit (CAFL), because it was thought that stresses below this limit were unlikely to cause fatigue damage. CSA S6-00 superseded this, adopting the identical provision to the AASHTO Load and Resistance Factor Design (LRFD) Bridge Design Specifications, which directly used Slutter and Fisher’s fatigue testing results to form the requirement for the fatigue resistance of stud shear connectors (CSA S6-00, Cl. 10.17.2.6). The semi-log (linear S vs. log(N)) fatigue curve used for shear stud design was not consistent with other fatigue details, which all used the same log-log (linear log(S) vs. log(N)) curve, shifted up or down depending on the severity of the detail. Additionally, a CAFL of 48 MPa was now specified.

The 2006 version of CSA S6 maintained the same provision, with new consideration for the fact that some stress cycles would exceed the CAFL, due to the variable nature of the true highway traffic loading and the fact that the equivalent truck weight being used for damage calculations was approximately one half of the

maximum truck weight. As such, an effective Variable Amplitude Fatigue Limit (VAFL) was introduced, although it was not explicitly called this, of 24 MPa, for infinite life design.

In 2010, a supplement to the 2006 publication of the CSA S6 (CSA S6S1-10) reworked the fatigue requirement for studs to be consistent with that of other fatigue details according to an investigation by Zhang (2007), (CSA, 2010). In this investigation, a regression analysis was performed on a large collection of push tests from many researchers. A log-log relationship was found closely approximating an existing fatigue category (detail Category D). The endurance limit for the detail did not change, since Category D had the same constant amplitude fatigue limit as the value previously used for studs (48 MPa, which resulted in an effective VAFL of 24 MPa when considering variable amplitude effects). Zhang also performed regression analysis on beam tests, but too few had been performed and published in the literature to draw any conclusions. The current code equation remains unchanged since 2010 and is given by Equation 2-7, taking a reorganized form of Equation 2-6 (CSA S6, 2014, Clause 10.17.2.3).

Equation 2-7

$$\Delta\tau = \left(\frac{C}{N}\right)^{\frac{1}{m}}$$

For Detail Category D in the Canadian code, C in Equation 2-7 is given as $721 \cdot 10^9$ and m is 3. The units of $\Delta\tau$ are MPa. The AASHTO design curve remains unchanged since the 1960s (AASHTO, 2014, Cl. 6.10.10.2), and still follows the log-linear form of Equation 2-4. The CSA, AASHTO, and Eurocode fatigue curves are shown in Figure 2-8 along with a cloud of data from over 250 push tests.

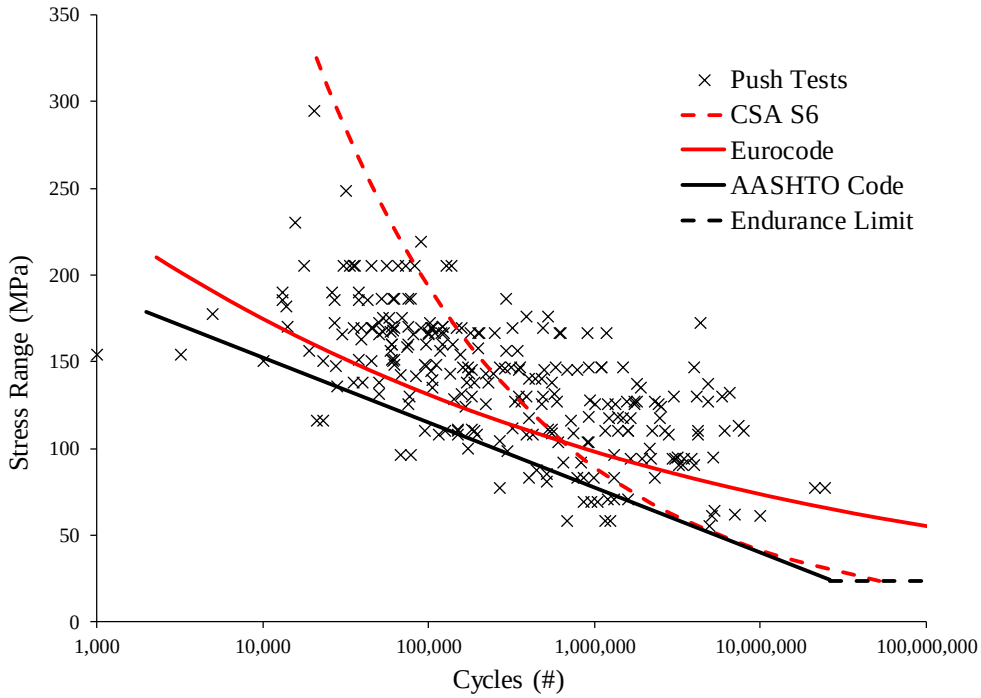

Figure 2-8: Code comparison of existing fatigue design curves.

It can be seen in Figure 2-8 that there is a very high degree of variability in the *S-N* data and in the design curves. The American design curve is the most conservative of the three, while the Canadian curve does not appear conservative at higher stress ranges. The majority of bridges, however, are designed at the endurance limit, which for USA and Canada is encountered for any bridge that expects more than 50 million loading cycles over its service life. Note that the *S-N* data cloud has very limited information at this long-life peripheral region. The design codes all make the assumption that repeated loading does not lessen the static strength of a stud. If the static strength of a stud decreases as a result of cyclic loading, fatigue and static strength checks should arguably not be independent from each other.

2.4 Studs in Grouted Shear Pockets

Several National Cooperative Highway Research Program (NCHRP) reports have been integral to the body of research surrounding the rapid replacement of bridge decks (Tadros, & Baishya, 1998) and the use of pocketed stud groups (Badie, Morgan Girgis, Tadros, & Nguyen, 2010) (Badie & Tadros, 2008). Tadros and Badie conducted push tests and beam tests with the goal of showing that the stud spacing limit for grouped shear studs could be doubled (they proposed that 1220 mm or 48 inches is adequate), and that fatigue design rules need not be changed for the case of grouped studs. With the larger pocket spacings, they used larger than average studs (31.8 mm diameter), to shear connect two full-scale composite beams. The beam slabs were 200 mm thick and 1200 mm wide, mounted on 18 x 119 wide flange beams (18 inches deep and 119 lb/ft) spanning 9.8 m. A total of 62 studs were used with 16 clusters on one beam (610 mm spacing) and 8 clusters on the other (1220 mm spacing). The beams were subjected to CA loading at midspan of two million cycles at 2 Hz, followed by static loading until failure.

It was concluded, based on observations between the beams and the fatigue design procedures used, that a pocket spacing of 1220 mm did not negatively affect the performance of the beam, and that regular stud fatigue design procedures may be used for precast applications. No fatigue cracks were observed in the studs upon panel removal and inspection. The larger studs were recommended for bridge designers because they reduce the number of studs required to be welded by 50% (they have twice the area of conventional 22.2 mm studs) and they reduce the size and number of shear pockets required; fewer shear pockets means less grouting, less labour, and gives the design engineer more flexibility in the layout out of panel reinforcement (Badie et al., 2010).

The Ministry of Transportation of Ontario (MTO), an owner of many bridges with prefabricated deck systems, also conducted an experimental program to study the effects of shear stud clusters in composite girder design (Huh, Lam, & Tharmabala, 2010). Huh et al. assembled six composite beams with shear stud clusters spaced at 400 mm and 600 mm, in addition to a control specimen with conventional uniformly spaced studs. The composite beam specimens had slabs that were 75 mm thick and 600 mm wide, mounted on W150 x 22 beams with a span of 4 m. Fatigue loading was applied to four of the six beams, but this loading was not meant to fail the connectors. Rather, the goal was to show that no significant loss of strength or stiffness would result. Constant amplitude cyclic loading was applied at a rate of 0.8 Hz for a total of 3

million cycles, and readings were gathered from strain gauges on the beams and a midspan deflection transducer. Based on the results from six composite beam tests and eight push tests, Huh et al. concluded that shear stud clusters can provide full composite action and stud clusters have little impact on the fatigue and ultimate strength characteristics of a composite system (2010).

Until recently, Canadian and American bridge codes limited the spacing of stud connectors in precast applications to the same standard as CIP construction at 610 mm or 24 inches. Recognizing the work of researchers including Badie et al. (2010) and Larose (2006), this limit has been doubled. The research presented on the fatigue of studs in precast panel shear pockets seems to have been motivated primarily by the idea of validating existing CIP design rules for precast applications.

2.5 High Strength Bolt Connectors

Research into the fatigue of high strength bolt connections has been minimal compared to that of stud shear connectors. Furthermore, while some investigators have examined the effects of repeated loading and the resulting decrease in static strength, very few have tested beam specimens with bolted connections in fatigue until failure. Welds are a primary cause of fatigue failures in metal structures, owing to the comparably high degree of surface imperfection that is present in a weld, in comparison with a rolled structural steel member. Welds also tend to coincide with stress concentrations due to local changes in geometry, and introduce unfavourable residual stresses at the surface of the welded component. These reasons, combined with the beneficial effect of bolt pretensioning (which minimizes the stress range experienced by a bolt), contribute to the expectation that bolted connections perform better in fatigue than welded shear connectors.

In 1979, Rabbat and Hanson investigated the performance of through-bolt connections between precast concrete deck slabs and supporting girders (1973). They used the shear-friction procedure of the 1971 American Concrete Institute building code to estimate the ultimate capacity of the connection. This shear-friction procedure is very similar to that found in the current CSA concrete code (A23.3, 2014) referred to as interface shear transfer. Static tests had been performed on bolted connections prior to 1979, but no data existed concerning fatigue, and specifically high-cycle fatigue. Rabbat and Hanson were performing their research for the Metropolitan Atlanta Rapid Transit Authority, and were looking for a connection detail for an elevated transit structure that would accelerate construction while minimizing traffic disruptions. Using a modified push test, steel-precast bolted connections were cycled for 2 million and 5 million cycles at 3 different load ranges. The specimen geometry was quite different from a classic through-bolt connection in that grout was used to fill the voids around the bolts, and a steel plate was used for the bolts to anchor to on the deck side. It was confirmed that cyclic loading reduced the strength of the bolts, in some cases as much as 14%. Pretensioning of the bolts tended to minimize fatigue effects. No fatigue prediction models were developed because the experiment was designed to determine residual strength, rather than fatigue endurance.

Dedic and Klaiber performed push tests on bolted connections in 1984 for the purpose of showing their value in rehabilitation work. Although they did not perform fatigue testing, they did obtain connector load versus slip (load-slip) curves and demonstrated that the bolts exhibited similar strengths and stiffness compared to conventional studs. The geometry of their researched connectors is shown in Figure 2-9.

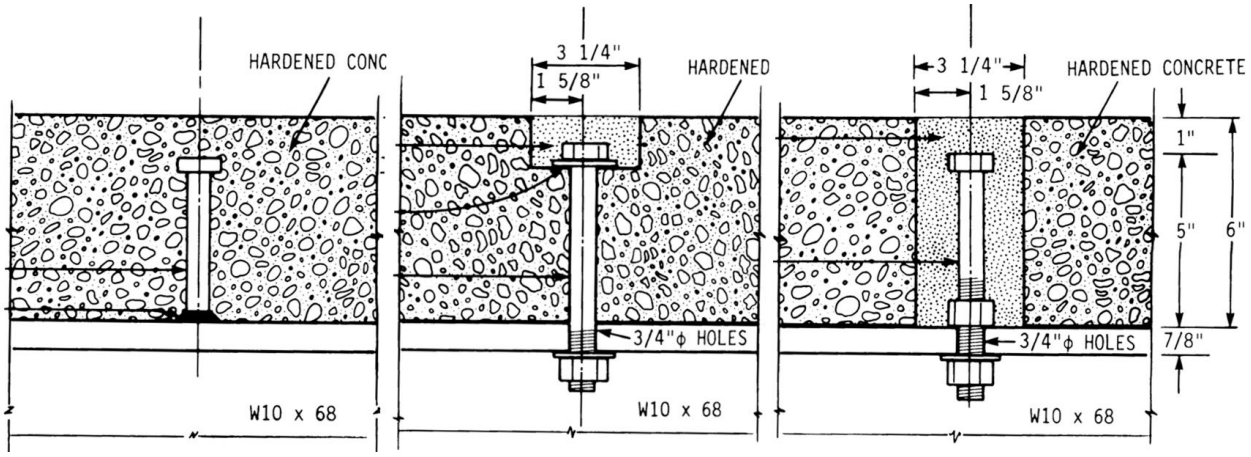

Figure 2-9: Details of connections investigated by Dedic and Klaiber (1984).

The through-bolt connection used by Dedic and Klaiber was epoxied (between the bolt shaft and the concrete), which may be the reason for reduced observed slip compared to others (to be shown). These tests were some of the first to establish the general shape of the load-slip curves for bolted connections; typically the initial stiffness is very high (higher than a stud), but after slip the stiffness is substantially reduced. Bolted connections have higher ultimate strengths than stud connections for the same steel area, and both generally exhibit significant ductility. Dedic and Klaiber concluded that ultimate strength formulas used for welded studs at the time could be used to estimate the capacity of high strength bolt connectors, and that bolted connections are well suited for rehabilitation work particularly where steel properties are unknown and welding is not an option (1984).

In addition to their experiments on the effect of stud clusters, the MTO also performed beam tests on the through-bolt connection system. Citing the success of implementing the grouted shear stud system, but also the drawbacks of on-site grouting, shear stud welding, and difficult slab replacement, Au, Lam, and Tharmabala studied the ability of the bolted connection detail to develop composite action, to withstand cyclic loading, and to perform at comparably high ultimate loads in flexure (2010). Two 4200 mm long reduced-scale beams (the same geometry as the specimens in Section 2.4) were tested, each with 38 pairs of 12 mm diameter A325 bolts at 110 mm spacing. Results from these experiments were compared to the control specimen with conventional stud shear connectors. Hairline cracks were reported on one of these specimens as a result of bolt tightening. The group noted that the specimen with these cracks had 38 MPa concrete, and the other specimen with 48 MPa concrete did not exhibit the same cracking. 3 million cycles of monotonic midspan fatigue loading were applied to each beam specimen. Au et al. found that although the level of composite action achieved were not as strong as conventional composite construction, it was “reliable and effective”. According to their tests, the fatigue loading did not affect the performance of the

system, and the ultimate flexural resistance exceeded the theoretical CSA code value (CSA S6, 2014). They recommended further testing to verify the results of their study.

Kwon, Engelhardt, and Klingner extensively studied the behaviour of post-installed shear connectors (2009, 2010). They examined the viability of using through-bolts, as well as embedded double-nut bolts to strengthen existing non-composite bridges by developing composite action. Full-scale beam tests, direct shear tests, and field implementations were used to assess the performance of the bolted connections.

The test setup shown in Figure 2-10 was used to test fatigue and static loading behaviour. Direct shear tests were performed on 22.2 mm bolt connectors yielding load-slip curves as well as fatigue *S-N* data points. The tests did not include load reversal and did not result in fatigue failures of the through bolt and embedded bolt connections despite 5 million cycles at stress ranges of 240 MPa and 310 MPa, respectively. These stress values are far higher than the welded shear stud AASHTO equation predicted (AASHTO, 2014). This is shown in Figure 2-11, in which the bolted fatigue runouts are superimposed on the chart from Section 2.3.2 showing push test of stud connectors and code equation *S-N* curves. Note that when bolt data is compared to stud data on the basis of stress, a factor of 0.75 is applied to the nominal bolt diameter to account for the reduction in area due to threading. As a result, a high strength bolt of the same diameter as a stud will have more strength, but not as much as the stress comparison suggests.

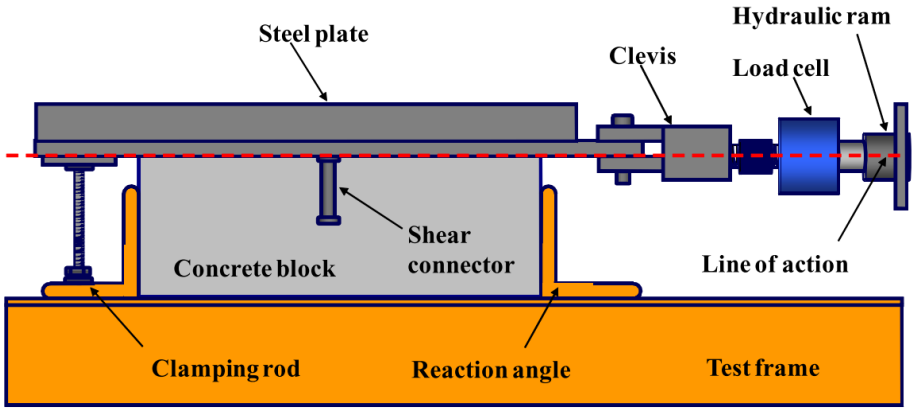

Figure 2-10: Test setup for single connector strength by Kwon et al. (2010).

Chen performed static push tests on through-bolt specimens at the University of Waterloo (UW) in 2012 to investigate the effects of various surface treatments at the steel-concrete interface (Chen, 2013). Although the surface treatments did not increase the friction forces and thus the connection strength as hoped, the load-slip curves obtained can be compared to those from Kwon et al., particularly for the base condition of no surface treatment. Figure 2-12 allows for stiffness and ductility comparison between the three connection types of different diameters. It is apparent that for the through-bolt connection slip (and ductility) is highly dependent on the bolt hole tolerances. Recall the 0.75 thread factor when comparing bolt and stud stresses.

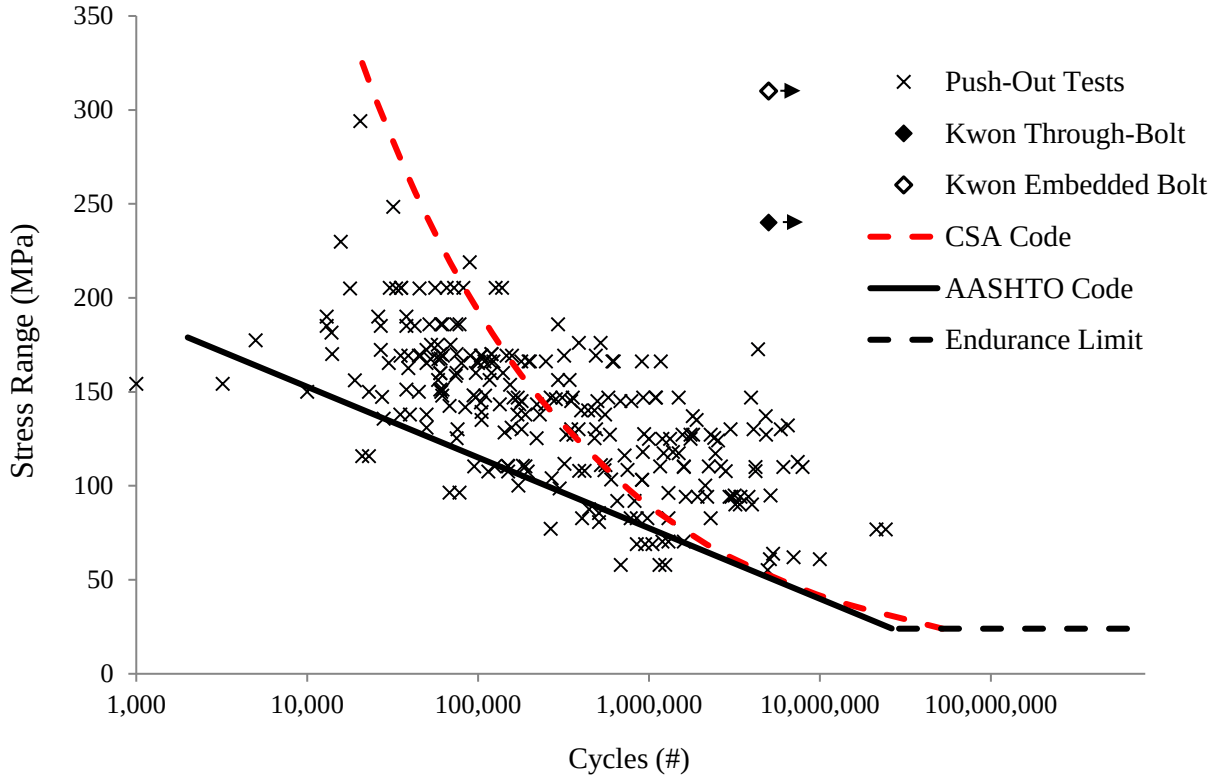

Figure 2-11: Kwon et al. through and embedded bolts compared to studs (2010).

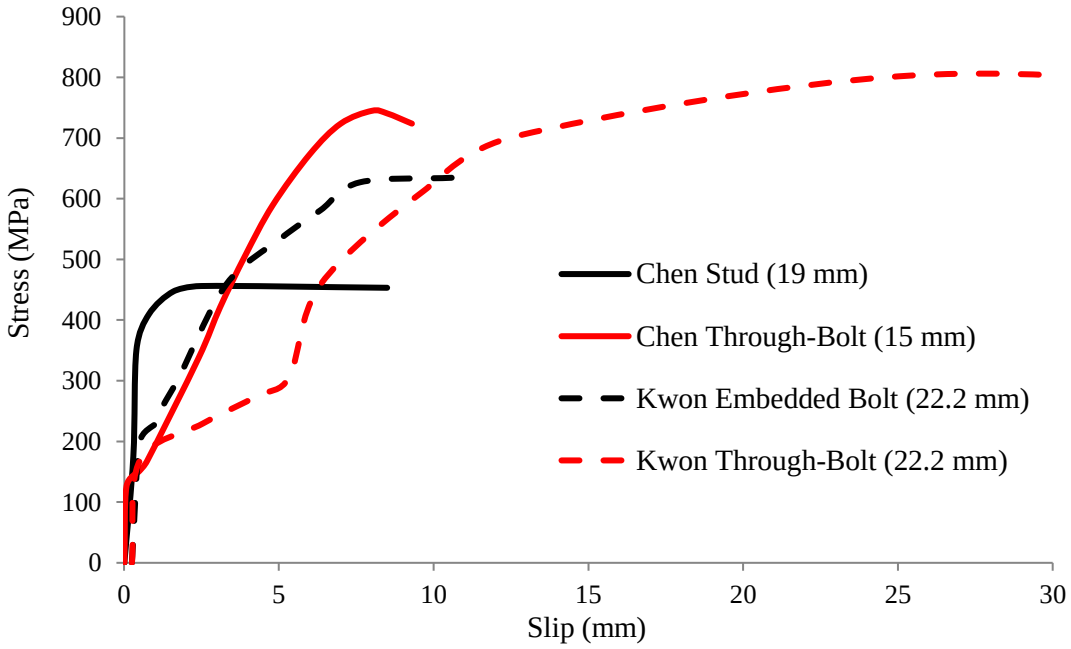

Figure 2-12: Load vs slip curves from Kwon (2010) and Chen (2013).

There are currently no code provisions for using high strength bolts in lieu of stud shear connectors in composite bridge construction, although the CSA S6 Code Commentary (CSA S6.1, 2010) does mention a successful pilot project conducted in 1977 near Waterloo, Ontario using bolted shear connections. The

bridge referred to is the three span, continuous plate girder Conestogo River Bridge, and the bolts used were embedded in the CIP deck (Dorton, Holowka, and King, 1977). Fatigue was found to govern over ULS in design, and the bolts were designed to be slip critical even when subjected to overloads. Currently any bolted connection used in a Canadian bridge must be slip critical, which means that service loads are not expected to move the connection into bearing, but rather the friction in the connection will be sufficient to carry the loads. Additionally, the only bolts permitted to be used are A325 and A490 high strength bolts. 22.2 mm diameter A325 Type 3 weathering steel bolts were used on the Conestogo River Bridge, and push testing was performed to ensure that 5 mm oversize holes would not be detrimental (typically holes are 1/16-inch oversize rather than 3/16-inch, but the extra space was needed to ensure concrete shrinkage would not stress the top flange) (Dorton et al., 1977).

The last project of interest when considering high strength bolts as shear connectors is the Amsterdam Interchange Bridge owned by the New York State Thruway Authority. The state launched a research and development program in 1973 to evaluate the effectiveness of the through-bolt connection for precast bridge decks and used the connections on the bridge on an experimental basis (Issa et al., 1995). Holes were drilled in the panels and through the top flange of the girders to allow fastening. Bolt pretensioning was found to be problematic due to cracking of the panels, much like the panels of Au et al. (2010). This is a challenge in the field that comes as a result of levelling and shimming precast panels atop the girders. In contrast, the embedded bolt detail does not face this problem, as a haunch is more easily accommodated while the grout is being poured into the pockets.

2.6 Fatigue Reliability Analysis of Components and Systems

As a consequence of stochastic processes in nature, no structure, component, or system can be perfectly reliable. Recognizing this, the goal of modern design codes is to have a target level of reliability, recognizing that some probability of failure must be tolerated. The basic reliability problem in the design of structures can be visualized by considering two random variables, R, and Q, representing the resistance of a structure and the load demand, respectively. A third variable may be defined, g, representing the margin of safety, which is given in Equation 2-8 as R minus Q. A component is safe when g is greater than zero, and it fails when g is less than zero.

Equation 2-8 $$g = R - Q$$

The level of safety in any structure may be measured using the reliability index (also called the “safety index”, or “level of safety”), denoted by β. The non-dimensional index is given in Equation 2-9 as the ratio of the mean of g to the standard deviation of g. The reliability index can also be thought of as the number of standard deviations that the mean safety margin falls on the safe side of the design point ($g > 0$). The reliability index is inversely related to the probability of failure, P_f, with the conversion between the two depending on the statistical distributions of R and Q.

Equation 2-9 $$\beta = \frac{\mu_g}{\sigma_g}$$

For the design of new bridges, CSA S6 specifies a lifetime target value of 3.5 (or 1 in 4,300 probability of failure) for the reliability index for those components that will not fail suddenly or will retain post-failure capacity, and the failure of which will not lead to sudden collapse (Hong, Goda, Lam, & Au, 2010). Section 14 of CSA S6 is for the evaluation of structures, and is not to be used for design, but has some further insight into target reliability levels. Figure 2-13 is taken from the CSA S6 Commentary on Clause 14.12.1 and shows a more general view of the approach to safety in CSA S6. Components that lie in a single load path, will fail suddenly, and are uninspectable should have a reliability index of 4.0 (P_f = 1 in 31,500). However, as the consequence of failure of a component or its inspectability and failure mode become less severe, a lower reliability is permitted, all the way down to 2.5 (P_f = 1 in 160). The distinction will continue to be made between design reliability targets and evaluation targets, since these are distinctly separate in CSA S6 (Section 14 separates evaluation from the rest of the code), and AASHTO (evaluation is covered in AASHTO's *Manual for Bridge Evaluation*, or *MBE*, and not in the *LRFD Specifications*).

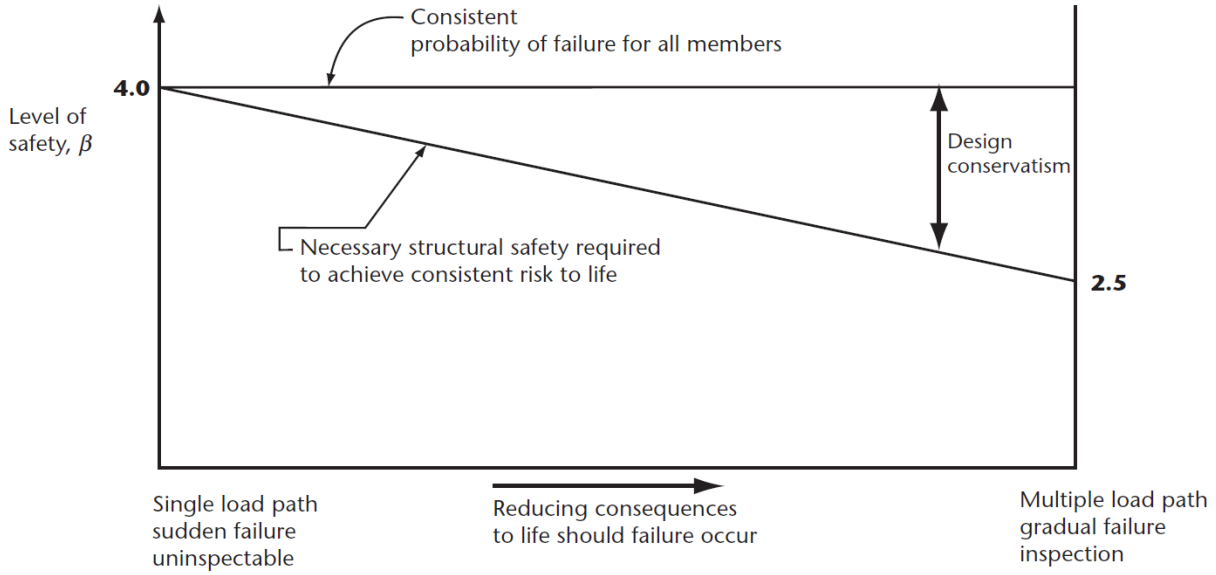

Figure 2-13. Relationship between risk and probability of failure (Figure C14.1, CSA S6 Commentary).

The history of how fatigue critical components came to be designed for two standard deviations from the mean, or 97.7% survivable probability, is unclear. The probability of failure at the outset points to a reliability index less than 2.5, prior to consideration of load as a random variable. It is believed by the author that there has been some influence of performance-based design during the development of current fatigue rules. In a 1985 report entitled "Calibration of Bridge Fatigue Design Model", Nyman and Moses point out that their recommended reliability levels were derived from the average performance of bridges in the USA and Ontario, with the presupposition that the average performance to that time was deemed acceptable and

economical (1985). The Eurocode recommends that the target reliability index for fatigue should be approximately between 1.15 and 3.75 depending on inspectability, repairability, and tolerance for damage for a 70-year bridge design life (similar to the 75-year design life mandated by CSA S6).

Nyman and Moses' comprehensive guide for the consideration of the reliability of fatigue details incorporated uncertainties in vehicular loading, analysis methods, and fatigue life, in order to make recommendations with the goal of having more uniform safety levels and fatigue lives for steel bridges (1985). Key variables included in their uncertainty model were the accuracy of the fatigue damage model (Miner's rule was chosen and assigned a coefficient of variation, or COV, of 15%), the stress range (mean and COV values were obtained for design categories of redundant and nonredundant components, as they were separated at the time), the girder distribution factor (COV of 13%), the impact factor (commonly now referred to as the "Dynamic Load Allowance", assigned a COV of 11%), and the truck volume (Average Daily Truck Traffic, or ADTT, assigned a COV = 10%). Other variables were also considered in their model, although statistical data was not available for all variables. Target safety index values were back-calculated by finding the safety index values from bridges deemed safe and economical at that time. Nyman and Moses found targets of β = 3.90 for redundant spans, and 5.28 for nonredundant spans, although they acknowledged that further study could show these values as being too high (1985).

In a subsequent NCHRP report, Moses, Schilling, and Raju made recommendations for evaluation procedures (1987). They reported that Miner's rule should be taken as accurate and justifiable as a means to convert a variable amplitude stress range into an equivalent constant amplitude range for design and evaluation, and they noted that some methods used an effective fatigue truck to represent typical traffic (something that is commonly done now). It is suggested that lower target reliability levels of 1.0 to 3.0 should be satisfactory for the fatigue evaluation of redundant and nonredundant members, respectively, since failure is less critical in fatigue than in static loading considerations. In referencing the use of a variable amplitude fatigue limit, they suggested conservatively ignoring the limit in reliability analysis (probabilistically, a guarantee cannot be made that any load value will not be surpassed), and they suggested that a slope of m = 3 should be used for *S-N* curves rather than the dual slope model suggested by the European Convention for Constructional Steelwork. By this time it was generally accepted that a practical CAFL exists, but an NCHRP study on variable amplitude loading found that "if any of the stress cycles in a stress spectrum exceed the CAFL, the fatigue life could be predicted by Miner's rule considering all cycles contributed to the damage" (1987). This is something that is still believed to hold true today, as discussed in a review by Baptista, Reis, and Nussbaumer (2017).

It is necessary to know how many cycles a fatigue component will be subjected to when performing a reliability analysis. The ADTT was taken as 2,500 in most studies in the 1980s (Nyman & Moses, 1985) (Moses, Schilling, & Raju, 1987), and it was estimated that some bridges may see well over 100 million stress cycles, but that most bridges see well below this number (closer to about two million). The current edition of CSA S6 specifies that new highway bridges be design to Class A standards, which see an ADTT of 5,000, translating to about 100 million cycles over a 75-year design life. However, the CSA S6

Commentary presents a disclaimer, stating that “forecasts for specific sites may show that actual truck traffic is considerably less than the design value” (2014). For most cases, the passage of a truck may be taken as a single stress range cycle for a fatigue component such as a shear stud. However, short, continuous, and cantilevered spans contain regions where this rule does not hold true (as it is the individual axles that are causing the significant fatigue cycles), and this must be taken into account.

Assessing the reliability of shear connectors can be done at the connector level or the system level. The most basic reliability analysis, a connector level analysis, involves quantifying the likelihood of failure for an individual connector. One such probabilistic analysis was carried out recently by Ovuoba and Prinz (2015) from the University of Arkansas. Specific emphasis was given to better define the CAFL, since this often governs stud design in bridges with moderate to high traffic demands.

Six composite push test specimens were tested with stresses ranging from 30 to 60 MPa, resulting in one specimen failure at approximately 13 million cycles (60 MPa), and five runouts with cycle counts as high as 31 million. A random fatigue limit model was applied to the obtained data, as well as other data from literature, using the statistical method called the maximum likelihood estimation (MLE) method. This method involves solving for population parameters (mean and standard deviation) to maximize the joint probability of predicting failure at all data points. Ovuoba and Prinz found that a CAFL of 44.8 MPa was predicted by the over one hundred push tests considered in the analysis (2015). This is compared to the value of 48 MPa that is presently used in design (CSA S6, 2014), (AASHTO, 2014). They recommended changing the existing AASHTO curve to be more similar to other fatigue details (CSA S6 did this in the 2010 revision), and proposed a new category specifically for studs. The category they suggested would be called D’, and would have a slope of $m = 4$, compared to $m = 3$ for most steel fatigue details. Even though the statistical analysis was completed, a mean confidence level of 50% was settled upon for their recommendation, citing the inherently conservative nature of the fatigue data resulting from push tests.

3 EXPERIMENT DESCRIPTION

An experimental program was conducted as the backbone of the research project. Specimens were carefully designed to accomplish several of the project objectives, including: obtaining *S-N* fatigue failure data for studs and high strength bolt shear connectors, investigating the effects of precast construction on the fatigue of studs in grouted shear pockets, and investigating bolted shear connection behaviour. Eighteen specimens were fabricated, instrumented, and tested including six specimens with welded studs in CIP concrete (CS), six with welded studs in grouted shear pockets (PS), three with high strength through-bolts (TB), and three with high strength bolts embedded in grouted shear pockets (EB) (see Figure 1-5 for reference). Each specimen type will now be described, followed by a general description of specimen fabrication, instrumentation, loading procedures, and the overall test matrix.

3.1 Specimen Material & Geometry

3.1.1 Welded Shear Stud Specimens

A total of twelve composite beams with shear studs were tested, six of which were constructed using traditional CIP methods (CS), and six that were constructed using precast slabs (PS). Each beam was simply supported with a 3,000 mm span and consisted of a W250x49 steel section (350W steel) connected to a 600 mm wide, 125 mm thick, 40 MPa concrete slab as shown in Figure 3-1 and Figure 3-2. Loading was applied by a spreader beam at points A and B, which were located 500 mm and 1,000 mm from the west support, respectively. Web stiffeners were provided at the supports to prevent buckling.

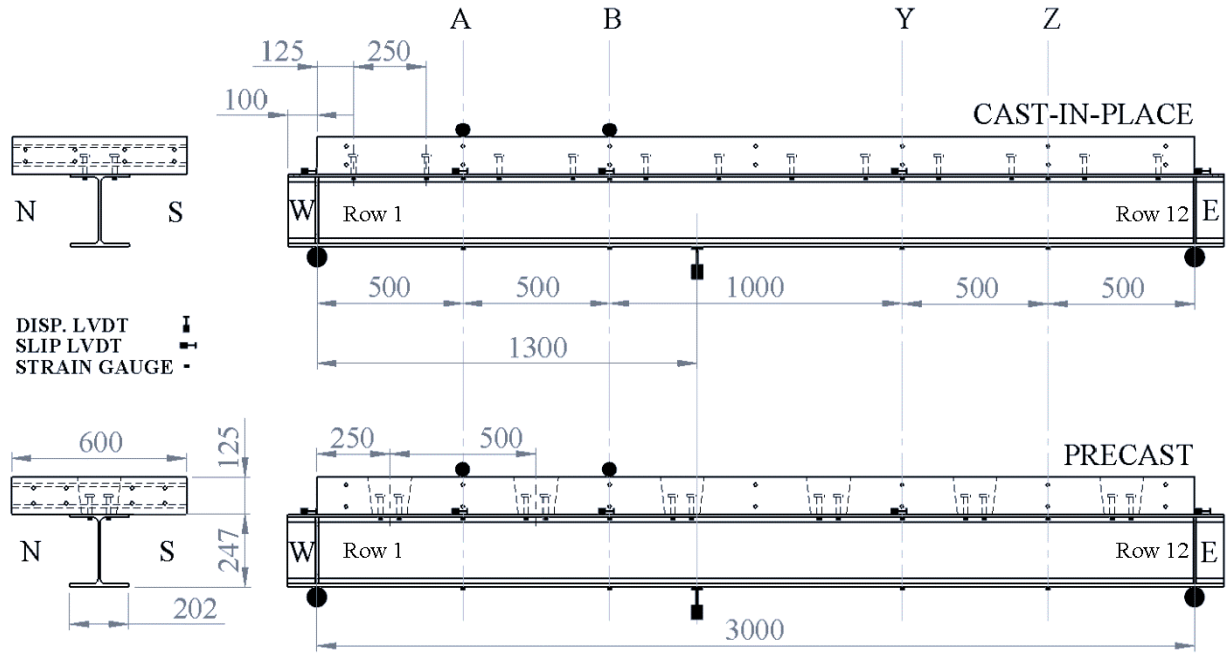

Figure 3-1. CS and PS beam specimen geometry and layout (dimensions in mm).

Figure 3-2. PS specimen during fatigue testing.

The shear connection between each steel beam and concrete slab was developed using a total of twenty-four Type B 16 mm (5/8”) diameter, 37 mm tall, Nelson headed shear studs, arc-welded to the top flange of each specimen using a typical stud gun. Type B studs have a tensile strength of 415 MPa and a yield strength of 345 MPa. For the CS specimens, the studs were welded in pairs and spaced at 250 mm, and for the precast specimens six stud clusters, consisting of four studs each, were spaced at 500 mm. The spacing of the studs within the clusters was 64 mm in both the longitudinal and transverse directions. A high performance, high early strength, low shrinkage, pre-packaged concrete was placed in the tapered pockets to create the shear connection in the PS specimens. The rapid hardening concrete product, King HP-S10 mix, has been previously specified by the MTO for infill strips and shear key pockets in prefabricated bridges and has a specified 28-day compressive strength of 60 MPa.

The deck reinforcement was designed according to CSA S6 (2014), which requires orthogonal reinforcement with a reinforcement ratio of at least 0.3% near the top and bottom surfaces of the deck. Identical upper and lower reinforcement mats were comprised of 400W 10M steel bars. The longitudinal reinforcement consisted of four 3,000 mm bars and the transverse reinforcement consisted of seven 600 mm bars. A cover of 20 mm was provided. Detailed drawings can be found for the welded shear stud specimens in Appendix A of (Porter, 2016).

3.1.2 High Strength Through-Bolt Specimens

The specimen geometry for both bolted specimen types were very similar to the welded shear stud specimens, differing only by their shear connector type and precast slab geometry. High strength through-

bolt (TB) specimens were prepared with the same 600 x 125 x 3,000 mm concrete precast slabs. Holes for twelve rows of two through-bolts were evenly spaced at 250 mm longitudinally, 102 mm apart in the transverse direction, and lined with polyvinyl chloride (PVC) piping with a 25 mm interior diameter. The through-bolts used in the specimens were 16 mm (5/8") diameter, ASTM A325 structural bolts (yield and ultimate strengths of 660 and 830 MPa, respectively). These bolts passed through the 25 mm PVC sleeves and through 17.5 mm (11/16") holes drilled in the top flange of the steel beams. The oversized PVC pipe diameter was selected as a tolerance control measure, permitting some variability in the location of the holes in the concrete. Steel bearing plates were fabricated and placed between the bolt head and the concrete deck to prevent concrete crushing during bolt pretensioning. The pretensioning procedure will be discussed in Section 3.2. Three configurations of TB specimens evolved during the test procedure, and are shown in Figure 3-3. These configurations arose as attempts to fail the through-bolt connector in fatigue and static loading were made during testing. Further description of these specimens can be found in (Balkos, 2017).

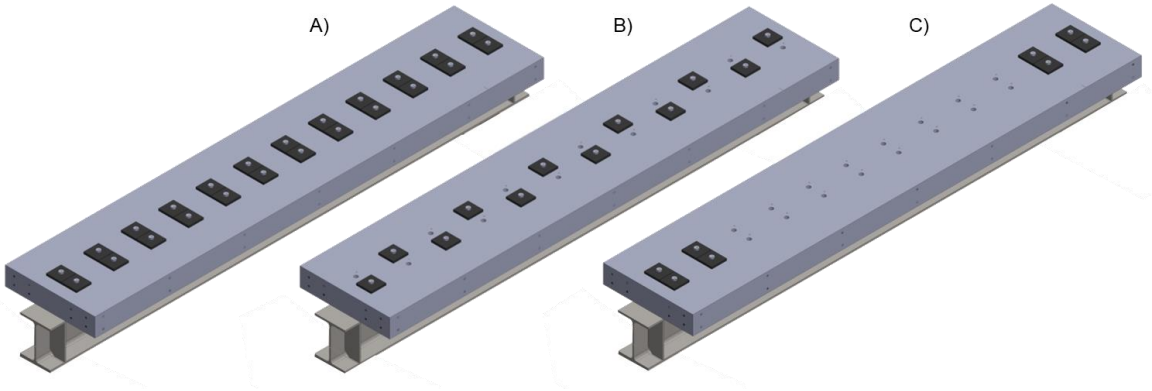

Figure 3-3. TB configurations for Specimens TB1 (A), TB2 (B), and TB3 (C).

3.1.3 Specimens with High Strength Bolts in Grouted Shear Pockets

The fourth and last specimen type fabricated and tested consisted of high strength bolts in grouted shear pockets, or “embedded” high strength bolts (EB). For consistency and ease of comparison with the PS specimens, six grouted shear pockets were chosen (each spaced at 500 mm along the length of the beam), each with a cluster of four 16 mm A325 bolts (5/8”) spaced at 75 mm in both directions. The 75 mm inter-cluster spacing was greater than the 64 mm used with the studs, and was necessary for the bolt washer and nut assembly to avoid contact with the beam fillet on the underside of the top flange. This also necessitated slightly larger grouted shear pockets. In the PS specimens, pockets with a square 120 mm base dimension tapered up to a 150 mm dimension at the top of the slab; the EB specimens required a 144 mm base dimension tapered up to 175 mm at the top of the slab.

The drilled holes in the top flange were 22.2 mm (7/8”) in diameter to allow for a 20.6 mm (13/16”) outside diameter thread blocker ring, which was mounted onto the 16 mm bolts between the washers, as shown in Figure 3-4. The thread blocker was a key piece of the assembly, ensuring ease of deconstruction regardless

of the state of slip between the bolt and the steel top flange. A double-nut configuration was used to increase the stiffness of the connectors, replicating the connectors of (Kwon et al., 2010). Direct tension indicator (DTI) washers were used to ensure the proper level of pretension in the bolts. The pre-packaged concrete used to embed the bolts in the pockets was King HP-S10, the same used in the PS specimens. This material will be referred to hereafter as a grouting material because of how it is being used, but it should be noted that the packaging refers to the product as a concrete.

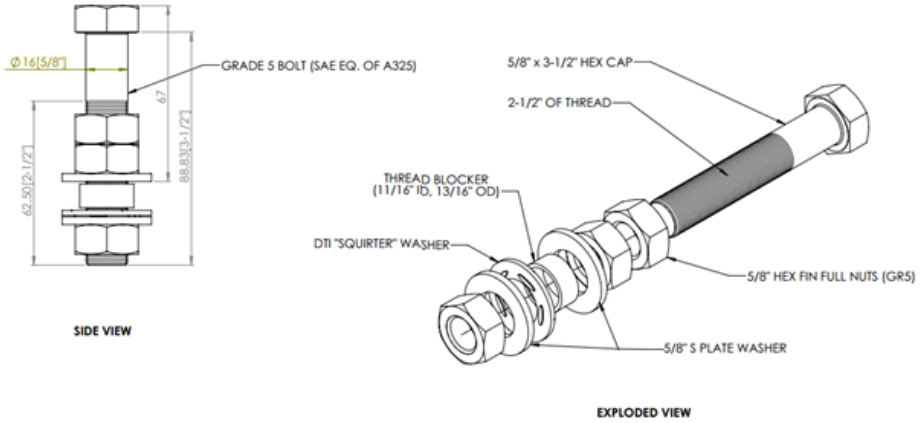

Figure 3-4: Bolt geometry for EB connection.

The nomenclature used in reference to all test specimens for the remainder of this thesis is as follows:

- CIP stud (CS), precast stud (PS), through-bolt (TB), and embedded bolt (EB) specimens;
- The west and east supports correspond to those shown on the left and right of Figure 3-1;
- Connectors are labelled from west to east with the row numbers 1 through 12 (N1, S1 etc.);
- Profiles A, B, M, Y, and Z correspond to cross-sections at 500 mm, 1,000 mm, 1,500 mm, 2,000 mm, and 2,500 mm from the west support.

3.2 Specimen Fabrication

Each specimen type required a unique fabrication process, despite many similarities. A discussion of the general process will be included herein, followed by a description of the unique requirements specific to each specimen type and their potential relevance in the field. The eighteen W250x49 beams were all prepared at UW's Engineering Machine Shop. Lifting holes and bolt holes were drilled in each top flange, and bearing stiffeners were welded at the supports. All formwork preparation and concrete casting was completed at UW, with concrete provided by a local ready-mix supplier, Hogg Concrete. Casting took place in three batches of six specimens each. The 28-day compressive strengths of cylinders from the three casts were 43, 36, and 35 MPa. Figure 3-5 shows the formwork for half of the welded stud specimens.

Studs were welded by a local metal fabricator, Ball Service Group Inc., with a typical stud gun. All procedures specified by CSA W59 (Welded Structural Construction, 2013) were followed, including standard bend tests to verify ductility at the start of the project. Fabrication of the CS specimens was completed after casting

and formwork stripping, while the other three specimen types required the additional step of mounting the precast panels onto the beams. For the PS and EB specimens, precast slabs were lifted, placed, and aligned onto the prepared beams prior to the mixing and placement of grout into the shear pockets. The HP-S10 rapid hardening grout was mixed using a small batch mechanical lab mixer. Tested cylinders gave 12-hour and 28-day compressive strengths of approximately 20 MPa and 60 MPa, respectively.

Figure 3-5: Precast formwork (foreground), and CIP formwork (background) for the stud specimens.

Bolted specimens required a greater effort to assemble than their stud connector counterparts. For the TB specimens, accurate positioning of the holes in the concrete decks proved to be a significant challenge. A plywood template identifying the hole locations was created to reduce tolerance issues. This template was used to mark the bolt hole locations on both the formwork and the steel beams. The PVC piping was fastened to the formwork at the intended locations of the through-bolts prior to casting. In order to fix the sleeve locations, a fender washer and hex nut assembly was installed at the top end of a threaded rod, which passed through the PVC sleeve and was anchored to the formwork with a T-nut (see Figure 3-6).

For both the TB and EB specimens, pretensioning of the bolts had to be completed until the bolts had a preload of 70% of their minimum tensile strength. This is mandated by CSA S6 (2014),and is particularly important for slip critical connections. For 16 mm diameter A325 bolts, this corresponds to a load of 85 kN. Direct tension indicating washers were used in combination with a calibrated torque wrench to verify this pretension. Specific information regarding slump and air tests, the concrete casting and curing process, and other elements not included herein can be found in (Porter, 2016) and (Balkos, 2017).

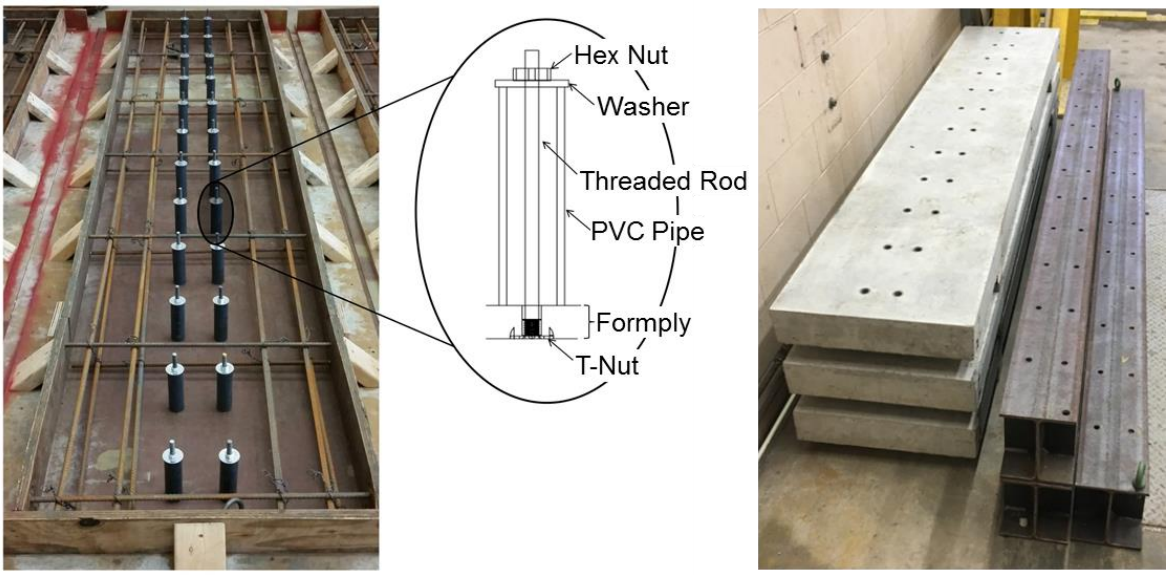

Figure 3-6: Formwork for TB specimens (left), and cast slabs and beams (right) (Balkos, 2017).

3.3 Specimen Instrumentation

The primary instrumentation goal for the stud specimens was to capture the progression of stud failure throughout the test and to collect data points that could be overlaid on top of existing *S-N* data to compare to previous tests from the literature. Studs could not be instrumented directly with strain gauges without the gauges being damaged during loading or impeding the shear connection itself, and visual inspection of studs could only take place afterwards during a specimen autopsy, at which time the specimen was deconstructed. The goal of the instrumentation on the bolted specimens was similar, although observing general behaviour such as slip and deflection was viewed as more important than detecting fatigue failures since these were not necessarily expected.

Specimens were instrumented with a combination of strain gauges and linear variable displacement transducers (LVDTs). “Profile” strain gauges were used at profiles A, B, Y, and Z (and in some cases a fifth profile in the middle of the beam, “M”), to gain information about the slab force at each of these profiles. The profile gauges themselves were mounted on the bottom of both the top and bottom flanges, and simple beam theory was later used to calculate the resultant tensile force in the steel section, and corresponding equal compressive force in the slab. These profile gauges were essential for verifying connector degradation throughout tests, since the force is the slab is primarily developed through connector shear forces (with some influence from friction at the steel-concrete interface). The other type of strain gauge, used only on stud connector specimens, was a “local distortion” strain gauge. Originally used by King et al. (1965), these gauges were placed beneath the studs on the bottom of the top flange of the steel beam and allowed for detection of fatigue failure (Porter, 2016). Since the placement of these gauges largely affected the magnitude of the strain readings, only the trend of the data was used in formulating the failure criterion, which was then used to determine the fatigue life of each stud.

To capture the interfacial slip behaviour of the beams during fatigue testing, a set of five LVDTs were positioned at each of the beam ends (W and E) and at profiles A, B, and Y. An additional LVDT was positioned 1,300 mm from the west support on the underside of the bottom flange to measure maximum deflection and observe any loss of stiffness that would occur as a result of shear connection degradation. Figure 3-7 shows the location and type of instrumentation used on the stud and bolted specimens. Minor variations in instrumentation existed throughout the testing. More instrumentation was provided on the through-bolt specimens, but will not be discussed in this thesis because the resulting data were not relevant. More information can be found in (Balkos, 2017).

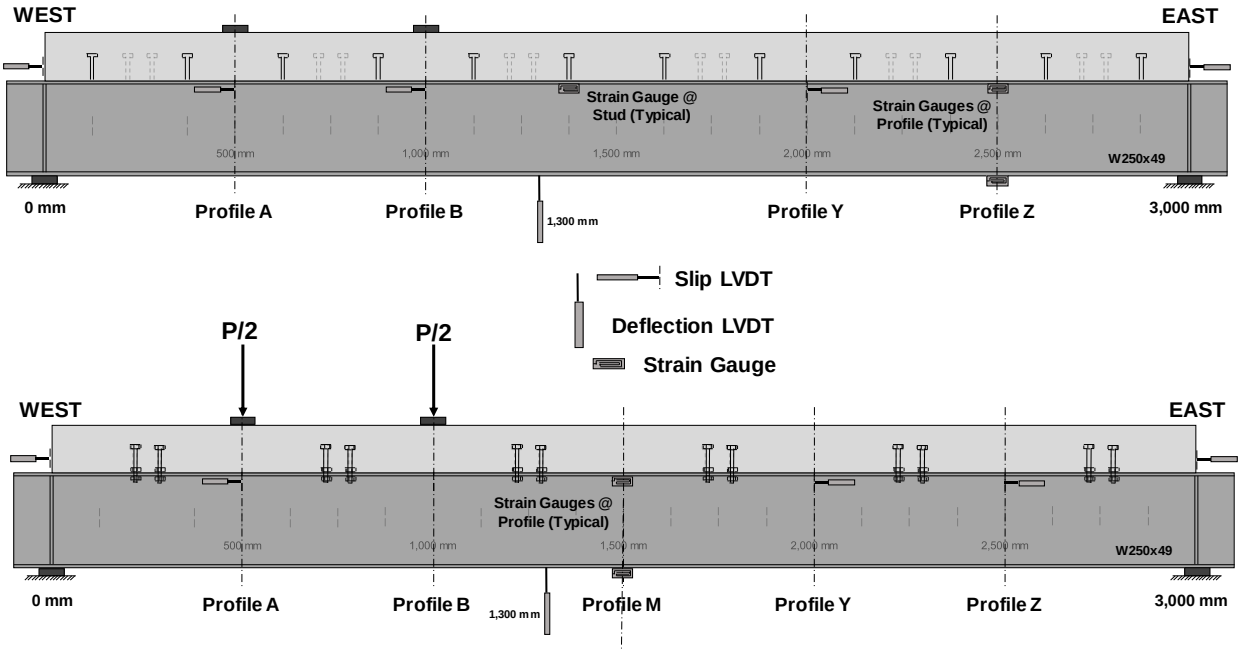

Figure 3-7: Beam test specimen instrumentation for the stud and bolt specimens.

Bolt slip behaviour in embedded bolted specimens was monitored with a low technology instrumentation solution. The nut and washer assembly was spray painted orange prior to the application of cyclic loading, so that slip could be detected by the presence of crescent shaped areas absent of paint, or areas on the leading edge of the slip where paint was damaged. This is shown in Figure 3-8.

Figure 3-8: Spray painting of the embedded bolts for slip detection.

3.4 Loading and Test Matrix

Most fatigue testing on shear connectors reported in the literature to date has been performed under constant amplitude (CA) loading. The effects of connector stress and slip during infrequent overload cycles (due to very heavy trucks or convoys for example) on fatigue performance may be significant, particularly for the case of a bolted connection that may slip under overload and would not have slipped under CA loading. For this reason, a variable amplitude (VA) loading history was used for the fatigue testing in the current research program, simulating typical in-service loading for a bridge subjected to Ontario highway truck traffic. The foundation of the VA loading history used in this study was data collected by the Ministry of Transportation Ontario (MTO) in 1995. This study contained the weights of 10,198 trucks that were randomly selected while traveling on the Provincial highway network. The results from this survey are presented in the form of a histogram in Figure 3-9 (left). These data were randomized to formulate a VA load-history. A segment of the first 25 cycles within this history is presented in Figure 3-9 (right). The load-history was scaled, and the Palmgren-Miner's linear damage accumulation rule was used to find the equivalent CA loading.

Unfortunately, only the stud specimens were able to be tested under the VA loading. This was in large part due to the equipment available in the laboratory, as well as the higher strengths of the bolts when compared to studs; the capacity of the test frame used to load the specimens must be approximately twice as high for VA loading to cause an equivalent amount of damage as compared to the CA case. The test frame used to apply specimen loading was a 500 kN capacity frame at the UW Structures Laboratory.

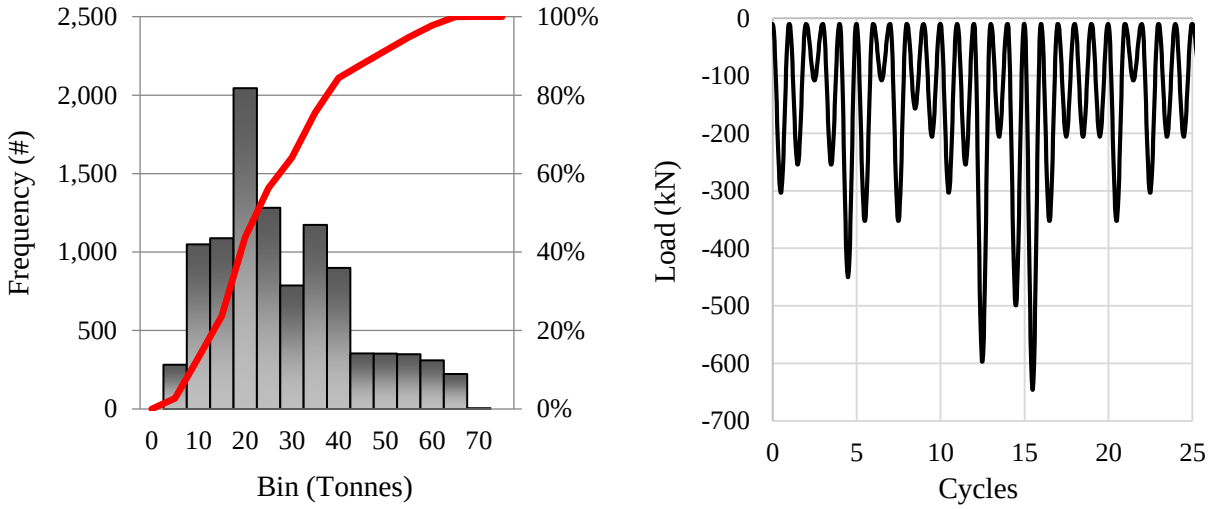

Figure 3-9: 1995 MTO truck data (L), VA loading history used in this study (R).

The test setup employed two-point loading, offset to create a varying interface shear profile along the beam span. This shear diagram dictated where connector failures would begin, allowing for careful monitoring of the critical area (the west end of the beam). As shown in Figure 3-10, the four connectors on the west end of the beam experienced three times the shear loading as all other connectors (Equation 2-5), the elastic shear flow equation, shows that the shear stress is directly proportional to the transverse shear value.

Fatigue loading frequency fatigue varied between 0.5 and 4 Hz, depending on the load value and specimen type. Static loading was performed at the start, at 1x and at 10x the theoretical fatigue life of each specimen for the stud specimens, and on a periodic schedule for the bolted specimens (no theoretical fatigue life could be calculated for these). A load of 200 kN was selected as a standard load for comparison purposes, and all static tests were performed to this value, which corresponds to an elastically calculation theoretical stress of 291 MPa for the four critical connectors on the west end of each beam. The initial static loading was intended to break any chemical bond adhering the concrete to the steel top flange during casting (for the CS specimens), and to collect baseline beam response data prior to potential cyclic loading damage.

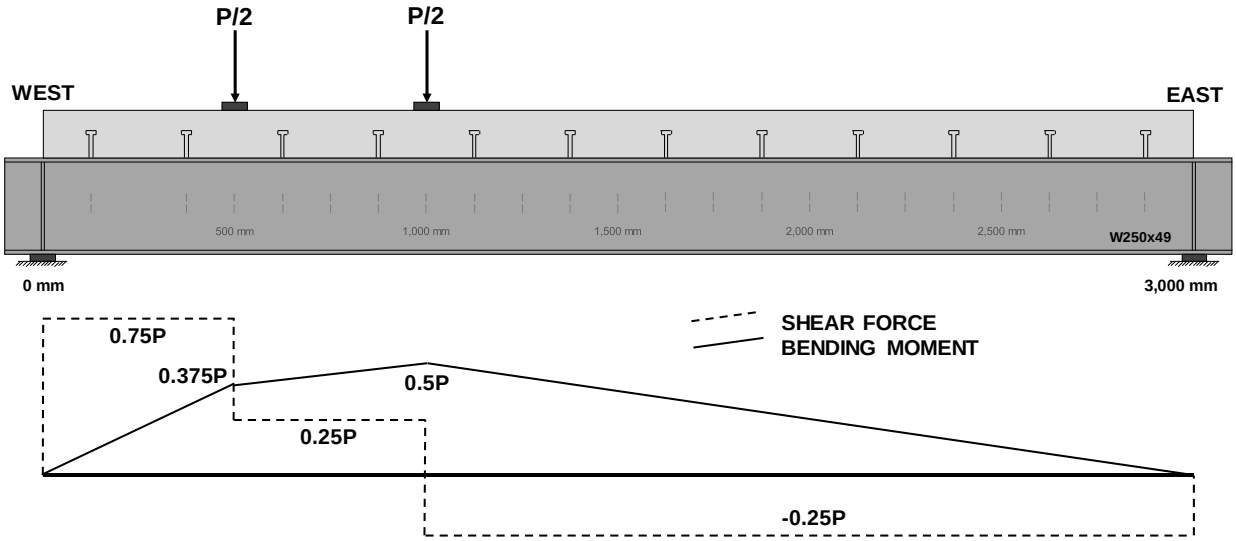

Figure 3-10: The two-point offset loading creates a varying interface shear profile.

The test program matrix for the stud-connected beams is presented in Table 3-1, along with the specimen names. Each specimen is named with two letters corresponding to the specimen type, and a number corresponding to the CA equivalent target stress range for the critical connectors (in MPa). Table 3-2 and Table 3-3 present the test program matrices for the high strength bolt specimens, including specimen names and corresponding test bolt stress ranges. Specimen names for the bolted specimens also include two letters corresponding to the specimen type, but the number that follows simply corresponds to the testing order. It should be kept in mind that the stress values shown in each table are not necessarily the actual stresses experienced by the connectors, since factors such as friction and partial composite interaction are at work in the composite beams. This is particularly true for the TB specimens, which transfer shear entirely through friction prior to connector slip, and feature a low-stiffness connection due to removed connectors in the case of TB2 and TB3 (see Figure 3-3). More information about specifics pertaining to loading and testing procedures may be found in (Porter, 2016) and (Balkos, 2017).

Table 3-1: Test program matrix for stud-connected beams.

CA Equivalent Stud Shear Stress Range (MPa)		Specimen Name	
Stud Rows 1-2	Stud Rows 3-12	Precast Stud (PS)	CIP Stud (CS)
67	22	PS067	CS067
100	33	PS100	CS100
120	40	PS120	CS120
140	47	PS140	CS140
200	67	PS200	CS200
300	100	PS300	CS300

Table 3-2: Test program matrix for high strength through-bolt specimens.

Bolt Shear Stress Range (MPa)		Specimen Name
Bolt Rows 1-2	Bolt Rows 3-12	Through Bolt (TB)
350	117	TB1
1,050	350	TB2
Ultimate Strength Test		TB3

Table 3-3: Test program matrix for specimens with high strength bolts in grouted shear pockets.

Bolt Shear Stress Range (MPa)		Specimen Name
Bolt Rows 1-2	Bolt Rows 3-12	Embedded Bolt (EB)
582	194	EB1
388	129	EB2
485	162	EB3

4 EXPERIMENTAL RESULTS AND DISCUSSION

Chapter 4 presents the results from the experimental beam testing program. Results from periodic static tests are discussed first, including raw data captured such as load, deflection, and slip data, as well as results calculated from sensor output, including strain profiles and slab forces. Static test comparisons are made between all specimen types. Following this, fatigue data are presented, with particular emphasis on the fatigue of stud specimens (CS and PS). Finally, specimen autopsies will be described and discussed. The fatigue failure definition is addressed as it is an issue with important implications. This definition requires consideration of strain gauge data in combination with autopsy observations and, consequently, the full discussion takes place near the end of the chapter.

In total, seventeen of eighteen specimens were tested under cyclic loading from October 2015 through to July of 2018. Overall, over 60 studs and 4 embedded bolts failed in fatigue, while no through-bolt failures were observed. As a result of fatigue resilience, the through-bolt specimens were modified and one test was reserved for ultimate strength testing.

4.1 Static Test Data and Results

Static test results are presented alongside theoretically predicted results. These predictions were made using several assumptions, which will be outlined here at the outset. An elastic transformed section analysis was performed on the composite cross-section assuming that plane sections remain plane, and assuming no strain discontinuity at the steel-concrete interface (complete composite interaction). The properties of the transformed cross-section are listed in Table 4-1.

Table 4-1: Transformed cross-section properties.

Property	Symbol (Units)	Value
Modular Ratio	n	7.2
Top to Centroid	y (mm)	129.1
Transformed Moment of Inertia	I_T (mm^4)	2.23 x 10^8
First Moment of Area of the Transformed Slab about the Elastic Neutral Axis of the Transformed Section	Q (mm^3)	6.93 x 10^5

The assumption of complete composite interaction is known to be false, since all connector types tested were mechanical connectors, requiring deformation to provide shear transfer. Furthermore, calculations show that a total of 48 studs would be required on the beam to develop the full flexural capacity of the cross-section at midspan; considering only 24 were provided, the beam would have a 50% shear connection in applications with typical a typical shear span (distance from point of zero to maximum moment). However,

the shear span on the experimental beam was not L/2, but L/3, due to the offset loading configuration used for testing. Therefore, the shear connection on the tested beams was 33.3%.

Theoretical calculations were performed to predict the load-deflection behaviour of the experimental beam in the linear range, the strain profiles at various locations along the beam, the connector and slab forces, as well as the CSA S6 code-predicted connector lifespan in fatigue.

4.1.1 Load-Deflection

The location of maximum deflection was calculated to be at a distance of 1,300 mm from the west support of the beam. The load-deflection results from static tests up to a load of 200 kN are plotted in Figure 4-1 next to theoretical predictions of a fully composite section, the steel beam acting alone, and the 33% shear connection existing on the beams (the latter prediction was completed using a reduced effective transformed moment of inertia as defined in CSA S16, see Porter, 2016). Theoretical predictions shown in the plot include the effects of shear deformation. The specimens shown, PS300, CS140, EB2, and TB1, were chosen because they represented the most typical load-deflection patterns of their respective specimen types. Note that the stud-connected beams were stiffer than their bolt-connected counterparts, being very close to theoretical predictions. The EB2 specimen had an initial stiffness equal to the stud-connected beams (up to about 50 kN loading), and overall a very similar stiffness to that of CS140 in the tested range. The total deflection at a loading of 200 kN was 24% larger for TB1, 7% larger for EB2, and 6% larger for the CS140 specimen when compared to the PS300 specimen.

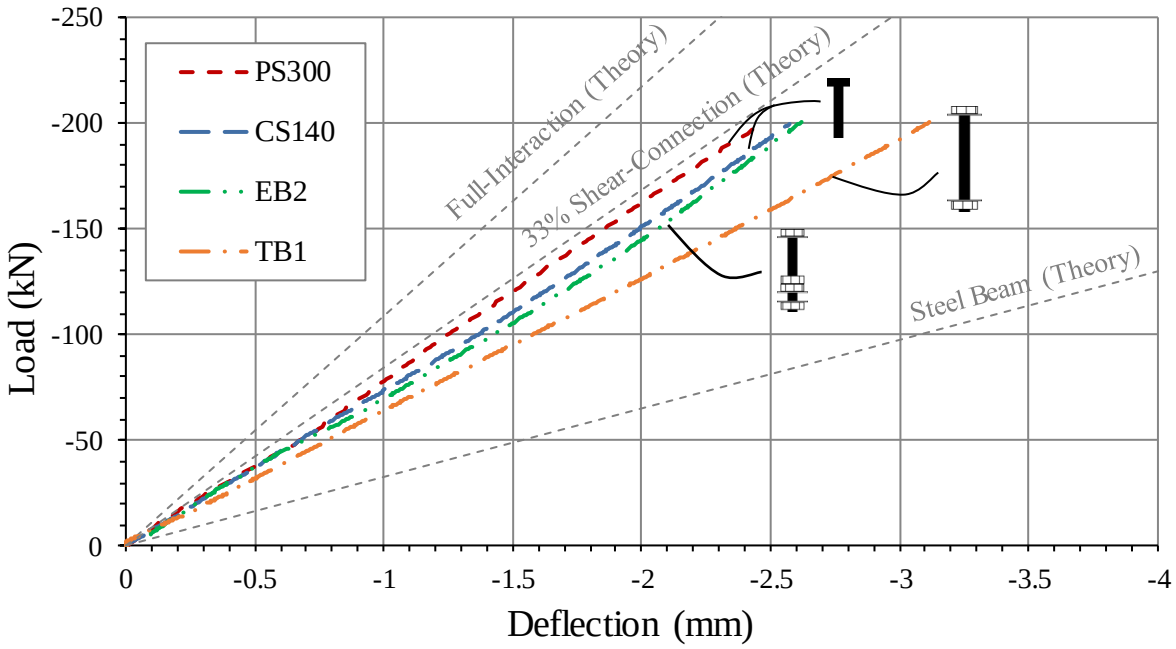

Figure 4-1: Load-deflection curves of each beam type prior to cyclic loading.

The stiffness loss of each specimen was tracked as cyclic loading was applied. In many cases the load-deflection behaviour did not change significantly, even as other signs indicated that there had been

degradation of the shear connection. However, for specimens where significant fatigue damage occurred, such as the PS300 and CS300 specimens, significant loss of stiffness was observed. To illustrate this, Figure 4-2 shows a comparison of deflection increases with cyclic loading between CS140 and PS300. It can be clearly seen that the stiffness of CS140 was minimally, if at all affected by the application of cyclic loading. Three lines are shown in the plot, corresponding to the specimen stiffness at the start of the test prior to cyclic loading (0%), at the number of cycles equal to the CSA S6 predicted failure for the critical studs (100%, or 258,000 cycles), and at ten times this value (1000%, or 2.6 million cycles). CS140 displayed no loss of stiffness despite the N1 and S1 studs (the first row of studs) being cracked. These cracks were discovered during the specimen autopsy procedure, which will be discussed in depth in this chapter.

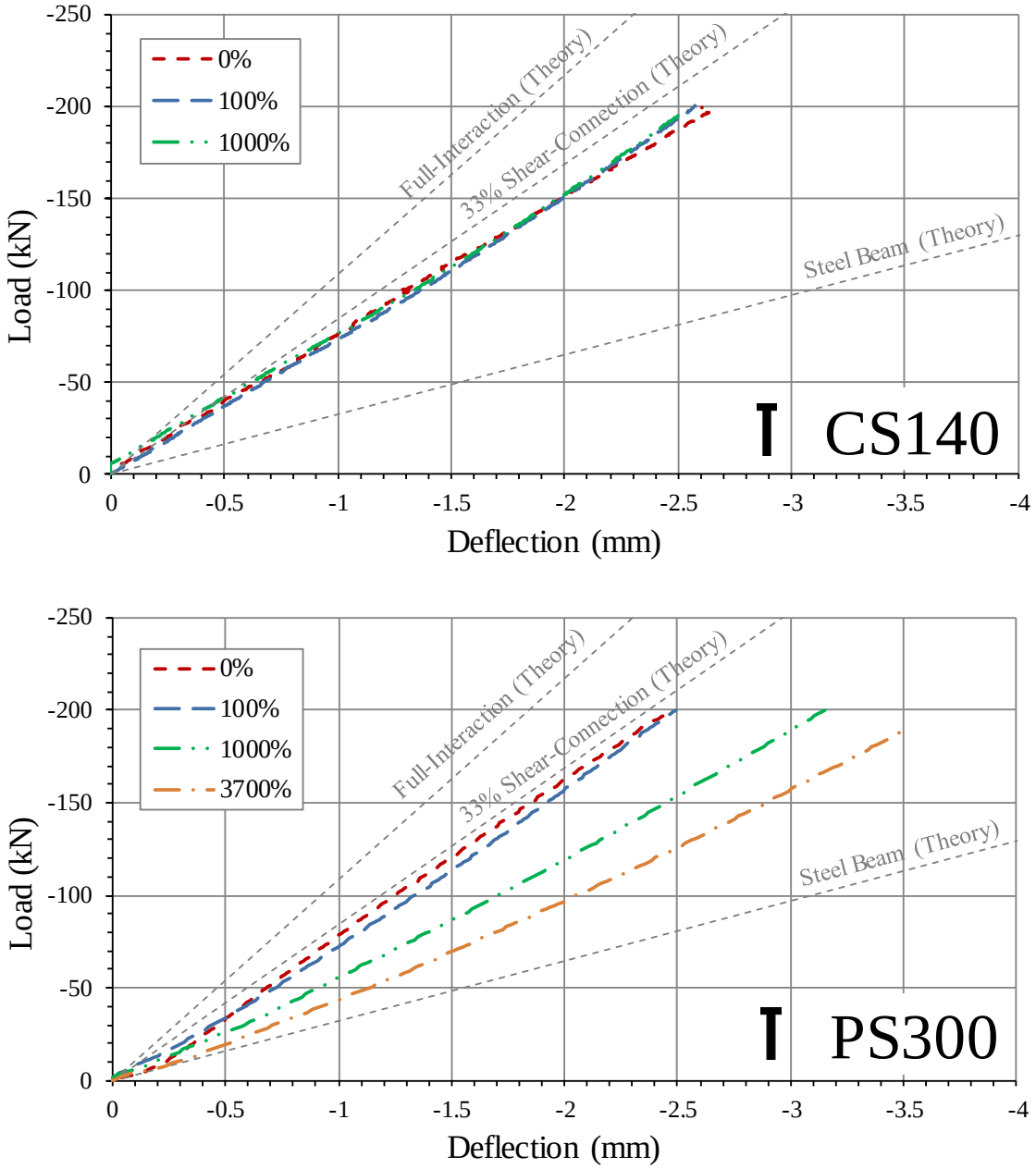

Figure 4-2: Comparison of increased deflection with cyclic loading between CS140 and PS300.

In contrast to the small amount of stiffness change observed in CS140, PS300 displayed very significant stiffness loss with the application of cyclic loading. In fact, PS300 experienced a 26% increased deflection at the 200 kN loading between the 100% (26,000 cycles) and 1000% (260,000 cycles) cyclic loading stages alone, with the stiffness decrease decelerating after that until the 3700% stage (1.2 million cycles). This loss is not surprising considering that the PS300 autopsy revealed that 18 of 24 studs were cracked by the end of the test, with the critical stud group completely detached from the top flange of the steel section. However, despite this loss, the stiffness test shows that significant composite action was still taking place. It should be noted that specimens PS140 and CS300 displayed similar patterns to the plots shown in Figure 4-2.

No significant stiffness loss was observed in the bolted specimens due to the application of cyclic loading. In large part, this is probably because very few fatigue failures were observed. However, even in cases where bolts did fail in fatigue, the few failures did not affect the beam stiffness (similar to CS140 in Figure 4-2). Interesting observations were made, however, with the TB1 specimen during a deliberate investigation that sought to quantify the effect of bolt failures if significant fatigue damage was to occur. The investigation involved the systematic removal of through-bolts, with static tests performed after 4, 10, 12, and all 24 bolts were removed. The results are shown in Figure 4-3 and show good agreement to elastic theoretical predictions in that the stiffness of the specimen with all bolts removed is closely approximated by the steel beam acting alone. This indicates that the slab provides minimal stiffness when no composite action is induced through the use of shear connectors.

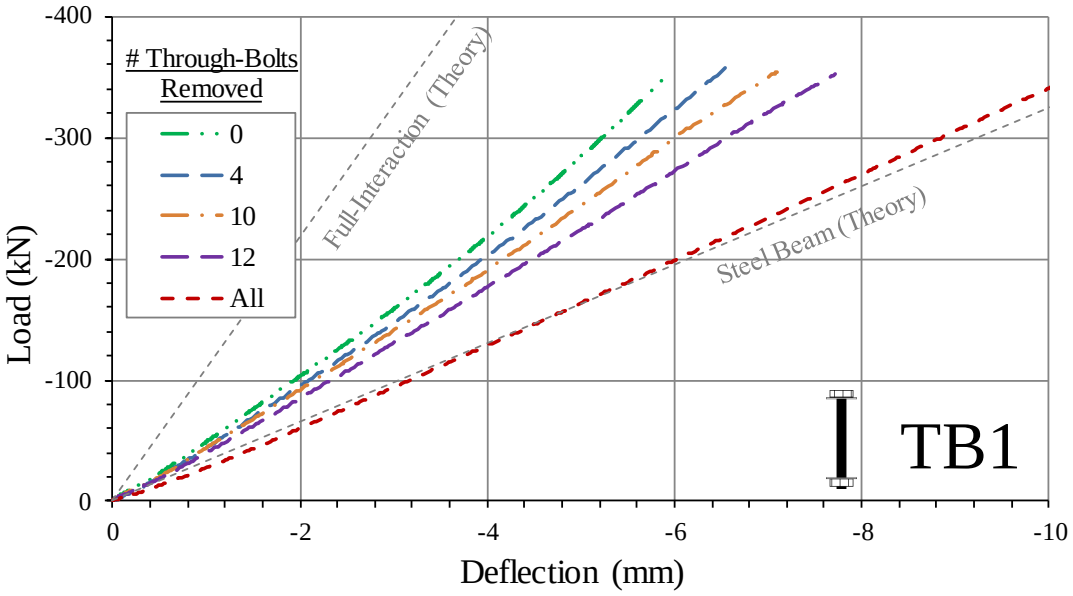

Figure 4-3: Stiffness loss with the removal of through-bolts in TB1.

4.1.2 Interfacial Slip

Gauges detecting slip between the bottom of the concrete and the top of the steel section (at the interface of the materials) were mounted at the ends of the beam (x = 0 and 3,000mm), and at profiles A (500 mm), B (1,000 mm), and Y (2,000 mm). EB beams had profile B gauges switched to profile Z at 2,500 mm. Like

the periodic stiffness tests, interfacial slip data proved not to be of great help in detecting the failure of specific connectors, but did help establish general trends, particularly when significant composite action was lost. More importantly, these gauges were used to develop “load-slip” curves, or “force-deformation” curves, which were used as inputs for a FE model discussed in Chapter 5.

Figure 4-4 compares interfacial slip values along the length of the beam for the three specimen types CS, PS, and EB for a load of 200 kN prior to cyclic loading. Slip data from TB specimens was not reliable enough to be useful for comparison here. Individual specimen slips are shown faded, while the specimen type average is shown in bold. The stud-connected specimens exhibited very similar slip levels on average, while the EB specimens show approximately twice as much slip. The slip at profile B was consistently very close to zero, which is to be expected as it is the location of maximum moment. Connectors transmit shear into the beam slab from either side, and towards, the location of maximum moment. In Figure 4-4 a positive slip value indicates relative motion of the slab sliding west in relation to the top flange of the beam (see beam diagram below for east/west).

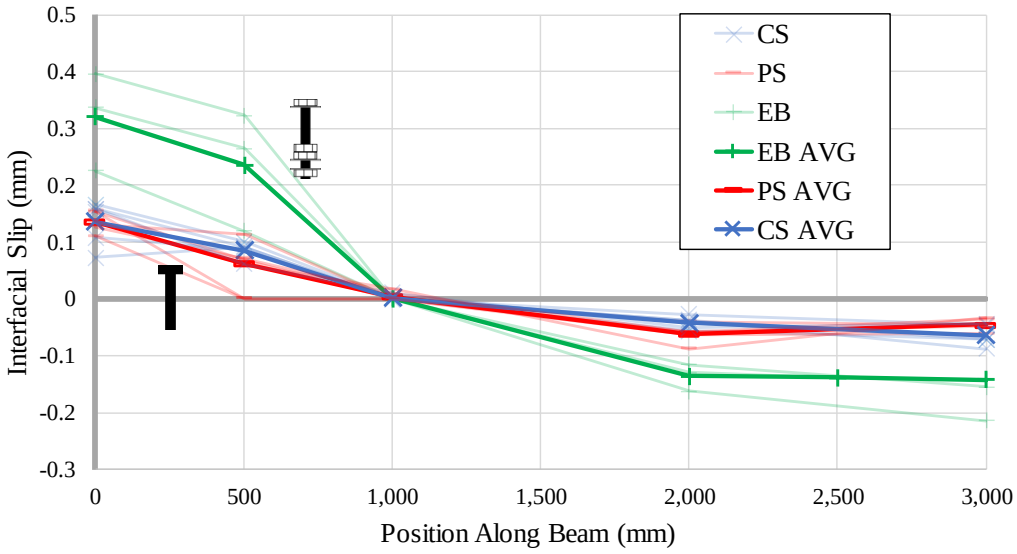

Figure 4-4: Interfacial slip on CS, PS, and EB specimens for a load of 200 kN prior to cyclic loading.

Increases in interfacial slip were tracked as cyclic loading was applied. For the bolt-connected specimens, no significant increases in slip were observed. For the stud-connected specimens, a clear trend of increasing slip was observed as cyclic loading was applied and connectors failed in fatigue. The CS140 and PS300 specimens that were featured in Figure 4-2 are shown again in Figure 4-5, this time with interfacial slip values along each beam length for a loading of 200 kN. Note that both specimens experienced increased slip values at 1000% of the expected fatigue life of the critical studs, particularly on the west end of each beam (x = 0). The average percentage increase in the west end slip of CS and PS specimens was 119% (2.2x) and 168% (2.7x), respectively, from the first cyclic load application to the 1000% cyclic loading stage. The west end of each beam is where the critical studs were located, and where fatigue damage was present in almost all tested beams. A further discussion of slip data will be presented in Chapter 5.

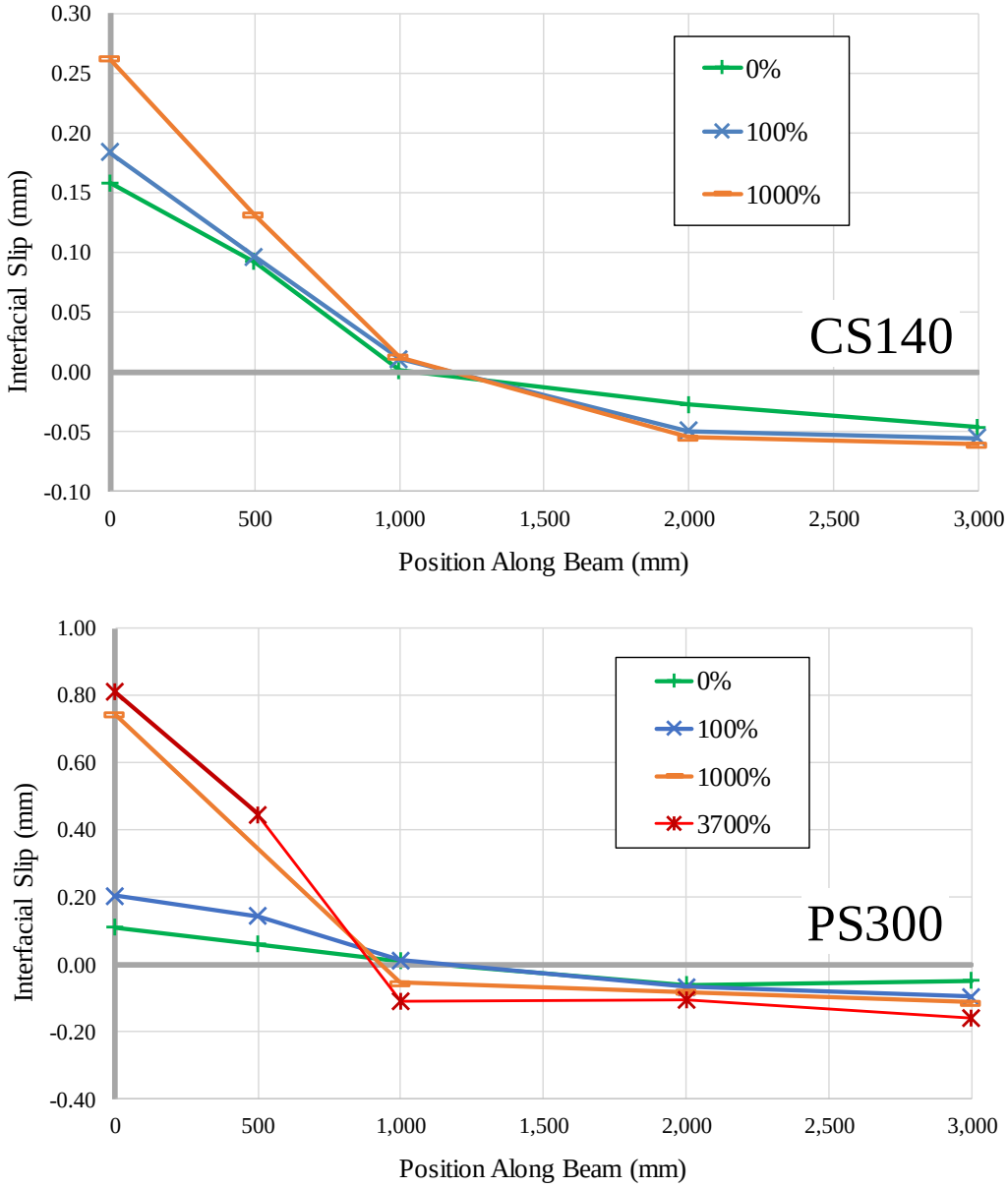

Figure 4-5: Increased interfacial slip with cyclic loading for CS140 and PS300 (P = 200kN).

4.1.3 Strain Profiles and Slab Forces

Strain gauges were placed on the bottom of the bottom flange and on the bottom of the top flange of the steel section at locations along the length of each beam. These gauges proved essential for the observation of shear connection degradation throughout the testing program. Not only did they provide direct information on levels of composite interaction along each specimen and over time, but they also allowed for the calculation of slab forces. These slab forces are primarily the result of connector shear forces, with friction playing some role. Initially, strain profile gauges were placed only near profiles A and B, and included concrete strain gauges as well as gauges on the slab reinforcing. It was found that gauges on the steel beam were much more reliable than the concrete or reinforcement gauges, and since the net compressive

slab force could be back calculated with only two steel section gauges, these other locations were abandoned in favour of more profiles. By the end of testing, each beam was instrumented with gauges at profiles A (500 mm), B (1,000 mm), M (1,500 mm), Y (2,000 mm), and Z (2,500 mm).

As expected, and consistent with the findings from load-deflection and interfacial slip data, specimens that experienced the most shear connection degradation from fatigue loading exhibited obvious neutral axis migration. This migration, which is clearly visible for the PS300 specimen shown in Figure 4-6, signals the loss of composite interaction. Note that in Figure 4-6, compressive strains are positive, and tensile strains are negative.

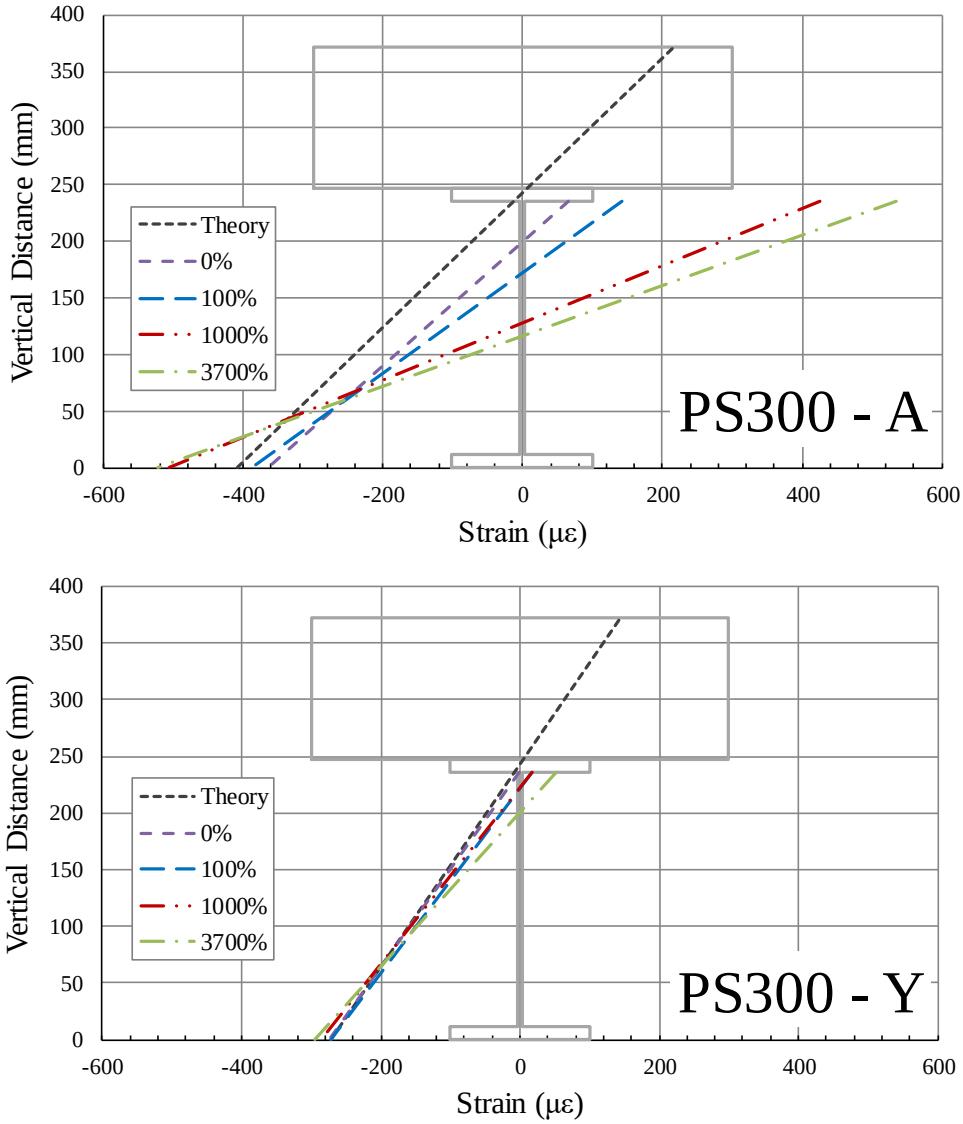

Figure 4-6: Strain profiles at profile A (500 mm, top), and Y (2,000 mm, bottom) for PS300 (P = 200kN).

Figure 4-6 shows the theoretical strain profiles at A and Y, assuming full composite interaction. Full composite interaction results in a neutral axis 129 mm from the top of the composite section, or 4 mm into the top flange of the steel beam. Prior to the application of cyclic loading (0%), the beam does not exhibit

full composite interaction. Instead, a strain discontinuity exists at the steel concrete interface (the concrete strains are not shown in the figure, but the bottom of the concrete section is in tension, so there must be a discontinuity). This discontinuity value may be termed the “slip strain”. When the slip strain is integrated along the beam length, slip values result such as those in Figure 4-5. Since it is known that mechanical connectors require deformation to provide shear transfer, and since slip was observed along the length of every specimen, it is no surprise that full composite interaction does not exist, even prior to the application of cyclic loading, at profiles Y and A. However, the level of composite interaction is much higher at profile Y, due to the fact that shear connectors in the profile Y region of the beam are not transferring as much shear, and their stiffness is significantly higher than the connectors around profile A adjusted for this slip level. Slip strain and related concepts are explored further in Chapter 5.

Note the gradual downwards migration of the steel neutral axis (where the strain profile crosses from tension to compression through the height of the steel), particularly at profile A. By the end of the PS300 test, it appears that no composite interaction remains, because the neutral axis has reached that of the steel section on its own (half the height of the section). This was validated by the PS300 specimen autopsy, which revealed that all studs contributing to the slab force at profile A were cracked to the point of no remaining connected area by the end of the test. This full loss of composite interaction was only found at profile A of PS300; other beams exhibited only slight neutral axis migration, while some exhibited none.

Figure 4-7 shows the strain profiles at A and Y for specimen EB1 at a load of 200 kN for various cycle counts. Cycle counts are used in lieu of percentages of fatigue life, since there is presently no way to estimate the fatigue life of the embedded bolt detail. When compared to Figure 4-6 it is apparent that less composite interaction exists at both profiles of EB1 prior to the application of cyclic loading. Additionally, less shear connection degradation occurs in EB1 throughout the test. A better way of using the same data to visualize and quantify the loss of composite interaction is through the calculation of slab forces along each beam.

As stated, the slab force calculation is made possible using the strain profile gauges, which readily allow for the calculation of the net tensile resultant in the steel section (a very simple calculation using Hooke’s Law and when materials are in the elastic range), which is equal to the net compressive resultant force in the slab due to equilibrium at the section. Figure 4-8 displays the slab forces along the beam length at a static loading of 200 kN, prior to the application of cyclic loading. Four individual specimens are shown, with one from each beam type. The theoretical slab forces based on elastic calculations assuming full composite interaction serve as an upper bound; the reality of incomplete interaction and interfacial slip prevents the full theoretical slab force, and thus limits the amount of shear force in the connectors.

Figure 4-8 reveals that all connector types perform similarly prior to the application of cyclic loading. It appears that TB2 has lower slab forces than the other beam types, but TB2 only contained half the shear connector area (recall Figure 3-3). The CS300 specimen appears to have the highest slab forces, indicating the highest level of composite interaction amongst these four specimens.

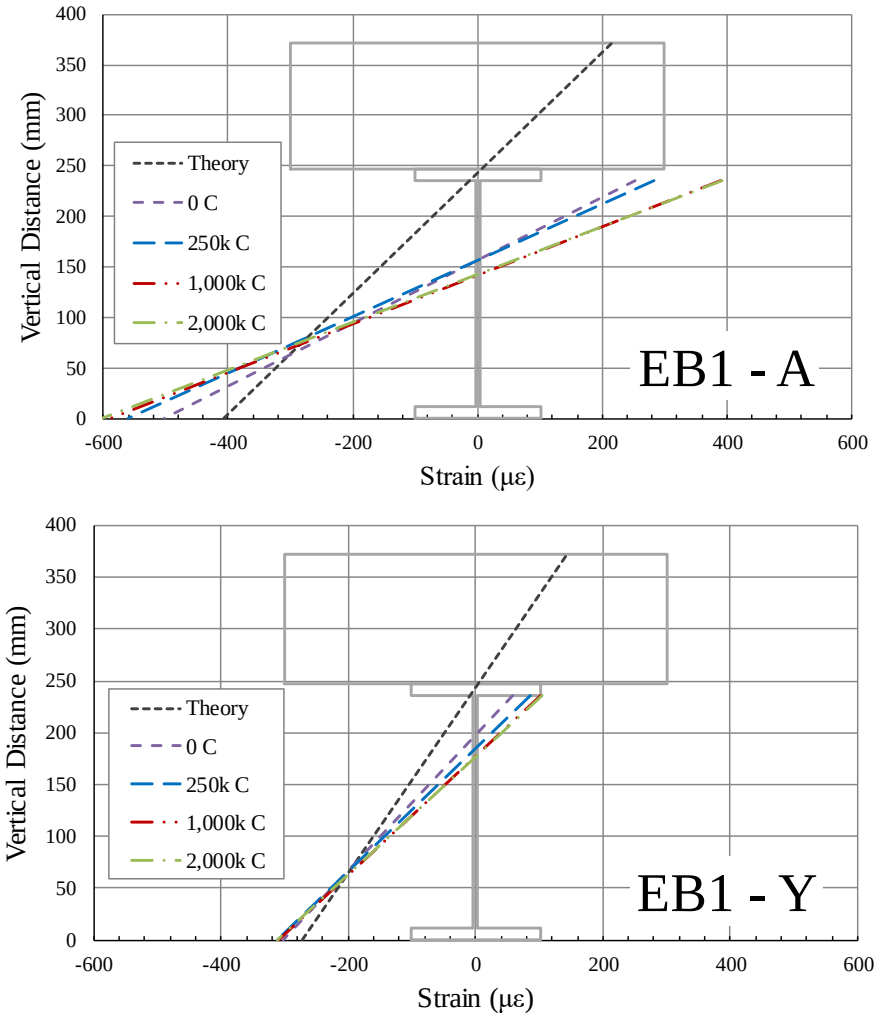

Figure 4-7: Strain profiles at profile A (500 mm, top), and Y (2,000 mm, bottom) for EB1 (P = 200kN).

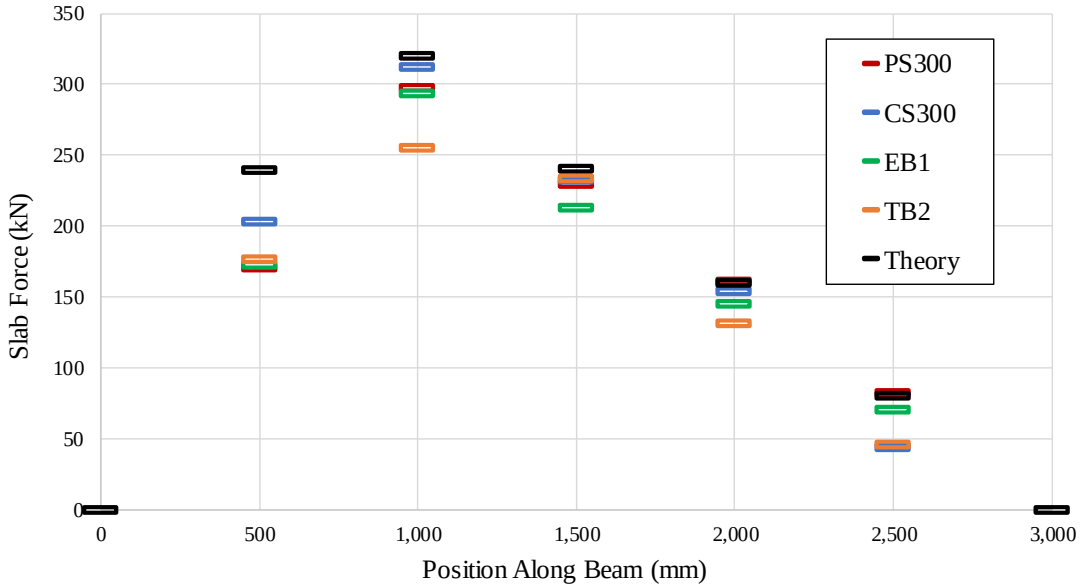

Figure 4-8: Slab forces calculated from strain profile gauges prior to cyclic loading (P = 200kN).

If the contribution of friction to shear transfer is ignored, connector shear forces can be directly calculated from the slab forces. For example, the slab force at profile A (500 mm) in CS300 is approximately 200 kN, which can be divided by the four studs west of that profile for a force of 50 kN per stud, or 252 MPa for the 16 mm studs. Although this exceeds the yield stress of the material for shear, it is believed that the net shear transfer occurs through a combination of stud shear and bending, so that no yielding occurs.

To compliment the strain profiles of PS300 shown in Figure 4-6, slab forces are shown for this specimen in Figure 4-9. The complete loss of composite interaction is shown at the 500 mm position along the beam (profile A), as the net compressive slab force at the end of the 1.2 million cycles is zero. PS300 is a precast stud specimen, and one shear pocket complete with four studs lies in between each profile shown on the x-axis of Figure 4-9 (profiles are located at 500 mm increments). Therefore, the complete loss of composite interaction at profile A indicates that the first stud pocket is not transferring any shear. However, there is still significant composite interaction taking place at the location of maximum moment (profile B at 1,000 mm). A comparison between the 0% and 3,700% data points at profiles A and B reveals that the second shear pocket began to transfer more shear as the first pocket was lost (pocket forces can be calculated by taking the difference between two data points). At the 1000% stage, the force in the second pocket had increased from approximately 125 kN to 200 kN. Between 1000% and 3700%, this force decreased to 175 kN as studs in the second pocket began to fail. As connectors lose capacity on one shear span, connectors on the other side of the point of maximum moment will also transfer less shear. This is not necessarily because they are losing capacity, but because the net compressive slab force at the point of maximum moment is being limited by the weaker shear span. This fact, as well as the concepts of redundancy and redistribution between connectors, are clearly illustrated in Figure 4-9 and underscore the value of a beam test over that of a push test, where none of these phenomena exist.

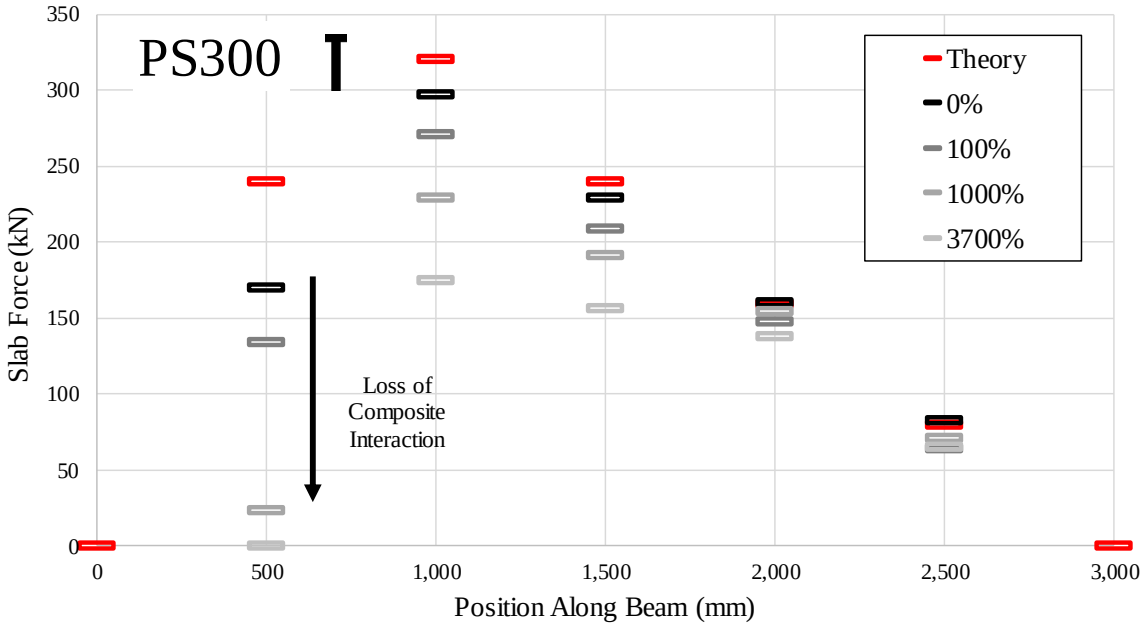

Figure 4-9: Slab forces calculated from strain profile gauges for PS300 (P = 200kN).

Slab forces for two embedded bolt specimens, EB1 and EB2, are shown in Figure 4-10 for comparative purposes. While stud specimens had the benefit of local distortion strain gauges to aid in failure detection (to be discussed in the following section), slab forces calculated from strain profile gauges were the primary source of quantitative data for detecting fatigue failures for bolted specimens, including EB1 and EB2. Specimen EB1 was loaded for 2 million cycles at a load range of 400 kN for a theoretical stress of 582 MPa on the critical bolt group, while EB2 was loaded for twice the number of cycles at a load range of 267 kN for a theoretical stress of 388 MPa for the critical bolt group. Slab forces are shown for a loading of 200 kN from periodic static tests at the start, end, and two middle points for each specimen.

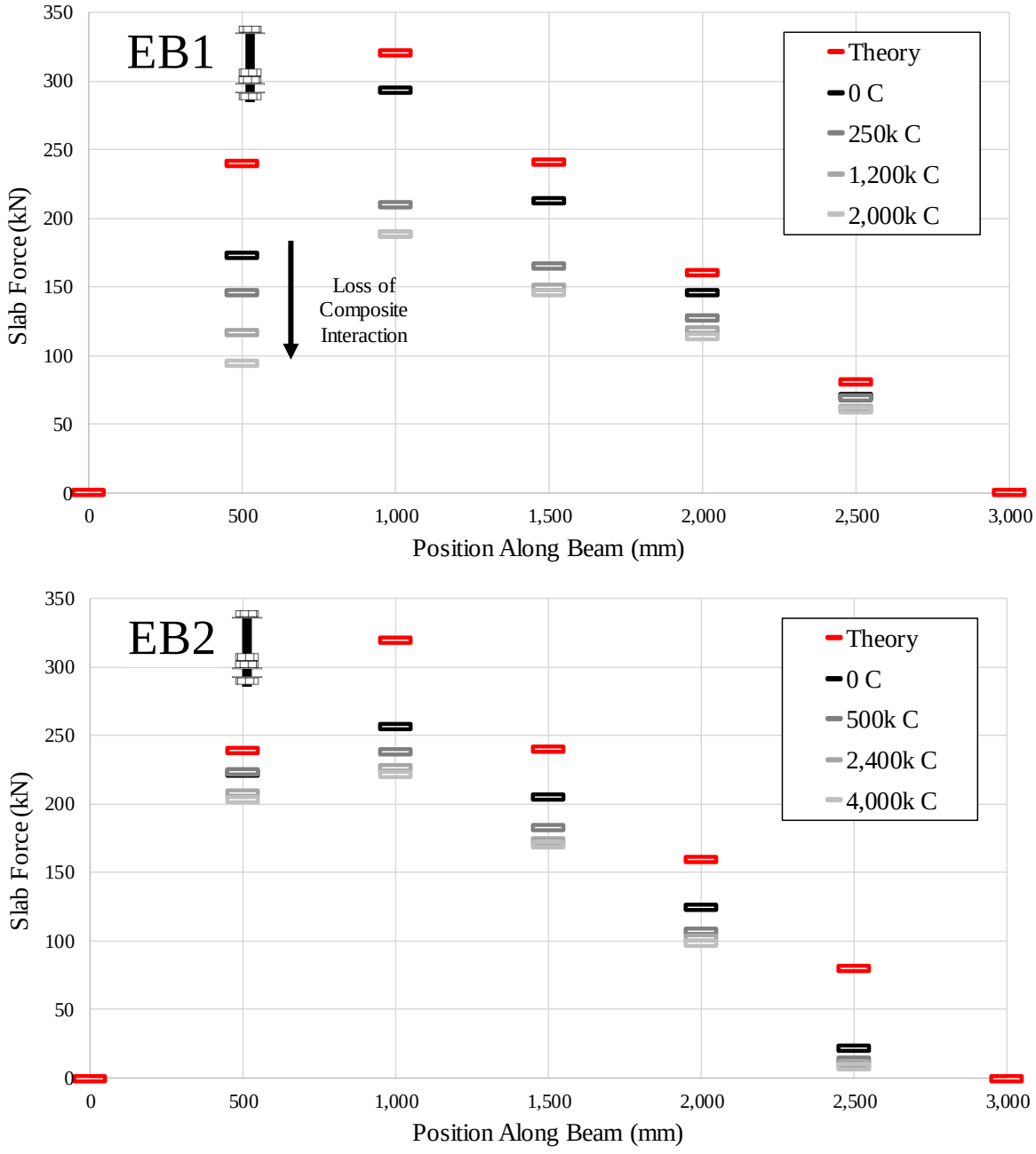

Figure 4-10: Slab forces calculated from strain profile gauges for EB1 and EB2 (P = 200kN).

The top plot of EB1 clearly shows the loss of composite interaction as the test progresses, while EB2 displays a very limited degradation that stabilizes after 2 million cycles. Both of these observations were confirmed during specimen autopsies where it was revealed that the critical bolt group had experienced fatigue failure in EB1, while the bolts of EB2 were intact. Interestingly, EB1 was still experiencing very significant slab forces at profile A despite complete failure of the bolts in the first shear pocket, because the failure plane through the bolts was located between the two nuts on top of the flange, and the lower nut was sufficient to maintain the pretensioned clamping force and transfer shear through a much-reduced effective connector height. For more static test results and associated discussion, see (Porter, 2016) and (Balkos, 2017).

4.2 Fatigue Test Data and Results

Fatigue test data will now be presented, with an emphasis on fatigue failure detection and a failure definition for stud connectors. After a definition is established in the follow subsection, an analysis of the fatigue life of each connector type, in the form of S-N data, will be completed. Periodic static test results were presented previously in the form of load-deflection curves, interfacial slip plots, and strain profiles revealing slab forces along the length of each specimen. For stud-connected specimens, data from static tests were presented at the initial stage prior to cyclic loading, as well as after the CSA S6 predicted fatigue life of the critical studs (100%), 10 times this value (1000%), and at the end of the test if the test continued past this point. For the bolted specimens, however, no fatigue prediction could be made, so data were presented with the cycle count itself.

Table 4-2 provides a summary of the fatigue tests conducted, in chronological order, including the number of cycles each specimen was subjected to and the equivalent stress range of the critical connectors (recall that stud specimens were subjected to VA loading, and bolted specimens were subjected CA loading). For stud specimens, the highest stress range in the VA load history was approximately twice the equivalent stress range shown in Table 4-2.

The data acquisition system used an algorithm to detect “peaks” and “valleys” from sensors throughout each test. Since each specimen underwent over one million applied loading cycles, a MATLAB script was used to process and manipulate the large data sets. For the stud specimens, the VA loading created a unique challenge in data processing. To plot results such as deflection, interfacial slip, or strain at a location of interest along with the number of cycles, a specific load value from the VA history needed to be chosen. The second highest load range from the VA history was chosen as the load for which all plots would be based upon. Rather than being twice the value of the equivalent load range (as the highest load range was), the second highest load range value was approximately 30% higher than the equivalent load range.

Table 4-2: Summary of fatigue loading.

Specimen	Critical Connector Equivalent Stress Range (MPa)	CSA S6 Predicted Fatigue Life	# Cycles at Test End
CS140	140.8	258,166	2,555,926
PS140	140.6	259,573	2,719,172
CS200	202.3	87,127	2,489,438
PS200	201.9	87,569	3,296,102
CS300	302.1	26,162	2,053,420
PS300	301.9	26,194	1,168,548
CS100	98.8	747,459	9,503,532
PS100	98.6	721,001	7,178,574
CS120	119.5	423,034	5,205,441
PS120	119.9	418,366	2,288,865
CS067	63.5	2,815,880	10,428,252
PS067	62.7	2,925,046	12,897,344
TB1	350	--	2,007,766
TB2	1,050	--	762,241
EB1	582	--	2,000,000
EB2	388	--	4,000,000
EB3	485	--	3,000,000

4.2.1 Fatigue and Stud Local Distortion

The concept of a local distortion strain gauge comes from the work of King, Slutter, and Driscoll at Lehigh University (1965). The idea for their use was that studs engage the top flange they are welded to in local bending as they are subject to shear force. It was thought that measuring these strains from local bending would give a qualitative measure of when fatigue cracking began and propagated, as evidenced by a loss of local distortion. Upon the recommendation of King et al., local distortion strain gauges were mounted underneath each critical stud for the initial tests. It was noticed early on, however, that the local distortion gauges were very useful, and that it was possible to observe fatigue failures in non-critical studs. As a result, nearly every stud was instrumented with local distortion strain gauges after this point.

Most local distortion strain gauges exhibited three distinct phases during the application of cyclic loading when a stud cracked in fatigue. These phases were an initial plateau, where the strain remained relatively constant, a second phase where strains rose to some peak value, and a third phase of descending strain values. The phases are illustrated in Figure 4-11, where peak values for studs N1 and S1 of PS140 are

approximately 1.05 million and 1.65 million cycles, respectively. The CSA S6 predicted fatigue life of both studs is also shown in the plot, at 263,000 cycles. For the case of PS140, the initial constant strain phase is not clear, since this test was relatively short. It is hypothesized that the behaviour of the local distortion strain data indicates that the following is taking place:

- In the first phase there is no fatigue damage on the stud;
- Rising strains in the second phase indicate plastic strain damage emanating from a fatigue crack that is growing;
- Strain growth peaks between the second and third phases as the stud begins to lose stiffness and force redistribution to neighboring studs commences;
- The third phase sees decreasing strains, which may decrease to a point consistent with flange strains from simple bending, but plastic strains from prior phases and mechanical interaction resulting from interlocking shapes of the cracked stud and flange will likely prevent this.

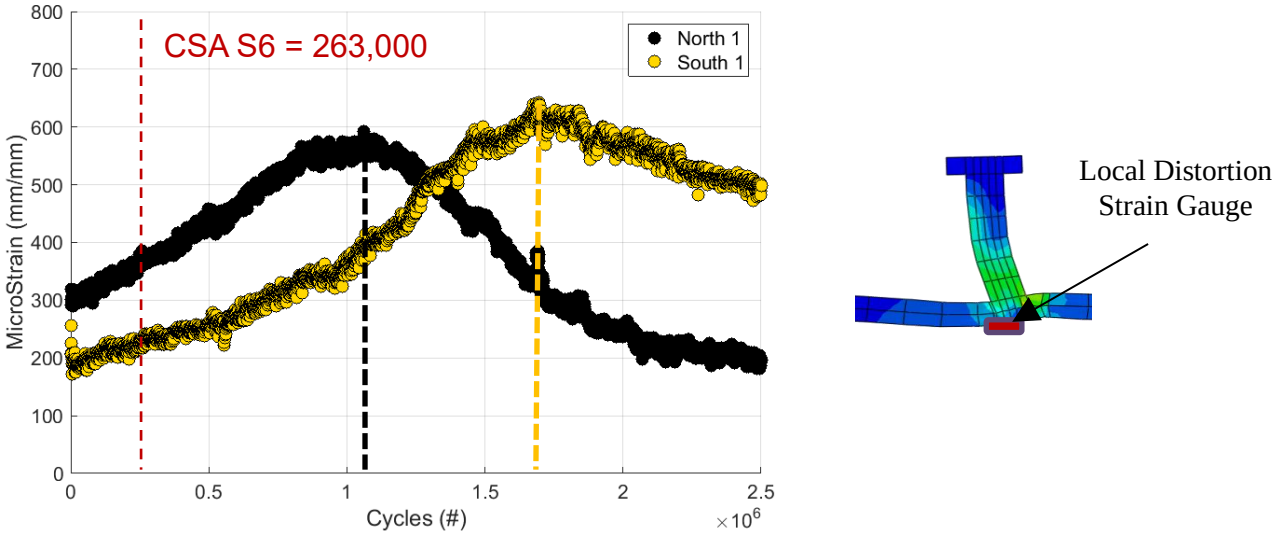

Figure 4-11: Local distortion strain gauge data for N1 and S1 of PS140.

An important step in vetting this hypothesis was to use autopsy observations to examine studs that were at various stages of local distortion. This work is presented in the following section.

4.3 Specimen Autopsies

After the application of cyclic loading and final static tests, the slab of each specimen was removed through saw cutting and chipping (stud specimens), or simple disassembly (bolted specimens), and connectors were inspected for damage. The general procedure for inspecting damage is laid out herein, following by an account of damage patterns observed and a confirmation of the hypothesis regarding local distortion strain gauges (see last section), all culminating in a definition of failure.

4.3.1 Autopsy Procedure

The autopsy procedure was significantly different for the stud specimens compared to their bolted counterparts. The former procedure, made more laborious by the irremovable stud detail and more extensive due to greater fatigue damage, will be discussed first. The initial task involved in each stud specimen autopsy was to remove concrete while causing as little damage to the studs as possible. This was completed by saw cutting, followed by using a sledgehammer and pneumatic hand tool to chisel away remaining concrete. The area around each stud suspected of being damaged was then cleaned with compressed air and a steel wire brush. At that point, a visual inspected was conducted to see if any cracking was visible in the shank or weld collar of the stud. Following visual inspection, a procedure known as a "bend test" was performed on each stud using a sledgehammer. A stud passed the bend test when it could be bent over 30 degrees from vertical without fracturing or falling off due to fatigue fracture. This is adapted from CSA W59 (Welded Structural Construction, 2013). The bend test is a sign of ductility and strength, and is a standard procedure for any stud welder to perform during the welding process (see Figure 2-5). Performing bend tests after studs are subjected to fatigue loading does not carry the same meaning as the initial welding bend test, as some studs that are cracked can still pass the bend test due to flexibility, but it was found to be a useful classification tool. In some cases, cross-sections were cut out of the flange longitudinally to investigate damage further. Specifically, if stud local distortion strain gauge data indicated that a significant crack might be present (phase 3 discussed in the previous subsection) despite a lack of visual evidence, a cut was made. Several cross-sections were also cut and analyzed of studs displaying phase one or two local distortion strain gauge behaviour to confirm the reliability of the failure definition.

The four autopsy steps, simplified, are summarized: remove concrete and clean around studs, perform a visual inspection and record results, perform bend tests and record results, and make cross-section cuts an inspect for cracks. Photos were taken and observations were recorded throughout. Figure 4-12 depicts the autopsy of CS140, showing the failed bend tests of studs N1 and S1, and the passed tests of N2 and S2.

Figure 4-12: Autopsy on CS140, showing N1/S1 failed bend tests and N2/S2 passed bend tests.

Figure 4-13 depicts the entire autopsy process in image form. Note that in the centre left image, stud N1 has visible cracks propagating into the top flange from base of the weld. This was also the case for S1 (centre right), but the bend test procedure has revealed the full extent and depth of the crack. The bright area on S1 indicates a formerly connected area, which has been freshly severed during the bend test itself. The bottom two images depict typical failed and passed bend tests.

Figure 4-13: Autopsy procedure in image form featuring N1/S1 and N2/S2 of CS140.

The autopsy procedure for the bolted specimens was markedly different than the stud specimens, taking very little time and cleanup effort. Both the through-bolts and the embedded bolts were loosened with a long socket wrench by hand. Through-bolts were easily removed from the slab holes and inspected for damage. For the embedded bolts, observations were made and recorded regarding bearing and slip. Specifically, spray paint (see Figure 3-8) was inspected for damaged or other evidence of bolt slip, and the thread-blocking rings installed on the bolts were inspected for signs of wear due to bearing. The slabs of the EB specimens were lifted up easily by the laboratory crane, and inspections of the undersides of the slabs and the tops of the steel beams were made. At this point the sledgehammer was used to remove the embedded bolt pockets from the slabs for more careful inspection of the bolts, as shown in Figure 4-14.

Figure 4-14: Autopsy procedure in image form featuring N1/S1 and N2/S2 of CS140.

4.3.2 Autopsy Observations

Autopsy observations will be presented using specimens CS140 and PS140 as typical examples, followed by a separate discussion of the autopsy of specimen EB1. Since no fatigue failures were observed in TB specimens, those autopsies will not be discussed (see Balkos, 2017, for more information). Recall that the 140 specimens were cycled with a VA loading equivalent to a CA loading of 140 MPa on the four critical studs N1-S2, and one third of this value on all other studs. The concrete in these specific beams had a 28-day compressive strength of 48.3 MPa and pocket grout strength of 54.1 MPa.

Specimens PS140 and CS140 were cycled more than ten times the CSA predicted failure of the critical studs, to approximately 2.75 million cycles, before the experiments were stopped and the beams were removed from the loading frame for autopsy. During the autopsies it was found that the critical studs were commonly connected to the steel with some remaining weld area. The lack of complete fracture is probably due to force redistribution, where neighbouring studs prevented the amount of slip necessary to fully fracture the cracked studs from the top flange.

Each stud in the critical group failed the bend test for specimen PS140, with little residual strength remaining. This was evident because the bend test blows were few and soft in comparison to a bend test for an uncracked stud. Figure 4-15 shows the group before the best test (left), and the fractured surface revealed after the bend test (right). The area that remained attached at the time of test termination is bright and silver in contrast to the dull brown fatigued area. The fatigue cracks occurred in the base metal of the steel top flange in the heat affected zone (HAZ) of the weld. The fatigue cracks of these studs were typical of others, protruding deep into the top flange from the front and back edge of the stud, and meeting at the last attached region. The studs are believed to have pivoted from this attached area, with enough flexibility to avoid being fractured from the top flange altogether. The remaining area of each stud was between 10% and 30% of the original uncracked area. The critical studs on specimen CS140 fractured earlier than those on PS140, and as a result there was less attached area remaining at the termination of the CS140 test. A distinct pattern was observed comparing all CS and PS specimens during autopsy: the primary crack growth direction was from the outside in CS specimens, and from the inside in PS specimens. This is shown in Figure 4-16.

Figure 4-15: Critical stud group of specimen PS140 before (left) and after (right) bend test.

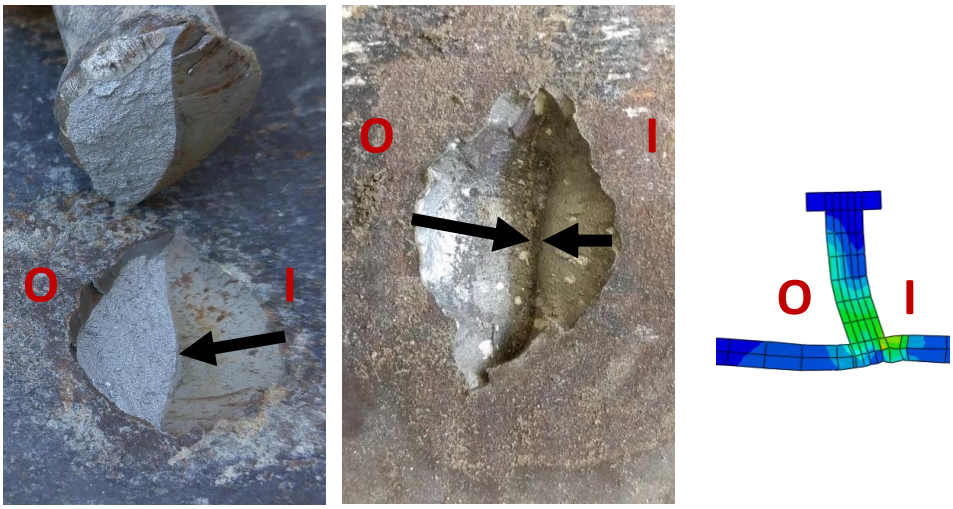

Figure 4-16: Crack growth direction for specimen PS140 (left), and CS140 (right).

The outside direction is not the logical location for the fatigue cracks to initiate considering the load effect on the stud. One explanation for this observation is that shrinkage of the concrete during curing caused the CS studs to experience cyclic tension on the outside part of the stud weld. Residual welding stresses may have played a role in crack initiation location as well. Further evidence of this crack growth pattern is provided in Figure 4-17. A detailed investigation into the cause of the fatigue crack growth direction patterns, and particularly the effect of shrinkage, is given in (Porter, 2016). In both CS and PS specimens, studs farther from the point of maximum moment failed first, consistent with the principles of incomplete interaction and slip.

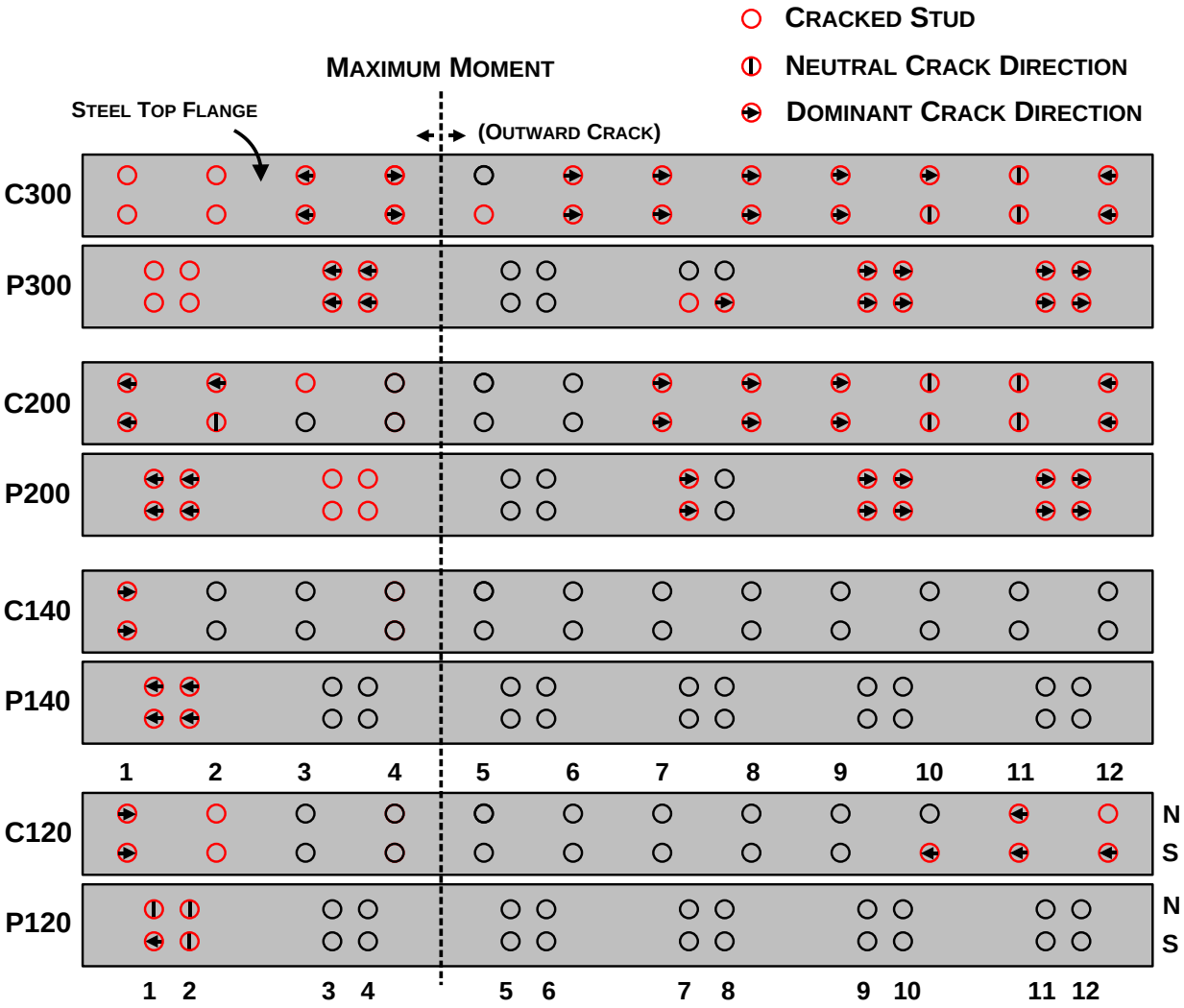

Figure 4-17: Dominant crack growth directions for various CS and PS beams.

In all, over 80 studs were found to have fatigue cracks on the twelve stud-connected specimens (Figure 4-19). Thirteen cross-section cuts were made to measure fatigue cracks accurately, and draw correlations between visually observed fatigue cracks, bend test results, and local distortion strain gauge data. Figure 4-18 shows the cross-section of a failed shear stud near its base, including the fatigue crack (red).

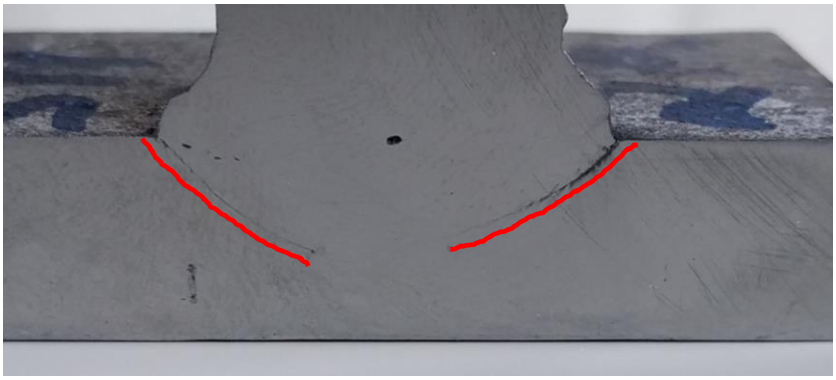

Figure 4-18: Cross-section of a failed stud connector (fatigue cracks highlighted).

Figure 4-19: Overview of all studs that failed in fatigue.

In the EB specimens no slip was detected using the spray paint, nor were any signs of bolt bearing present. In all cases the thread blocking rings were easily removed when the bolts were loosened, rendering them unnecessary to the bolt assembly (they were used in anticipation of bolt slip, to prevent bolt threads from making slab removal difficult after bearing into the top flange of the steel). Only four bolts failed in fatigue in all EB specimens, and these were the four critical bolts in specimen EB1. These bolts are shown in Figure 4-20. The progression of images shows the bolt group from the underside of the slab following slab removal.

One of the bolt segments fell to the ground immediately, while the other three were removed easily by hand. The fatigue failure surface was between the nuts located on top of the flange. As a result, the lower nut was still inducing composite action in the slab after fatigue failure through mechanical interaction (see Figure 4-10). The lower images of Figure 4-20 show that concrete was being pulverized throughout the cyclic loading procedure at the critical pocket. Even though the load range at which the A325 bolts were being cycled would pass strength requirements for the bolts, the CSA S6 ultimate limit state (ULS) strength requirement for the concrete bearing on the bolts was being violated, indicating that concrete crushing would occur (see Clause 10.11.8.3.2 of CSA S6, 2014).

Figure 4-20: Failed bolt group of EB1 and concrete pulverization left on the top flange.

4.3.3 Fatigue Failure Definition

The criterion for failure could be considered the onset of a decrease in stud capacity, the start of a fatigue crack, or the complete fracture of a stud with so that no capacity remains. This criterion is important but can be difficult to identify in an instrumented test. For the purposes of this research, stud failure has been defined as the point when the capacity of a stud to transmit shear force begins to decrease. From the observation of test results and autopsies, this occurs after an initial fatigue crack begins to form in most cases. The crack may be in the stud shank, the weld, or in the base metal (beam flange). Autopsy findings combined with local distortion strain gauge data indicate that the peak local distortion strains correspond to the commencement of shear transfer decrease. Table 4-3 provides the evidence necessary to enforce the fatigue failure definition based on the local distortion strain gauge data.

Table 4-3: Autopsy findings and local distortion states used to establish a failure criterion.

Local Distortion	Specimen	Stud	Cross-Section	Autopsy Findings	Bend Test
No Response	CS100	N10	Yes	3 mm (e) crack in shank	Not Tested
No Response	CS120	N11	Yes	2 mm (e)	Pass
No Response	CS067	N12	Yes	no cracking	Pass
Post Peak	CS100	N2	Yes	12 mm (w)	Pass
Post Peak	CS067	S1	Yes	10 mm (w)	Pass
Post Peak	PS120	S1	Yes	3 mm (w) & 10 mm (e)	Pass
Post Peak	CS100	S10	Yes	no cracking	Not Tested
Post Peak	CS120	S10	Yes	3 mm (e)	Pass
Post Peak	CS100	S11	Yes	9 mm (e)	Pass
Post Peak	PS200	S11	Yes	11 mm (w) & 7.5 mm (e)	Not Tested
Post Peak	CS100	S2	Yes	visual cracking (not measured)	Pass
Post Peak	CS300	S4	Yes	11 mm (w) & 3 mm (e)	Pass
Rising	CS300	S5	Yes	1 mm (e)	Pass
Rising	CS120	N10	No	no visual cracking	Pass
Rising	CS120	N2	No	visual cracking	Pass
Rising	CS120	N3	No	no visual cracking	Pass
Rising	CS120	N4	No	no visual cracking	Pass
Rising	CS200	N4	No	no visual cracking	Pass
Rising	CS300	N5	No	no visual cracking	Pass
Rising	PS300	N6	No	no visual cracking	Pass
Rising	PS300	N8	No	visual cracking	Pass
Rising	CS120	S2	No	visual cracking	Pass
Rising	CS120	S3	No	no visual cracking	Pass
Rising	CS120	S4	No	no visual cracking	Pass
Rising	CS200	S4	No	no visual cracking	Pass
Rising	PS200	S4	No	visual cracking	Pass
Rising	PS300	S5	No	no visual cracking	Pass
Rising	PS300	S6	No	no visual cracking	Pass
Rising	PS300	S8	No	6.6 mm (w)	Failed

Not every failed stud is shown in the table, but only those that contribute to the failure definition. The table includes the local distortion phase at the time of the autopsy, the results of bend tests, and the length of fatigue cracks from select cross-section cuts. Those studs exhibiting post peak location distortion behaviour all had significant fatigue cracking (3 mm or more), apart from S10 on CS100. Furthermore, almost every stud listed in Table 4-3 that did not display post peak local distortion strain gauge behaviour had only insignificant amounts of cracking (3 mm or less). There was only one case of significant cracking that was not detected through the local distortion strain gauge method, and this was S8 of PS300. This stud failed the bend test to reveal a 6.6 mm crack. It is possible that the gauge placement in this case was not accurate enough to capture the reduced stiffness of this stud.

4.4 Fatigue Life (*S-N*) Analysis of Connectors

Based on the results of the stud failure investigation, failures were defined corresponding to the number of cycles required to reach a maximum local flange distortion strain at each stud. Table 4-4 summarizes the results for the initial stud failures on each beam. These failure points (number of cycles) were plotted against individual stud stress levels (equivalent CA stress) to create *S-N* plots, allowing for comparison between each other, other testing programs, and various design standards. Data can be plotted for each individual stud, but the initial failure of the first stud pair in each beam is of higher importance than the failures of subsequent studs. Plotting of these secondary stud failures is not strictly valid since the stress ranges used correspond to the initial stresses, but the actual stress range values are unknown due to the redistribution of forces between studs after the initial failures. Figure 4-21 (left) shows the results for the initial stud failures and for all stud failures. North American codes and tests from literature are provided for comparison.

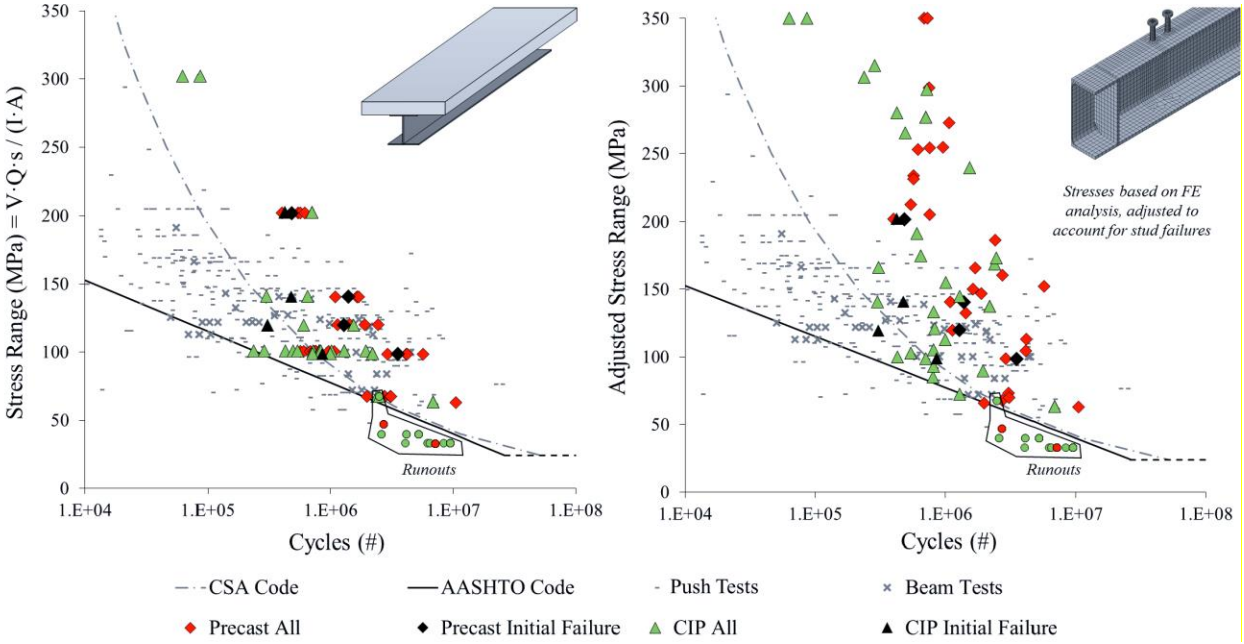

Figure 4-21: *S-N* results for studs in CS and PS specimens (left), and adjusted results (right).

As shown in Figure 4-21 (left) and in Table 4-4, the PS specimens had longer fatigue lives than their CS counterparts at the same stress range levels, and all the results of this study fall within the envelope of test results reported by others. The specimens tested exceeded their code-predicted fatigue lives (CSA S6, 2014), with the exception of one CS specimen. The precast specimens exceeded their code predicted fatigue lives by an average of 446%, while the CIP specimens exceeded their code predicted fatigue lives by an average of 220%.

Table 4-4: *S-N* results for initial stud failures.

Specimen	Stud Shear Stress (MPa)	# Cycles to Failure (% of CSA S6)	CSA S6 Predicted #
CS067	63.5	6,875,000 (242%)	2,815,880
PS067	62.7	10,500,000 (361%)	2,925,046
CS100	98.8	886,000 (114%)	747,459
PS100	98.6	3,548,000 (472%)	721,001
CS120	119.5	306,000 (72%)	423,034
PS120	119.9	1,289,000 (307%)	418,366
CS140	140.8	475,000 (184%)	258,166
PS140	140.6	1,392,000 (536%)	259,573
CS200	202.3	424,000 (487%)	87,127
PS200	201.9	484,000 (552%)	87,569
CS300	302.1	Static failure on overload	26,162
PS300	301.9	Static failure on overload	26,194

4.4.1 Revised *S-N* Plots

A SAP2000 FE model was created to compute stud stresses after one or more studs had failed. The goal of obtaining these stresses was to revise the *S-N* results for secondary stud failures by correcting stress ranges based on an equivalent stress range using the Palmgren-Miner damage accumulation rule. The SAP2000 model was programmed using the CSi Application Programming Interface (API). Studs were represented as multi-linear elastic links with a load-slip behaviour based on the measured load-slip from several beam tests. The model was verified by comparing general behaviour to that of an ABAQUS model (also discussed in the following chapter) and the experimental results.

In the experimental program it was observed that studs would fail in a slow manner, redistributing forces to adjacent studs as fatigue cracks propagated, and even transmitting shear through mechanical interaction due to the shape of the fatigue failure surface. In the SAP model, however, failed studs were given a zero stiffness to assess the effect of force redistribution on the remaining studs. It was found, not unexpectedly, that the stud shear force was increased significantly on adjacent studs after initial and secondary stud failures. For example, after the first row of studs failed, the shear force in the second row was increased by 39% (see Figure 4-22).

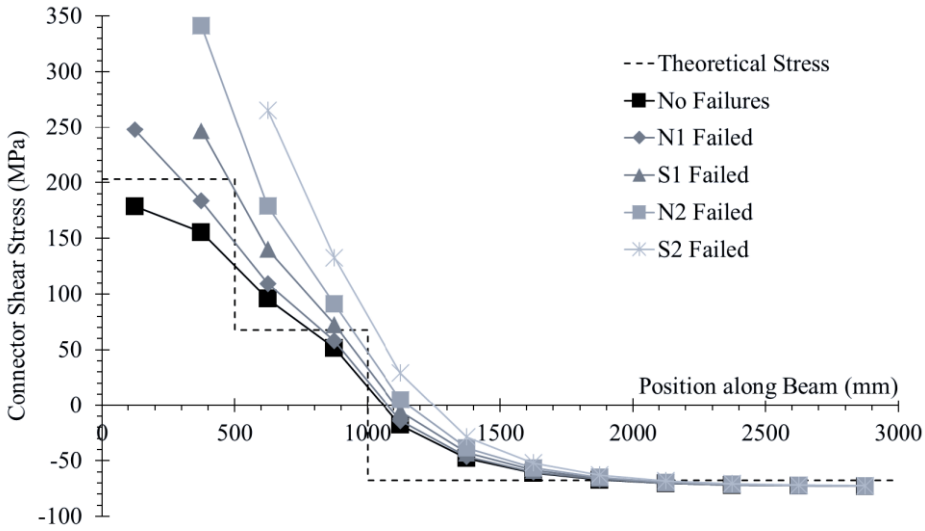

Figure 4-22: Stud force redistribution due to stud failures, as predicted by SAP2000 FE model.

Figure 4-21 (right) displays the revised *S-N* plot, using stress range values accounting for stud shear force redistribution due to preceding stud failures. A table summarizing the stepwise stress range increases with successive stud failures for each specimen is provided in (Sjaarda, 2017). Note that many of the failures close to the current design criteria curves on Figure 4-21 (left) were secondary failures, which are shifted upwards in Figure 4-21 (right). In Figure 4-23, mean and "mean minus two standard deviation" *S-N* curves based on the failure data are plotted and compared with the AASHTO and CSA design curves. Looking at this figure, it can be seen that the mean curves are above the AASHTO and CSA design curves, whereas the mean minus two standard deviation curves fall on or slightly below the design curves. The conservative definition of failure (significant cracking, but not total separation of the stud) assumed in this study may explain this result. The low consequence of single stud failure observed in this study raises the question of what an appropriate design survival probability should be for this connector type. It is this question that is explored in the final chapter of this thesis.

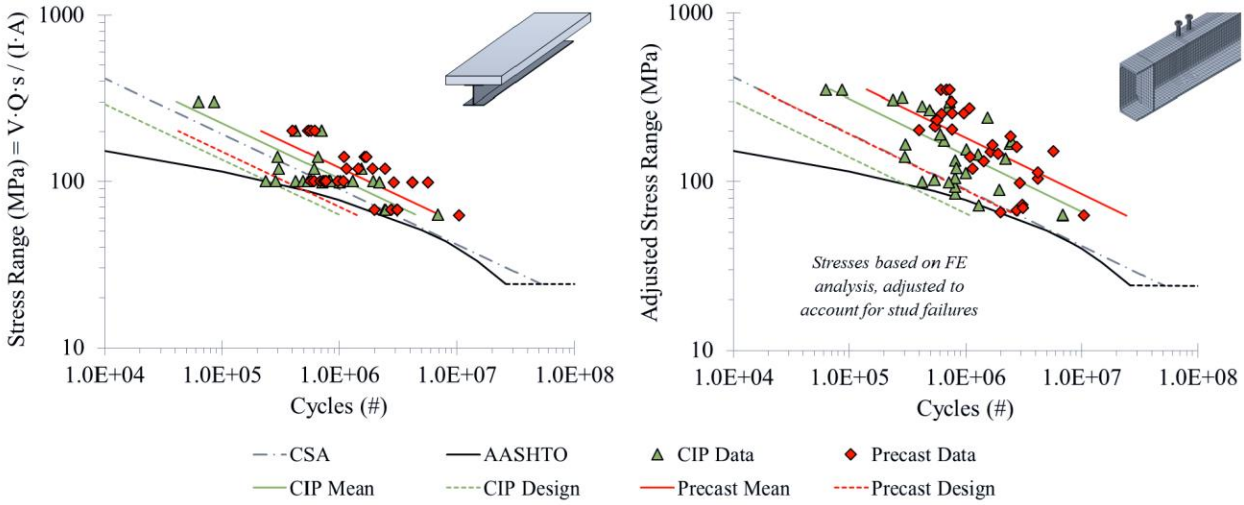

Figure 4-23: Fatigue design curves based on observed stud failures.

5 COMPOSITE BEAM MECHANISTIC MODELLING

A finite element (FE) composite beam model was created to extend the results of the laboratory experimental work to applications in full bridges. The goals of the mechanistic model were twofold: develop a simple and reliable composite beam model using data from the beam specimens tested, and investigate the consequence of one or multiple connector fatigue failures on the structural integrity of a full bridge. The former is presented in this chapter, and the latter is covered in Chapter 6. Specifically, this chapter outlines a composite beam mechanistic model that is validated by the test data and by a more complicated FE model, and presents a compelling use for this model that involves evaluating the performance of connectors using only knowledge of their load-slip behaviour.

5.1 General Modelling Approach

There were several FE models generated throughout the duration of the research project, each with a different level of complexity and a specific application. Models were used to confirm aspects of the experimental design, confirm other models and hand analyses, and aid in the explanation of experimental results. Three models that were developed are listed below, followed by a brief description of the first two. The SAP2000 Model, which was selected as the model to achieve thesis objectives numbers 4 and 5 (investigate bolted connection behaviour, and perform full scale reliability analysis, see Section 1.3), will be the subject of all later sections in this chapter.

- Abaqus Experimental Model (specimen)
- Abaqus Full Bridge Model (full bridge)
- SAP2000 Model (specimen or full bridge)

5.1.1 Abaqus Experimental Model Description

The first Abaqus model developed was a representation of the experimental specimen setup. The model contains non-linear material properties and 8-node solid elements with rigid simple supports. A screenshot of the Abaqus experimental model is shown in Figure 5-1.

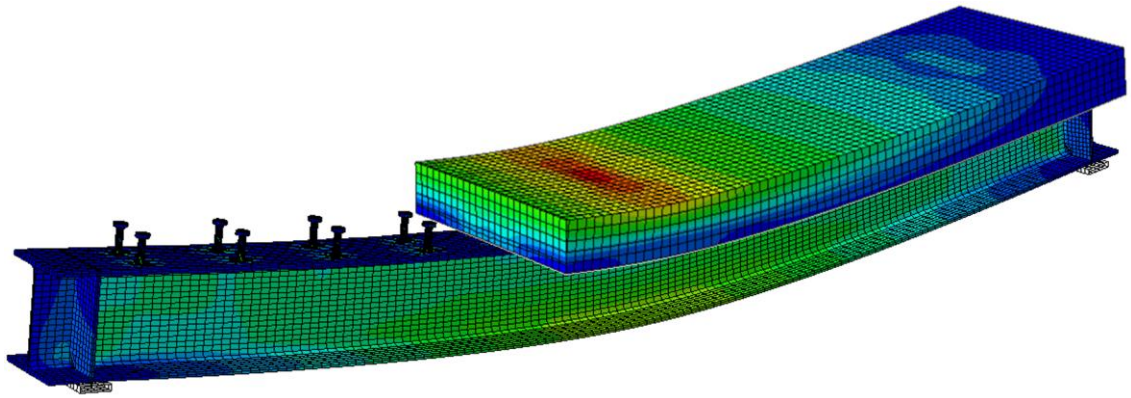

Figure 5-1: Abaqus experimental model.

The initial purpose of this model was to analyze the forces being transferred to the slab with a single static load, to confirm the results of the laboratory beam tests. Further to the initial purpose, the model allowed for the study of the redistribution of stud forces by neglecting certain studs (to simulate failure), and an analysis of the effect of concrete shrinkage on the stud forces through the application of a temperature load on the slab. A similar model was developed by Taylor Porter, and a further description of the model type, as well as results generated from its execution, is included in (Porter, 2016).

5.1.2 Abaqus Full Bridge Model Description

A full multi-span bridge model was also created in Abaqus as it was initially thought necessary to study the system effects of failed connectors in a reliability analysis. The Abaqus scripting feature was used to generate a parametric model that can be adjusted and executed iteratively through text files written in the Python programming language. Figure 5-2 shows a 139 m long three span continuous bridge that was modelled with the program. Shell elements were used to represent the flanges, web, and stiffeners for the steel section, as well as the concrete deck. Slot link connectors with a custom load-slip curve were used to model the shear connectors, and all material was input with non-linear properties. The model was only executed to verify its integrity and accuracy, before it was abandoned due to its comparably long run times and the difficultly with extracting results data as compared to the SAP2000 Model.

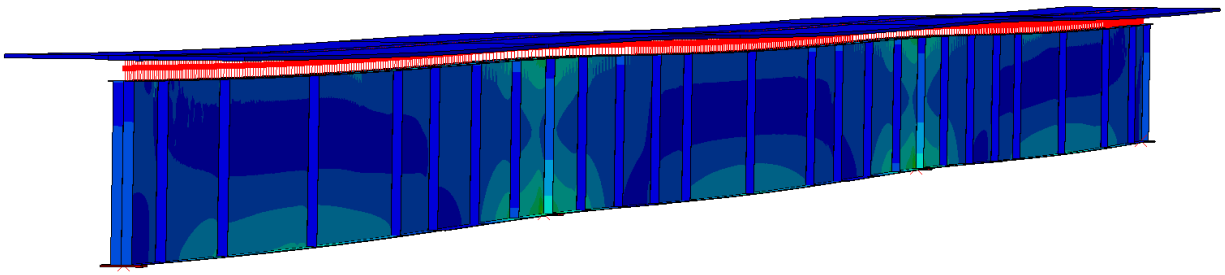

Figure 5-2: Abaqus full bridge girder model.

5.2 SAP2000 Model Description

A SAP2000 model was created to represent both the experimental specimen and a full bridge, and is programmed using the CSi Application Programming Interface (API) (2014). The model works in conjunction with a spreadsheet, which contains necessary geometry and material data. The spreadsheet contains the load-slip properties of the shear connectors, represented as multilinear links with load-slip behaviour defined by the user. This load-slip behaviour is the key variable for this model and will be discussed in detail. The model contains simplifications, including linear elastic material behaviour for the steel and concrete, which allow it to run analyses quickly. As a result, validation of the model was necessary to assess the significance of these simplifications.

Figure 5-3 depicts the prototype composite beam to be modelled and a schematic of the model. The concrete deck is represented by shell elements, while the model uses beam elements for the steel beam.

The two are connected using multilinear link elements representing shear connectors. The model uses a "division" size specified by the user, which splits the deck and steel beam into segments. The division size is recommended to be small (about 25 mm) to allow for versatility in accommodating different connector spacings and for more locations where data is output (link elements can only connect to shell and beam element ends and edges). To prevent ingress (overlap) between the concrete deck and the steel beam, gap link elements were used at every division and given rigid properties in the vertical direction. Friction is not included in the beam model at any point in this research, but is possible to implement by altering the gap link element properties.

The SAP model is set up for parametric analysis, allowing material properties, loading, and geometry (including connector spacing), to be specified by the user. However, for discussion purposes in this chapter, the geometry and loading setup has been set to match the beam specimens from the experimental program described in Chapter 3. Validation was completed using the Abaqus experimental model, as well as the static tests conducted prior to fatigue testing on the experimental beam.

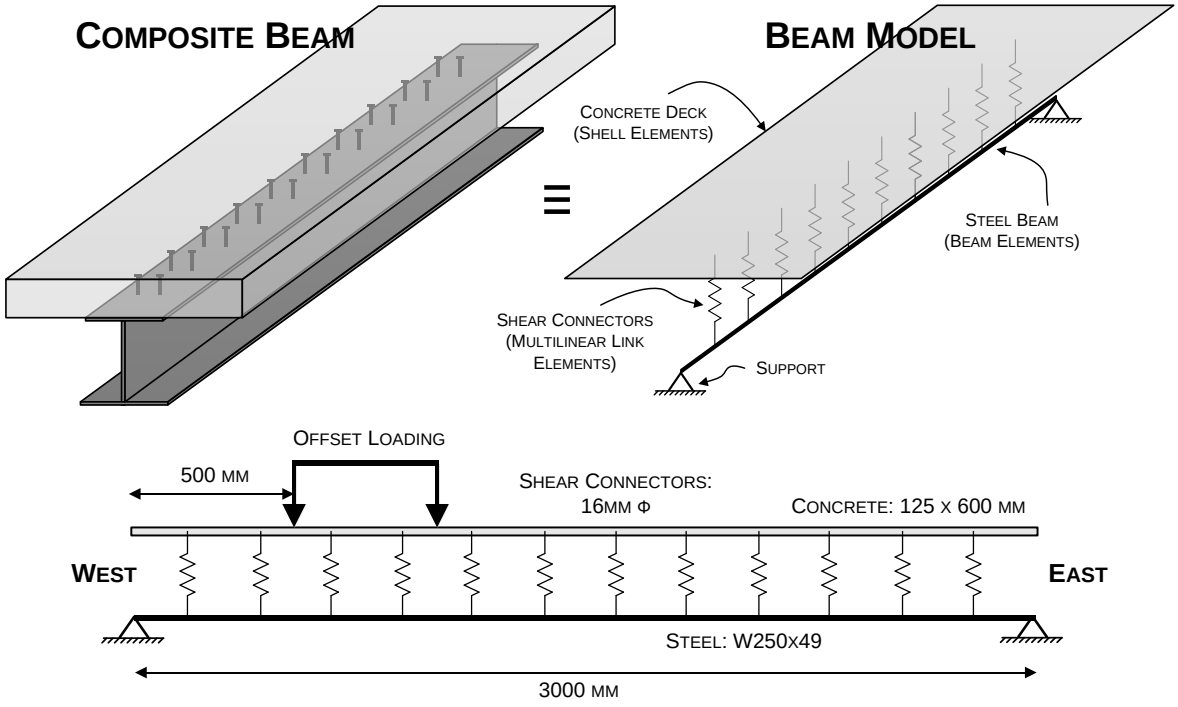

Figure 5-3: FE beam model showing element types, geometry, and loading setup.

5.2.1 Model Geometry and Loading

As stated, the model geometry and loading was setup to match that of the composite beam specimens described in Chapter 3. To recap, the specimens were simply supported with a 3,000 mm span and consisted of a W250x49 steel section connected to a 600 mm wide and 125 mm thick concrete slab. The strength of the concrete was input into the model as 45 MPa, and 24 welded shear studs per beam, each 16 mm (5/8") in diameter, were used at a spacing of 125 mm (2 studs per row). The loading configuration

consisted of two point-loads that were offset from the beam midspan to create a varying shear diagram along the length of the beam. This geometry corresponds to a degree of shear connection of 33%.

5.2.2 Load-Slip Relationships

Five load-slip relationships were used as link inputs for the SAP2000 model to generate the results that will be discussed. Two of these come from push tests completed by Chen et al. in 2013, using studs and through-bolts, and the other three correspond to relationships drawn from the CS, TB, and EB beam tests from the experimental program in this research project. The PS load-slip results were not appreciably different from the CS results, so they were not included in this study. To obtain connector load-slip data from the beam tests, the profile linear variable displacement transducers (LVDTs) were used to obtain slip values for select connectors, and the profile strain gauges on the steel were used to calculate the force in the slab transferred by those connectors. The resulting curves may be more aptly named "force-deformation" curves rather than load-slip, because the loading was not applied directly to the connectors in the way that a push test is performed. Each load-slip curve was approximated by linear segments, following the measured load and slip data. The curves, with loads normalized for a single stud, are shown in Figure 5-4. Each curve is given an abbreviated name for reference (shown in the Figure 5-4 legend). The first two letters correspond to the specimen type (CS, TB, or EB), and the last letter corresponds to the test type (P for push test, and B for beam test). For example, the through-bolt load slip curve derived from push tests is called "TBP". In Figure 5-4 the signs on both axes are given as negative indicating compression from the push tests, but the load-slip relationship holds true for shear transfer in any direction (positive and positive axes would also be accurate).

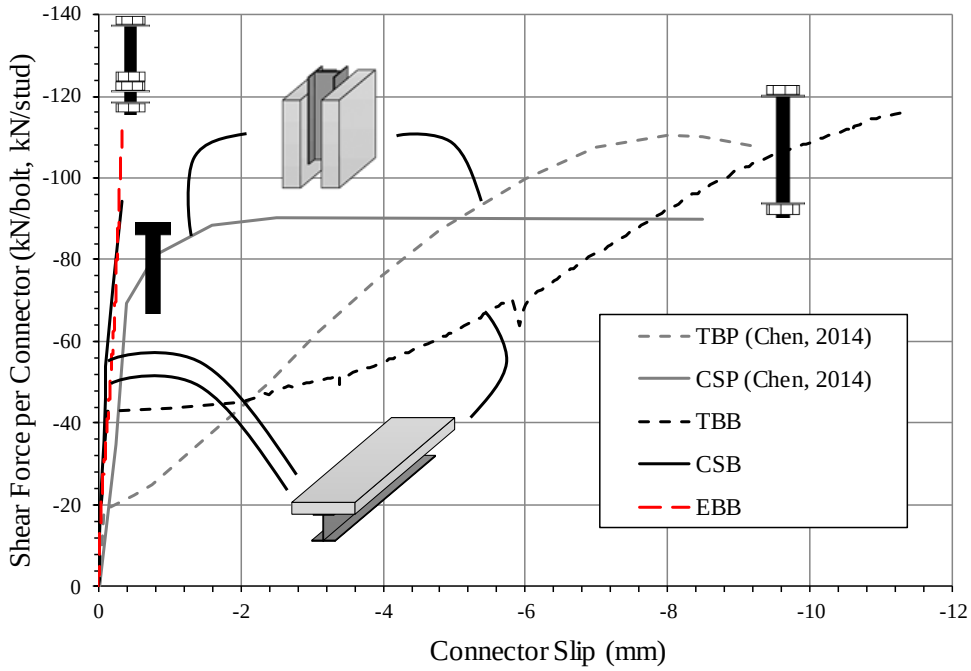

Figure 5-4: Force-deformation (or "load-slip") curves used as SAP model inputs.

Figure 5-5 shows the same load-slip curves over a shorter connector slip length, so that the initial stiffnesses of the curves can be compared. Several things stand out from these figures: the curves derived from beam tests are stiffer than those derived from push tests of the same connector type, particularly in the initial stages of connector slip, and the embedded bolt load-slip curve closely resembles that of the stud for the two beam tests. The higher stiffness in the beam test load-slip curves is a result of boundary conditions and geometry differences in the two tests. Neighbouring studs prevent slip in beams, even as connectors yield, and this does not occur in push tests. The early reduction in stiffness for the through-bolt connector is a result of the bolt slipping into bearing as friction is overcome. After this point, the stiffness is increased again and ductility and strength are achieved through dowel action of the bolt.

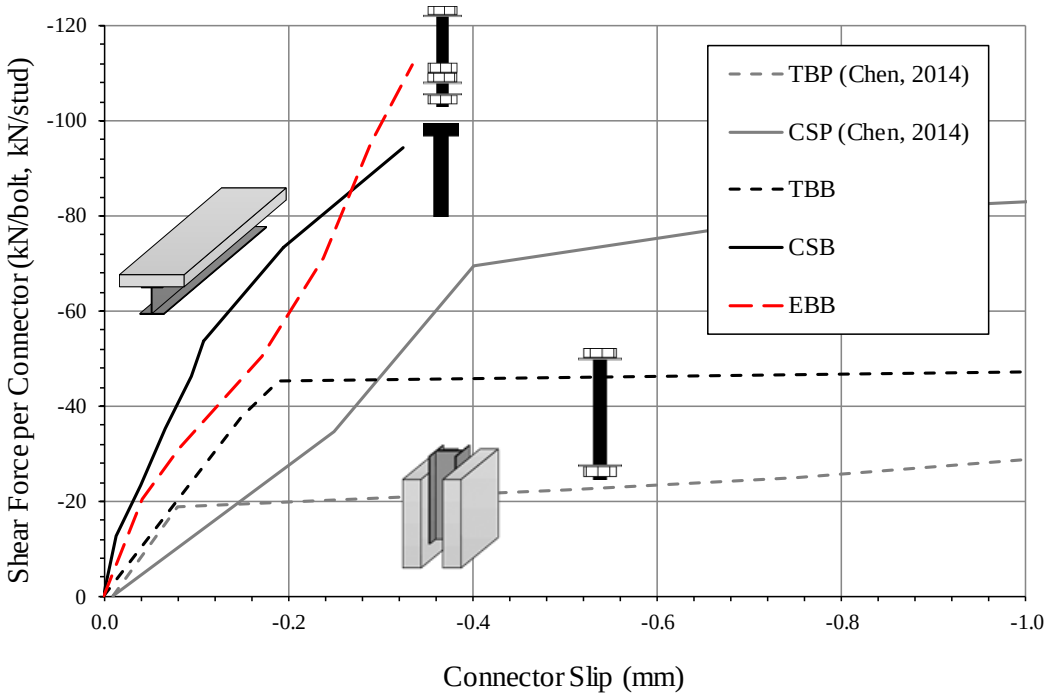

Figure 5-5: Initial slopes of load-slip curves.

5.3 SAP2000 Model Results and Discussion

Results from using the five load-slip curves as model inputs will now be presented and discussed. The goal of this is to show that the model can realistically model composite beam or girder behaviour using only load-slip curve inputs, and to examine the differences in the resulting composite interaction when using bolt or stud connectors. The model will then be a useful tool to evaluate future novel connectors by circumventing the high cost of multiple beam tests, but still evaluating connectors for the composite interaction they are meant to induce. In this way, the model is shown to be a much better shear connector evaluation tool than push tests, which merely serve to provide information about the ductility and strength of a connector through a non-representative test setup.

5.3.1 Comparison of Model Connector Stress and Interfacial Slip Results

A comparison of connector stresses and interfacial slips between the SAP2000 FE results using the five load-slip curves as link inputs will now be shown and discussed. The first objective is to validate the simplified composite beam model. This validation will be done with the CS specimen type since the Abaqus experimental model (described in Section 5.1.1) was built with this connector type. This model, along with the CS experimental test results, are compared with the SAP2000 results. Figure 5-6A shows connector stresses along the beam length for the Abaqus FE analysis, the SAP2000 model with the CSB input, the SAP2000 model with the CSP input, and the experimental results of the CS specimen.

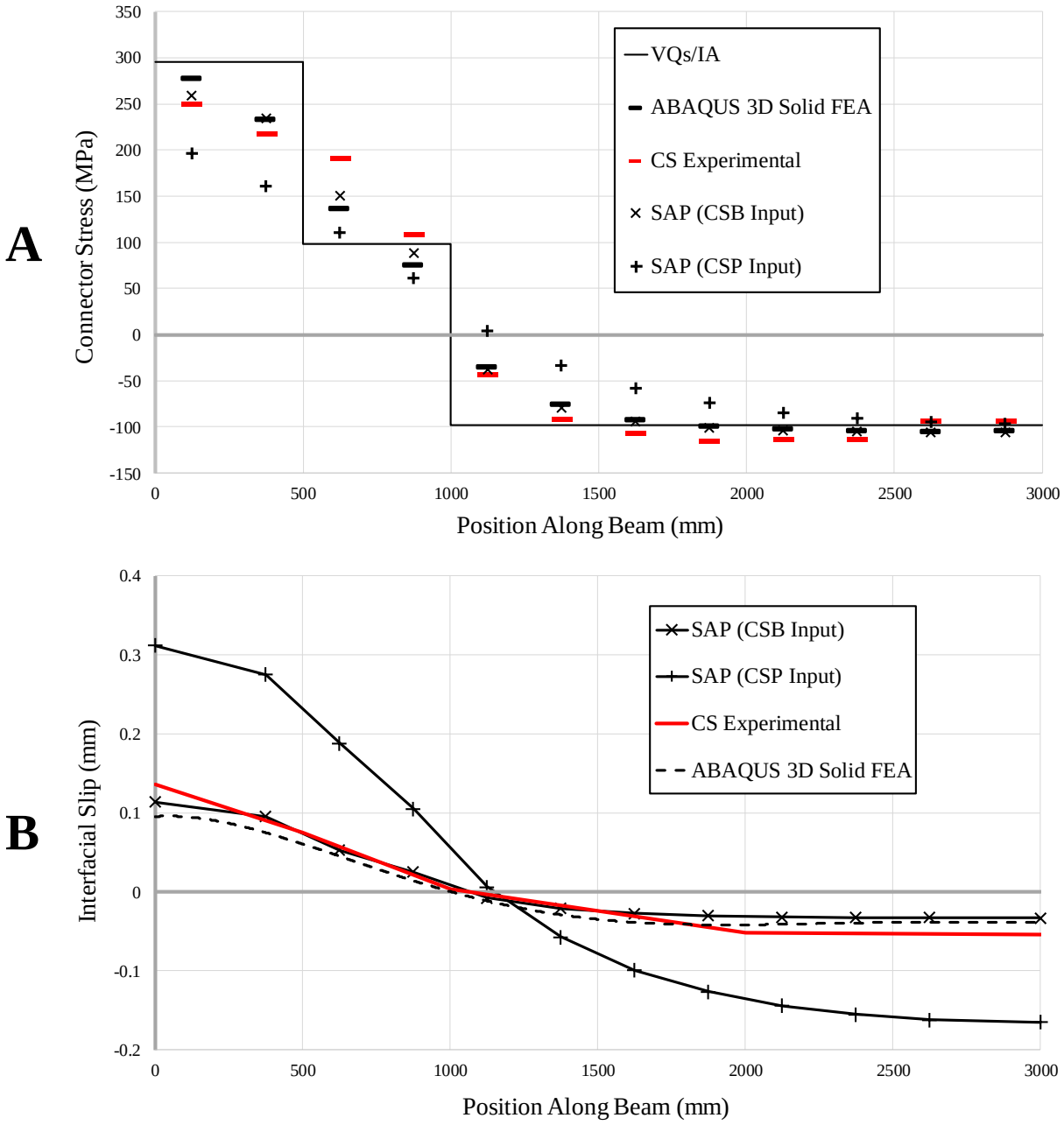

Figure 5-6: CS connector stresses (A) and interfacial slip (B) along the beam for a load of 200 kN.

The stud stresses calculated from elastic theory assuming full composite interaction are also shown. These results correspond to a beam loading of 200 kN (100 kN at both 500 mm and 1,000 mm from the west end of the beam). The elastic stud stresses were computed using Equation 5-1 (a version of Equation 2-5), where *V* is the transverse shear, *Q* is the second moment of area of the transformed section, *s* is the connector spacing, *I* is the moment of inertia of the transformed section, and *A* is the area of the shear connector.

Equation 5-1 $$\tau = \frac{V \cdot Q \cdot s}{I \cdot A}$$

Note the high degree of correlation between the connector stresses predicted by Equation 5-1, the Abaqus model results, the experimental measurements, and the SAP model using the stud beam test (CSB) load-slip curve as the multilinear link input. The SAP model results are within 5% of the Abaqus FE results and 12% of the experimental measurements on average. This confirms that the use of beam test load-slip curves data as model inputs will result in accurate composite interaction modelling. However, using the stud push test (CSP) load-slip curve results in significantly lower stresses (on average 30% lower than when using the beam test load-slip curve). Using push tests to approximate the interface shear resistance will result in an underestimation of connector stiffness and force.

In addition to examining stud connector stresses, the interfacial slip values along the length of the beam can also be compared. Figure 5-6B shows the predicted slip values for the SAP models with CSB and CSP inputs, the Abaqus model, as well as the CS experimental test results. It is apparent that the SAP model using the stud beam test load-slip curve gives slip values that are similar to the solid Abaqus model and the experiment, but the SAP model results using the push test load-slip curve gives much larger slip values.

With a validated model, the model use may be extended to the other three connector load-slip curves presented in Section 5.2.2. Figure 5-7 presents connector stresses along the beam length for the SAP2000 model using all five load-slip inputs. The embedded bolt (EB) connector forces fall in between those of the studs and the through-bolts, consistent with what was observed in the experimental program. Notable here is the sharp decrease in through-bolt connector forces when using push test load-slip data as model inputs as compared to beam test data. While both the TBP and TBB load-slip curves have a plateau of reduced stiffness after bolt slip occurs, the TBP plateau begins sooner; the load of 200 kN used to display the connector forces was enough to cause the through-bolts to slip under a push test load-slip assumption, but not a beam test constitutive assumption.

5.3.2 Comparison of Model Degree of Composite Interaction Results

While connector stress and slip are important metrics, the primary goal of the analyses is to assess the connectors in terms of the degree of composite interaction they induce. Figure 5-8 shows the degree of composite interaction along the beam length, according to the definition shown in Figure 2-4 and given in

Equation 2-2. Interaction values along the beam length vary significantly, reflecting the restraint of slip around the leading face of each connector, and less restraint on the trailing face. The "leading" connector face is the one farthest from the maximum moment (in this beam the maximum moment is 1,000 mm from the west end, denoted as the zero position along the beam).

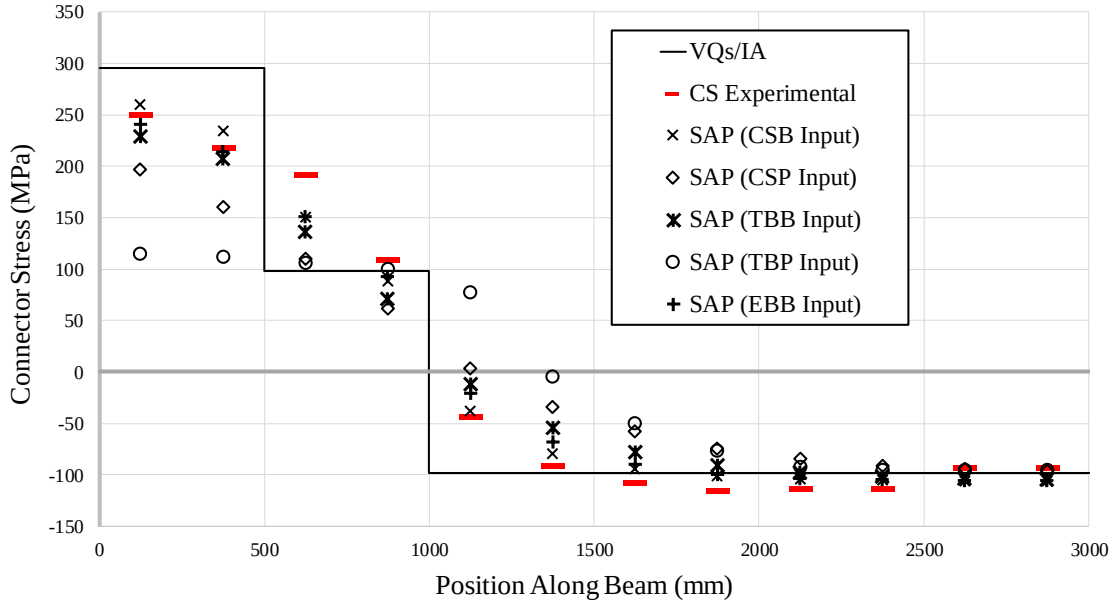

Figure 5-7: Connector stresses along the beam for a load of 200 kN.

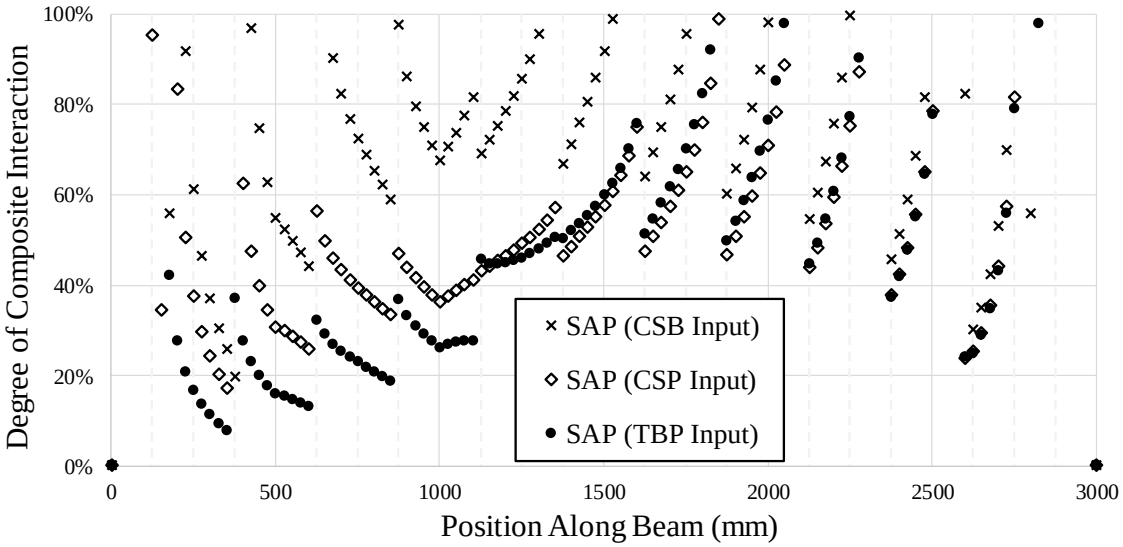

Figure 5-8: Degree of composite interaction along the beam length for a load of 200 kN.

In general, the analysis results using the stud beam test load-slip curve to define the link elements shows higher values of composite interaction, with an average value of 69.6%, whereas using the stud push test curve links averaged 50.4%. Both show a parabolic trend, with the degree of composite interaction peaking around midspan. To explain the increased interaction near the point of maximum moment and the midspan one must look to Figure 5-6, and observe where there is the lowest amount of slip for the highest connector

force. The amount of composite interaction at any point is completely driven by the compatibility of displacements, which is why the type of load-slip curve used to define the flexibility of the connector is so important to the results. All three results also exhibit larger variation toward both ends of the beam. This is because the percentage difference in the compressive force in the slab is larger on either side of the outside connectors (those toward both beam ends) than it is on the inside connectors.

The difference between the stud push test results and the through-bolt results can again be seen primarily on the west end of the beam, where the slip is highest. Prior to the initiation of slip in the through-bolt connection (at a connector load of about 19 kN for TBP, see Figure 5-5), the stiffness of a stud and a through-bolt connector are comparable. As a result, in the region of the beam where bolt slip has not occurred (from about 1,300 to 3,000 mm), similar levels of composite interaction develop. Composite interaction results have only been shown for three of the five load-slip inputs to preserve plot clarity, but similar observations can be made with all results.

5.3.3 Summary of Results

Table 5-1 summarizes the key outcomes from using each of the five shear connector load-slip inputs. These key outcomes include deflection, average degree of composite interaction, and maximum steel stress at the bottom flange. Comparing the SAP model results to each other, it is readily apparent that those based on beam test load-slip data feature higher levels of composite interaction, and lower deflection and steel stress. Differences in the maximum stress in the beam are small compared to differences in the degrees of composite interaction, because the maximum stress occurs where the beam moment is highest and shear is lowest; composite interaction is most affected in areas of high shear where slip has accumulated. The maximum moment is, by definition, the end of the shear span and the location where the interfacial slip vanishes.

Table 5-1: Summary of beam behaviour outcomes using different load-slip curves as inputs (200 kN).

Model Load-Slip Input:	CSB	CSP	TBP	TBB	EBB
Maximum Deflection	2.14 mm	2.68 mm	2.86 mm	2.35 mm	2.22 mm
Average Degree of Composite Interaction	69.6%	50.4%	44.4%	62.7%	66.1%
Maximum Steel Stress	101.2 MPa	109.1 MPa	112.8 MPa	104.7 MPa	102.6 MPa

A simple FE model has been presented in this chapter, which allows for the input of a load-slip curve for a given shear connector type and outputs beam behaviour including degree of composite interaction, deflection, material and connector stresses, and interfacial slip. The load-slip curve input can be in the form of force-deformation data from a beam test, or load-slip data from a push test. In the following chapter, this FE model will be put to use in a full bridge girder reliability analysis.

6 RELIABILITY ANALYSIS OF STUDS IN COMPOSITE BRIDGE GIRDERS

In this chapter, a modified version of the composite beam model presented in the preceding chapter is used to assess the reliability of stud shear connectors designed using current code provisions, and to suggest modified design procedures based on the reliability analysis results. The design of shear connectors involves a deterministic calculation, with each stud assumed to have the same specific strength (that associated with the 50% survival probability curve based on the push test data). Only individual stud failure is considered according to the current design practice, with no interaction between ultimate strength and fatigue strength considered. The analyses presented in this chapter consider the probabilistic characteristics of both the welded stud resistance and the highway traffic loading. Additionally, the effect of stud fatigue failures on the ultimate capacity of the bridge is considered. Observations are made using an example bridge, designed according to current code provisions. The results of this portion of the study culminate with key observations and point towards a revised design procedure, calibrated for the level of reliability upon which the Canadian Highway Bridge Design Code (CSA S6, 2014) is based.

6.1 Reliability Analysis Using Simulation

6.1.1 Fundamental Reliability

Prior to completing reliability analyses for the stud shear connection, it is necessary to define or review what is meant by “reliability” and define the specific reliability problem for the stud shear connection failure. A description of the pertinent analysis parameters is also necessary. To begin, “safety margin” will be discussed. The safety margin has to do with a limit state function, which corresponds to the boundary between desired and undesired performance of a component, structure, or system (Nowak & Collins, 2012). When considering the ultimate limit state (ULS), this undesired performance corresponds to an unsafe situation. If we define *R* as the resistance of a component (or “capacity”), and *Q* as the load effect on that component (or “demand”), then *g*, the limit state function (or safety margin), can be defined as the difference between the two, given in Equation 6-1 .

Equation 6-1 $$g(R,Q) = R - Q$$

If *g* is greater than zero, the component, structure, or system in question is safe, but if *g* is less than zero, there is a negative safety margin, and an unsafe situation exists. The factor of safety, *FS,* is closely related to the margin of safety, but it is the ratio of the resistance (*R*) to the load effect (*Q*), rather than the difference.

Equation 6-2 $$FS(R,Q) = \frac{R}{Q}$$

Often both *R* and *Q* are continuous random variables (RVs), each having a probability density function (PDF). If this is the case, then *g* is also a random variable with a PDF, and the three RVs can be represented

graphically, such as in Figure 6-1. The probability of failure is the probability that *g* is less than zero, or the area underneath the PDF of *g* to the left of zero, as shown in Figure 6-1.

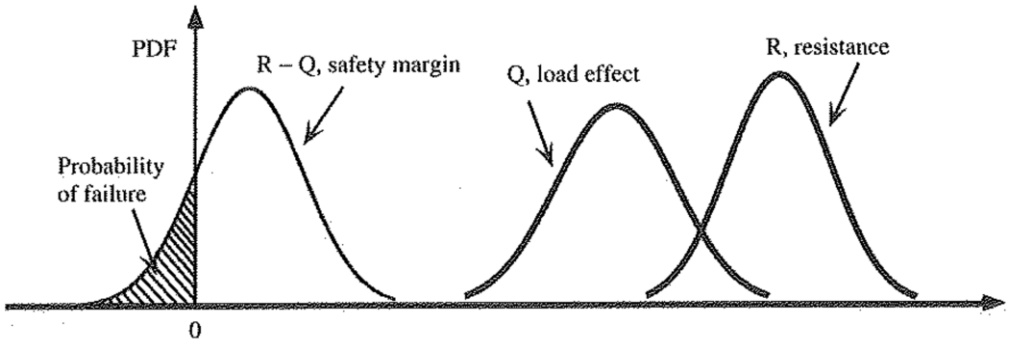

Figure 6-1: PDFs of load, resistance, and safety margin (Nowak & Collins, 2012).

In general, a component, structure, or system is more reliable if the probability of failure is low, which is the case when both the average safety margin is high, and the variation in the safety margin is low. A measure of this reliability is called the reliability index, denoted by β. The reliability index is the number of standard deviations of *g* between the mean value of *g* and the first point of failure ($g = 0$). Assuming that *g* is normally distributed, β is given by Equation 6-3, where μ and σ are the mean and standard deviation of *FS*, respectively.

Equation 6-3
$$\beta = \frac{\mu - 1}{\sigma}$$

If *g* is lognormally distributed, β is given by Equation 6-4, where λ is the mean of ln(*FS*), ζ is the standard deviation of ln(*FS*), and *V* represents the coefficient of variation of *FS* (σ/μ).

Equation 6-4
$$\beta_{LN} = \frac{\lambda}{\zeta} \approx \frac{\ln\left(\frac{\mu}{\sqrt{1+V^2}}\right)}{\sqrt{\ln\left(1+V^2\right)}} \qquad \lambda \approx \ln(\mu) - \frac{1}{2}\zeta^2 \quad \text{and} \quad \zeta \approx \sqrt{\ln\left(1+V^2\right)}$$

6.1.2 Fatigue Resistance and Demand for Stud Shear Connections

The discussion in the previous subsection will now be applied to the reliability problem of the fatigue failure of a stud shear connection. In this problem the fatigue resistance variable *R* is the total number of load cycles a particular shear connection can withstand prior to failure, and the fatigue demand variable *Q* is the total number of load cycles applied to the connection for the lifetime of the bridge. Strictly speaking, for this problem *Q* should not be thought of as the load effect, since load effects are encapsulated within *R*. Hence, the term “demand variable” is used. The function *g* represents the number of cycles in reserve when it is positive, or it represents failure, when it is negative. Definitions will now follow for what one load cycle on the shear connection corresponds to physically, as well as failure of a shear connection.

The passage of a truck over a bridge will generally cause a single large load cycle for a shear connector. However, the exception to this rule is a very short span or a cantilevered span where individual truck axles and vibrations play a significant role. Every load cycle is comprised of a peak shear load and minimum shear load as the connector resists interfacial slip. During the passage of a truck on a typical simple span composite bridge the peak and minimum loads are of opposite sign. The magnitude of load during the load cycle is the algebraic difference between this peak (maximum) and minimum. For the purposes of reliability analysis in this chapter, each cycle corresponds to the passage of a truck over the bridge (a discussion is included at the end of the chapter to address this assumption).

Shear connection failure means that the connection ceases to perform its intended function of allowing adequate composite action through the transfer of longitudinal shear forces. Shear connections are comprised of many studs; therefore, the connection may still perform its function after the fatigue failure of one or more studs. In fact, it will be shown in this chapter that over 50% of the studs in a typical highway bridge may fail before safety is a concern. The total resistance of the connection, R, is the sum of the number of cycles required to fail the first connector, and the subsequent number of cycles required to fail each subsequent connector until safety becomes a concern.

For a given bridge, the resistance of the stud shear connection is comprised of several random variables, which together dictate the number of cycles until failure. These include:

- the fatigue resistance of each stud,
- the weight of the trucks crossing the bridge,
- the dynamic load factor for the trucks (also called the dynamic load allowance, DLA), and
- the girder distribution factor (also called the transverse amplification factor).

Normally, only the first variable in the list would be classified as a resistance variable, since the latter three have more to do with the load and its associated affect on the shear connection. However, for the formulation of this fatigue reliability problem, it is convenient to group these together into the random variable R.

The fatigue demand variable, Q, is the total number of cycles or in other words the total number of trucks that will cross the bridge in its service life (a variable called N_c in CSA S6, 2014). This is a random variable, but due to limited knowledge, the deterministic code design value will be used for the purposes of this chapter. This value only depends on the number of design lanes on the bridge, the design life of the bridge, and the expected average daily truck traffic (ADTT), as well as the assumed number of cycles per truck passage, N_d. Equation 6-5 shows that Q is equal to the product of N_d (the design number of cycles per truck passage), p (a scaling factor equal to or less than 1 accounting for multiple design lanes), y (the design life of the bridge in years), and ADTT. The value of Q is 87.6 million cycles for a typical simple span composite bridge (N_d = 1) with three design lanes (p = 0.80), a typical service life of y = 75 years, and a design ADTT of 4,000 (the CSA S6 design value for Class A highway bridges).

Equation 6-5 $$Q = N_c = N_d\, p(ADTT)365y$$

If *Q* is assumed to be deterministic, the distribution of *g* takes the same form as the distribution of *R*. For the stud shear connection this distribution will be shown to be lognormal later in this chapter.

6.1.3 Simulation Procedure

The Monte Carlo Simulation (MCS) method is necessary to determine *R* due to the great number of random variables involved in the stud shear connection problem and the geometrical complexity encountered in solving for connector stresses during the fatigue life of a bridge. Although it may appear that there are only four RVs (as shown by the list in the previous subsection), a closer inspection reveals that *each stud on the bridge* represents a random variable on its own (stud strengths are independent and identically distributed variables, or IIDs), because each stud on the bridge is in a unique location. This problem is similar to a "*k*-out-of-*n*" reliability problem, where a certain number of studs, *k*, must function out of the total (*n*) for the system to function (Eryilmaz, 2019).

The approach taken to assess the reliability of the stud shear connection in this chapter is to use an example bridge, designed according to the current CSA S6 rules for the fatigue of shear studs. This example bridge will be represented using the FE model presented in Chapter 5 of this thesis. The FE model will be used to determine the failure order and stress history of each stud on a bridge as stud fatigue failures occur. This can be done for the deterministic case, where each of the RVs in the problem take on their mean values for a single trial to test the fatigue life of the stud shear connection, or it can be done probabilistically, where each variable is assigned a random variate for every failure trial, and many trials are completed in order to estimate the distribution of *g* and the overall reliability of the connection, *β*.

The random variables used in the model and their associated statistical parameters are given in Table 6-1. For the MCS procedure, a new bridge geometry is given at the start of every trial consisting of studs with random strengths according to the statistical strength distribution observed during the beam testing program described in Chapter 4 of this thesis. A moving load analysis is performed for a fatigue code truck with a random weight, DLA, and distribution factor. The number of cycles until failure of the most vulnerable stud (stud with the lowest number of cycles until failure based on the stud stress range and fatigue strength) is calculated, and then that stud connector is reprogrammed with a reduced stiffness to simulate failure. Damage is calculated for each of the other studs for use in a miner's sum calculation, which will be repeated after every analysis for each stud that has not failed. A new trial then begins with the modified bridge geometry, and subsequent stud failures are determined using the accumulated damage calculation. Each trial consists of a full shear connection failure, including the failure of many individual studs (close to 50% of the studs). A new fatigue code truck weight, dynamic load allowance factor, and girder distribution factor are sampled every 20 million cycles; in this way, a single effective truck load is used for many cycles at a time, but a random sampling is still maintained over the life of the bridge. While these variables are

properties of a given structure, and not a given truck, they may change over the length of the structure (for different studs), or over time (with truck routes changing) so sampling multiple variable values is considered appropriate. A single trial for the simulation procedure can be summarized with the following steps:

1. All studs on the example bridge are assigned random strengths (based on experimental data),
2. An effective truck load is sampled and applied to the bridge in a moving load analysis,
3. Stud stress ranges are recorded, and the number of cycles until failure is calculated for each stud (using Equation 2-7), N_i,
4. The lowest calculated N_i value is saved as N_f, and damage is calculated for all studs using this N_f (the failed stud has a damage of 1, and all other studs sustain damage of N_i/N_f),
5. The failed stud is reprogrammed to have a reduced stiffness reflecting failure, and steps 2 through 5 are repeated until a critical number of studs have failed, resulting in a failed shear connection.

Table 6-1: Probabilistic MLA simulation variables.

Variable Description	Symbol	Mean Value	COV (%)	Source
Stud Fatigue Curve Intercept	*logC*	12.33	4.1%	UW Beam Tests (Ch 4)
Fatigue Code Truck Weight	--	0.52*[CL-625 ONT]	6%	CSA S6 Commentary (2014)
Dynamic Load Allowance Factor	DLA	1.25	11%	Nyman & Moses (1985)
Girder Distribution Factor	F_v	0.676	13%	Nyman & Moses (1985)

The remainder of this chapter is devoted to the description of the example bridge, and a discussion of the reliability analysis results.

6.2 Example Bridge Characteristics

The bridge used to assess the reliability of existing shear stud design procedures consists of a concrete deck on steel girders. This bridge type is very common in North American, particularly for medium spans. The bridge is simply-supported with a span of 30 metres, and has a 225 mm thick, 30 MPa concrete deck atop six steel girders, which have a spacing of 2.5 metres on centre. There are three design lanes on the bridge supporting a Class A highway in Canada. The CSA S6 “code truck” used for analyses was the CL-625-ONT Truck (see Clause A3.4.1 of CSA S6, 2014). The geometry of an interior girder is shown in Figure 6-2, and features a constant cross-section along the bridge length for simplicity. For the design of the shear studs, headed studs, 22.2 mm (7/8-inch) in diameter were used in rows of two.

All new highway bridges in Canada are required to be designed as Class A unless otherwise approved (CSA S6, 2014), because the cost of retrofitting a bridge to bring it to Class A standards far exceeds the cost of designing and building it for the highest use case initially. These bridges have an average daily truck

traffic (ADTT) of 4000 trucks over a design life of 75 years, resulting in about 100 million cycles, depending on the number of design lanes on the bridge. For the current CSA S6 design curve, a stud experiencing over 50.2 million cycles is designed at the endurance limit (horizontal line at the right of Figure 2-8). It follows that the importance of the stud fatigue design curve is concentrated in the endurance limit value, where most stud designs fall.

Elements of the design procedure for the studs will be shown in order to highlight the disparity between the number of studs required to satisfy the ultimate limit state (ULS), and the fatigue limit state (FLS), and to highlight certain assumptions implicit in the procedure. Although the procedure from the CSA S6 code is used, the procedure from the AASHTO code is similar. Table 6-2 shows various design values used in the design calculations.

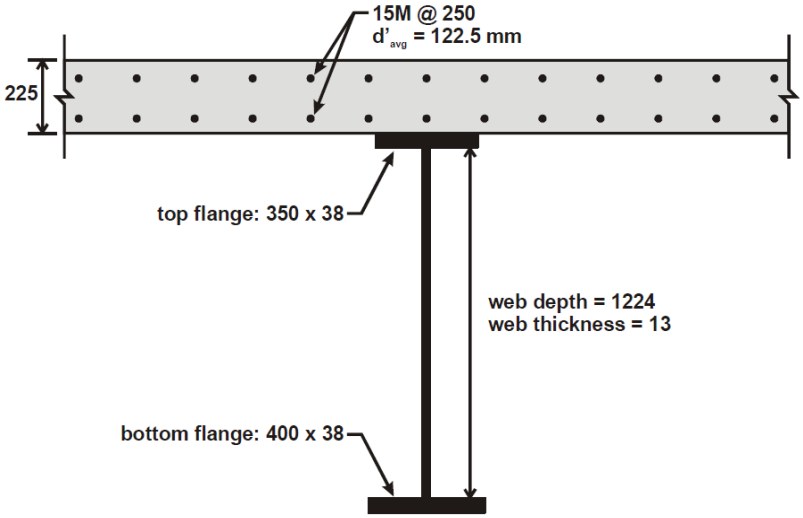

Figure 6-2: Interior girder cross-section.

Table 6-2: Reference table for example bridge design values.

Variable Description	Symbol	Value	Units
Stud ultimate strength	F_U	415	MPa
Concrete modulus of elasticity	E_C	25,588	MPa
Compressive force in slab at midspan (ULS)	$C_C + C_R$	10,978	kN
Design life cycles	N_C	$87.6 \cdot 10^6$	cycles
Fatigue code truck factor	-	0.52	-
First moment of area of the transformed slab about the elastic neutral axis of the transformed section	Q	$21.244 \cdot 10^6$	mm^3
Transformed moment of inertia	I_T	$30.340 \cdot 10^9$	mm^4
Resistance factor for concrete/steel/shear connectors	$\Phi_c/\Phi_s/\Phi_{sc}$	0.75/0.95/0.85	-

The stud ultimate strength of 415 MPa matches that of a Type B stud, prescribed by CSA S6 (Cl. 10.4.7, 2014). The modulus of elasticity of concrete comes from an assumed 28-day concrete strength of 30 MPa and a calculation given in Cl. 8.4.1.7 of CSA S6 (2014). The compressive force in the slab at the location of maximum moment (midspan) for the ultimate limit state was calculated to be 10,978 kN; the plastic neutral axis is in the steel top flange for this condition, indicating no web local buckling of the Class 3 web, and allowing fully plastic behaviour. The design life cycles, N_c, was calculated using Equation 6-5. The fatigue code truck factor of 0.52 is given by CSA S6 (2014) and is shown in Table 6-1. This calibration factor accounts for the difference between the design truck, and the trucks that cause fatigue damage (more information can be found in the CSA S6 Commentary, CSA S6.1 C10.17.2.2, 2014). Both Q and I_T are derived from the section geometry, shown in Figure 6-2, and the material resistance factors for concrete, steel, and shear connectors, are prescribed by CSA S6 in Cl. 10.5.7 (2014).

6.2.1 Ultimate Limit State Design

The number of shear studs required for ULS can be determined considering the amount of horizontal shear that must be transferred into the slab of a composite girder to develop the full flexural capacity of the cross-section (considering steel to be “elastic perfectly-plastic” and using the equivalent stress block method for concrete). In Table 6-2 this value is given as 10,978 kN. The static strength of an individual stud, for the 22.2 mm stud diameter, is calculated in Equation 6-6, and taken as the lesser of the maximum force limited by the stud steel at ultimate capacity, and the crushing of the deck concrete:

Equation 6-6
$$q_r = 0.5\phi_{sc} A_{sc} \sqrt{f'_c E_c} \leq \phi_{sc} F_u A_{sc} = 144.1 \text{ MPa}$$

In Equation 6-6, the first term of the left side of the inequality represents concrete crushing, and the right side represents the limited strength of the steel stud. For 30 MPa concrete, the concrete strength is the limiting factor. The total number of studs required on the girder (two shear spans) is given below:

Equation 6-7
$$\#Studs\ (ULS) = \#Shear\ Spans\left(\frac{C_c}{q_r}\right) = 2\left(\frac{10{,}978 \text{ kN}}{144.1 \text{ kN}}\right) = 154 \text{ studs}$$

Equation 6-7 is in accordance with Cl. 10.11.8 of CSA S6 (2014), which also states that shear connectors may be spaced uniformly, or according to the variation in the interface shear. An assumption is made in the design that each connector has sufficient ductility to reach maximum strength at the same time, regardless of spacing and interfacial slip distribution.

Although the total horizontal shear force necessary to develop the capacity of the cross-section is required by code to be able to be transferred, a partial shear connection is sufficient to carry factored loads in most cases. In CSA S16 “Design of steel structures”, the minimum partial shear connection permitted is 40% (CSA S16, 2014). When considering the reliability of the shear stud connection in the current study, it is suggested that this partial degree of shear connection may be relied upon in the event of multiple shear stud fatigue failures. Figure 6-3 illustrates the loss of ultimate strength capacity, M_r, with partial shear connection levels ranging from a full connection to the non-composite case. The sharp decline below a 10% connection is due to the slenderness of the Class 3 web in the example bridge plate girder.

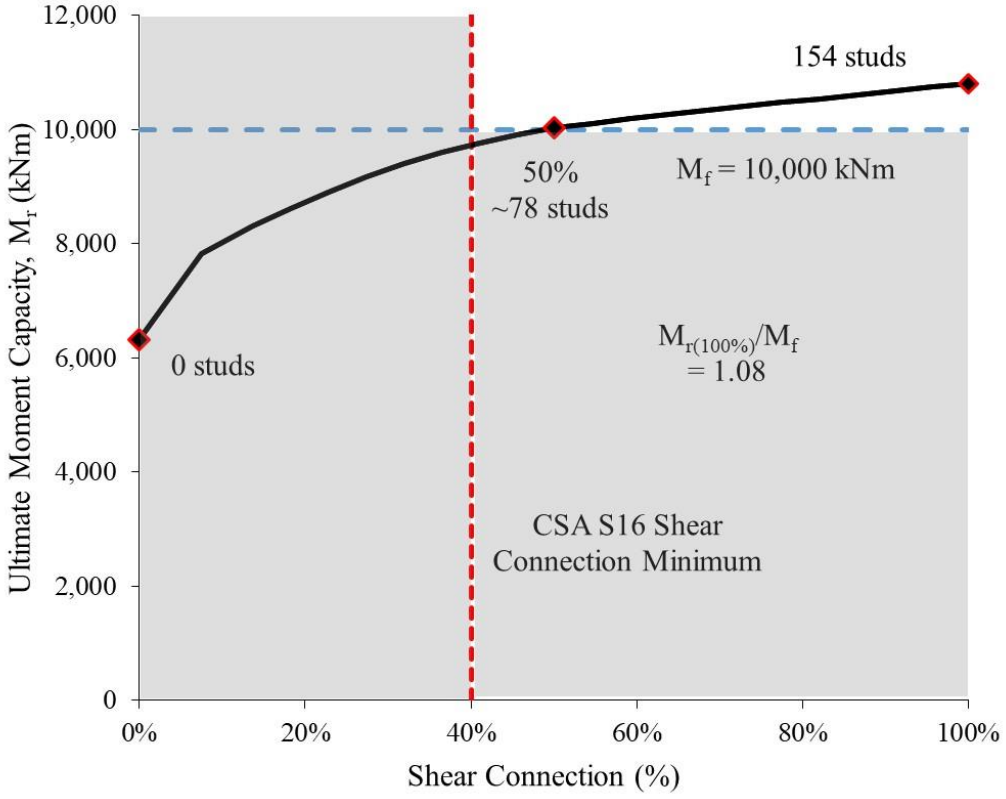

Figure 6-3: Ultimate capacity of the bridge girder with varying shear connection.

Figure 6-3 also shows M_f, the factored design moment at ULS. The ratio of M_r with a 100% shear connection to M_f is a potentially key factor when considering the reliability of the shear connection in fatigue. The closer the ratio is to a value of 1.0, the less tolerance a girder has for the degradation of the shear connection. However, it should be kept in mind that the structure will probably have far more studs than required even for $M_{r(100\%)}$ under the current code fatigue requirements (this will be demonstrated in the following subsection). Also of note, since the curve in Figure 6-3 is relatively flat on the right-hand side, even a ratio of 1.08, which is present in the current example, is enough to allow a shear connection degradation to the 50% level (approximately 78 studs) from 154 studs, with the structure still having sufficient ULS capacity. As stated earlier, fatigue design limits will almost certainly govern shear stud design and the number or

studs required will exceed the 100% shear connection amount often by more than a factor of two, allowing significant degradation before any ULS concerns arise.

6.2.2 Fatigue Limit State (FLS) Design

The procedure to calculate the number of studs required at FLS under the current code provisions will now be demonstrated. This procedure involves ensuring that the calculated stud stress range, τ_{rs}, is below the allowable stress range for the number of cycles expected. While the allowable stress range is a constant value, which can be determined from the CSA S6 fatigue curve, the calculated stud stress range varies with the design longitudinal shear force range (V_{sr}) and the stud spacing as given in Equation 6-8.

Equation 6-8
$$\tau_{rs} = \frac{V_{sr} Q}{A_{sc} I_t}\left[\frac{s}{n}\right]$$

In Equation 6-8, n is the number of stud connectors per row on the girder top flange and s is the row spacing. Other variables in Equation 6-8 are given in Table 6-2. The design shear force range can be determined for each stud location from the moving load envelope of shear from the passing of the design truck, including the dynamic load allowance (DLA). The design longitudinal shear force range for fatigue is the fatigue truck code factor (Table 6-2) multiplied by the total range of shear force per girder as the design truck passes over the bridge, V_g. The latter can be computed based on the shear value per design lane, V_T, using the transverse amplification factor (girder spacing, S, divided by the truck load distribution width, F, equal to 0.675 for the example bridge, see Table 6-1).

Equation 6-9
$$V_{sr} = 0.52 V_g = 0.52\left[\frac{S}{F}\right]V_T$$

The design shear force range (V_{sr}) is directly proportional to the stud stress range provided the bridge cross-section and stud row spacing remain constant, as shown in Equation 6-8. Multiple stud row spacings are normally chosen for material and labour savings where the design shear forces are lower (spacing may follow variations in interface shear as noted in Cl. 10.11.8 of CSA S6). In Figure 6-4, an economical spacing plan for the example bridge is shown, along with a comparison between the allowable stress range and the elastically calculated stress range commonly used in design (from Equation 6-8).

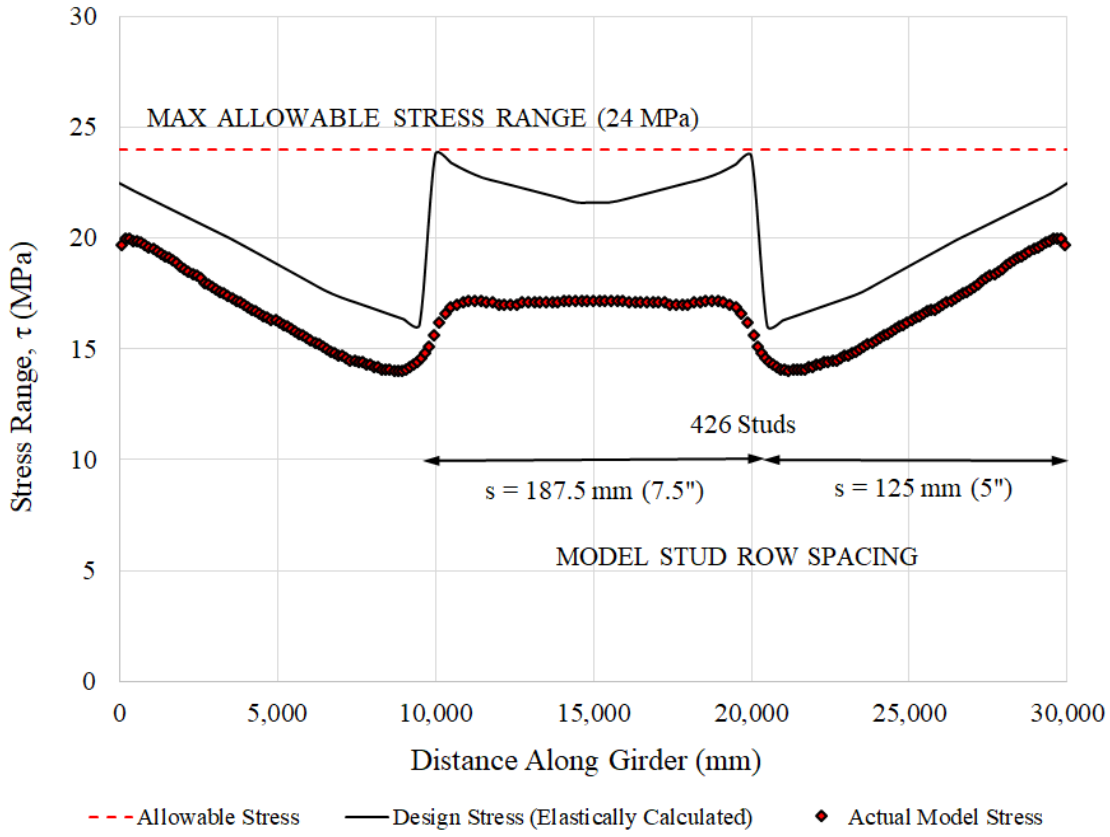

Figure 6-4: Allowable and design stud shear stresses.

Rather than computing the stress on each connector in an elastic manner, using Equation 6-8, the stress can also be determined using the design spacing in an FE model and finding the resulting stud stresses. These are shown in Figure 6-4 for the SAP2000 FE model. The actual stress ranges are 15-30% lower than those expected by calculation. The reason for this is that the elastic stress calculation assumes 100% composite interaction. Studs, like any other mechanical shear connector, require deformation to resist shear force and this results in less interfacial shear force to be transferred due to compatibility.

The allowable stress range for the welded studs is 24 MPa, which is the product of the endurance limit for a 'Category D' detail, and 0.52. The 0.52 factor, called the "fatigue code truck factor" in Table 6-2, represents the proportional weight of an "equivalent" truck for fatigue design compared to the 625-tonne code truck. More specifically, the factor is meant to describe the proportion of fatigue damage done by the average truck cycle compared to the damage from one passage of the code truck on the bridge. To recap, any bridge designed in Canada that will experience more than 50.2 million cycles over its design life requires studs to be designed at this 24 MPa endurance limit to ensure that the heaviest trucks do not exceed the real constant amplitude fatigue limit (CAFL) of 48 MPa. The example bridge is expected to experience 87.6 million cycles as a Class A bridge; if Class B were used, the number of design cycles would change to 21.9 million and the allowable stress would increase 33% to 32.1 MPa.

6.3 Reliability Analysis Motivation

The two-spacing plan shown in Figure 6-4 of 125 mm and 187.5 mm uses two connectors per row (n = 2) and results in a total number of 426 shear connectors. This is almost three times as many connectors as required for code compliance of a 100% shear connection (154), and more than five times than that required for strength purposes (78). With the close spacing of studs required under the current code fatigue provisions, bridge constructors may have difficulty fitting in transverse rebar, and material and labour costs for stud welding will be high. It is therefore essential that the following reliability analysis be conducted, to discover if the great number of studs provided is necessary to achieve the CSA S6 (2014) targeted reliability index. The first objective of this chapter is therefore to estimate the reliability of shear connections designed under the current rules, and the secondary objective will be to propose modified design rules to bring that level of reliability into better agreement with code targets.

6.4 SAP2000 FE Model Description

The model employed for reliability analysis was described in detail in Chapter 5, but a summary will be provided here, including specific modifications for full girder modelling. The concrete deck is represented by shell elements, the steel girder with beam elements, and the two are connected using linear link elements representing shear connectors. The model uses a “division” or discretization length, which must be a common denominator of each stud spacing, and the half the length of the bridge itself. The two-spacing plan shown in Figure 6-4 of 125 mm and 187.5 mm is ideal for model input because it results in a beam and shell element discretization length of 62.5 mm, and it allows for symmetrical geometry.

The stiffness of the link elements representing shear connectors is a key input to the model, because it determines how much force the studs will attract and affects the resulting composite interaction level. For this model, a commonly used equation developed by Ollgaard, Slutter, and Fisher (1971) was used to simulate stud stiffness, and it was confirmed through analysis that the studs remained in the linear range of load-slip behaviour (consistent with expectations for the fatigue/serviceability load level). The model contains simplifications, including linear elastic material behaviour for the steel and concrete, which allow it to solve quickly. As a result, validation of the model was necessary to ensure that results were not negatively impacted by these assumptions in a significant way (Sjaarda et al., 2018).

The FE model, depicted in Figure 6-5, was used in a series of analyses of increasing complexity, with results and verifications observed at each stage. The four analysis levels and a brief description of each are included in Table 6-3. Following this, the results of each analysis are presented and discussed.

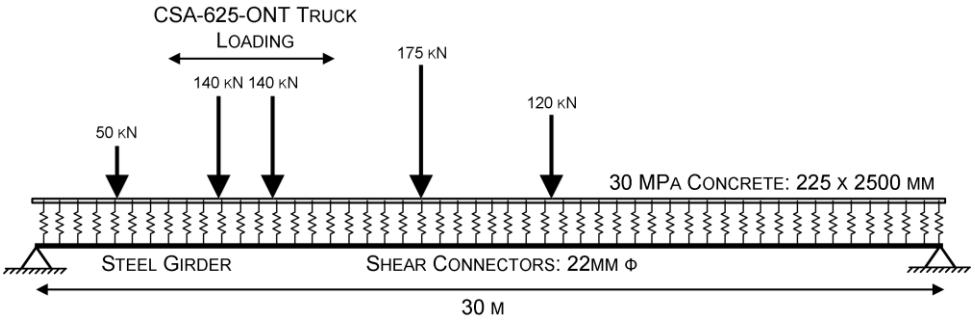

Figure 6-5: Depiction of code truck on SAP2000 model.

Table 6-3: SAP2000 Model analysis levels.

Analysis Level	*Description*	*Application*	*Runtime*
Static Analysis	A single static analysis is performed with the code truck placed at a position specified by the user. Shear connector loads and slips are reported, as well as strain profiles and deflections of the bridge along its length.	- Use strain profiles to compute degree of composite interaction - View slab separation	5 s
Moving Load Analysis (MLA)	A moving load analysis is performed using SAP2000's moving load function. Shear, moment, and connector force envelopes are reported.	- Find accurate stress ranges for shear connectors - Find maximum force effects (shear/moment)	30 s
Deterministic MLA Simulation	After a MLA is performed, the connector with the highest stress is reprogrammed to have a reduced stiffness, simulating a fatigue failure. The model is reanalyzed continuously. The location and stress of the failed connector and the overall deflection of the beam is reported for each analysis.	- Observe the progressive failure of a shear connection - Compare the fatigue life of the connection as a whole to the fatigue life of an individual connector	# stud failures * (30 s) = ~120 * 30 s = 1 h
Probabilistic MLA Simulation	The truck loading and the stud strengths are given probabilistic properties. Multiple full shear connection failures are performed in a Monte Carlo simulation to obtain the reliability of the shear connection as a whole.	- Find reliability of shear connections in bridges designed under current code rules - Recommend design rule changes to bring design into alignment with the code targeted level of reliability	# trials * (1 h) = 100 * 1 h = 4 d

6.4.1 Static Analysis Results

Select results from a single static analysis will be shown in this section, with the code truck placed in the approximate position for the maximum bending moment. This analysis is completed considering only the truck loading, and neglecting dead loads. The location of the 50 kN axle is 4,687.5 mm from the left support, resulting in a maximum moment of 1,332 kN·m underneath the 175 kN axle (located 16,125 mm from the left support). Figure 6-7 compares the stud connector stresses computed using elastic theory with the link stresses reported by the FE program. The discontinuities in the elastically calculated stress coincide with

the location of each of the five truck axles, and the two locations along the girder where the connector spacing changes.

An observation of special interest is that the actual link stresses reported by the FE model reflect the elastic predictions well in areas of constant shear or connector spacing but diverge at the points of discontinuity. As discussed previously, this is due to the mechanical nature of the connectors, requiring slip to transfer shear and resulting in partial composite interaction. This phenomenon was validated by the experimental beam test results, and a simple experiment of increasing the stiffness of each link in the FE model confirms that a rigid shear connection would not exhibit this behaviour.

It may seem that the difference between the elastically calculated stress, which is used as the design stress for studs, and the actual connector stress is trivial. However, the locations of divergence correspond with the critical locations for shear connector design; the maximum shear at a given location found from a moving load envelope of shears always corresponds to a truck position with an axle at this same location. As a result, the difference is important and results in the 15-30% lower FE stresses shown in Figure 6-6.

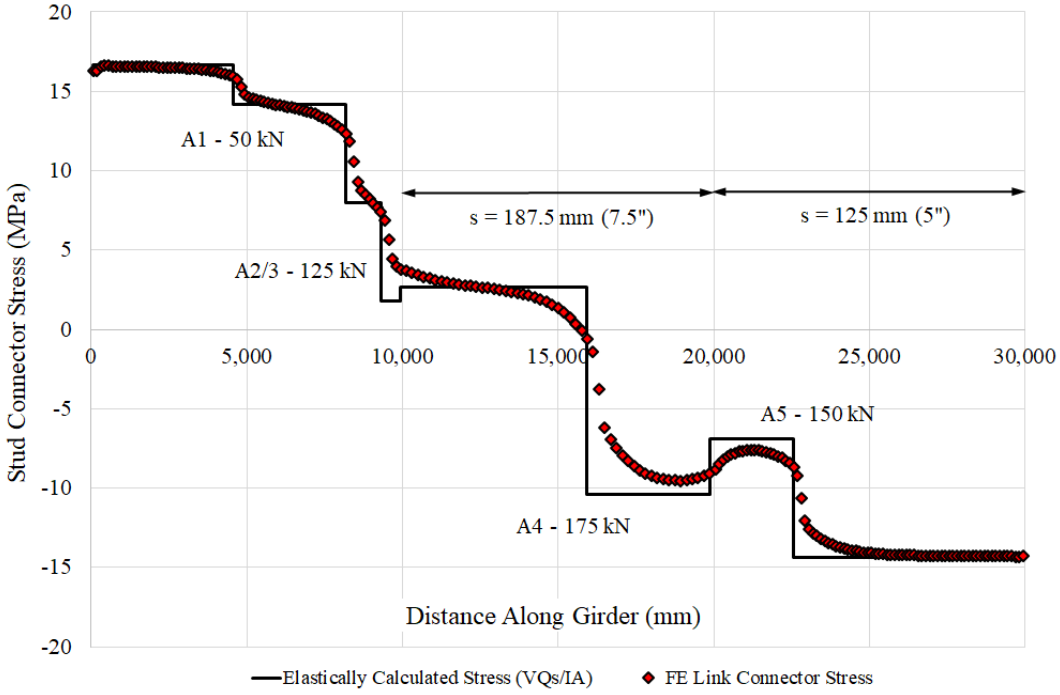

Figure 6-6: Stud connector stress comparison from fatigue code truck near midspan.

As noted in Table 6-3, a static analysis is also useful for viewing the degree of composite interaction along the girder length, as well as checking the slab separation. The former is shown in Figure 6-7, where concrete shell element stresses have been used to find the degree of composite interaction (the same procedure outlined in Chapter 5). This plot reveals an average degree of composite interaction of 85-90%.

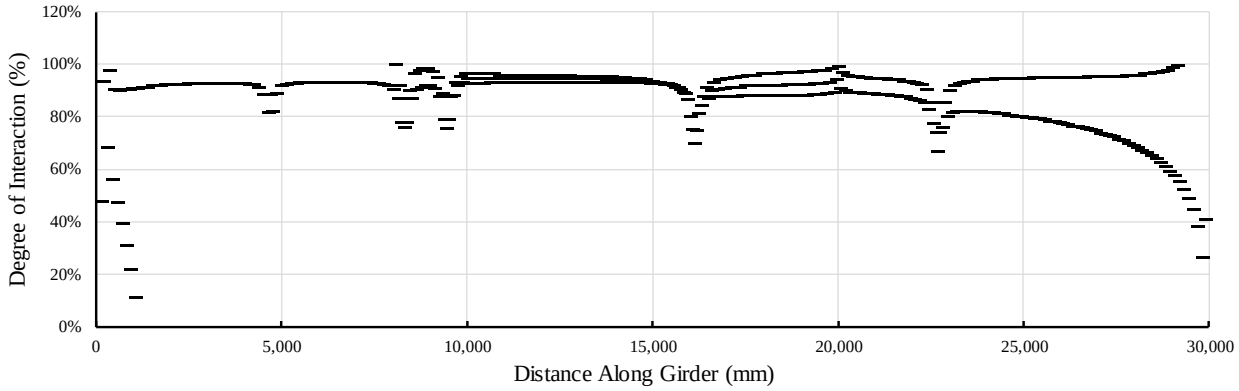

Figure 6-7: Degree of composite interaction along the girder length.

6.5 Moving Load Analysis Results

The second tier of analysis, moving load analysis (MLA), makes use of the SAP2000 moving load analysis function. This is necessary because the design of shear connectors depends not on the highest stress produced from the passage of the fatigue code truck, but on the stress range (the difference between the most positive load effect and the lowest or most negative). For this, an envelope of stress ranges must be produced from a moving load to find the maximum stress range at each location along the bridge girder. The connector stress data previously shown in Figure 6-4 was generated from the results of a single moving load analysis.

6.5.1 Deterministic MLA Simulation

To assess the reliability of the shear connection as a whole, and not just the reliability of a single connector, information about the progressive failure of studs must be obtained. Since the studs that undergo the highest stress range with the passage of a fatigue code truck are located at the ends of the girder, these studs can be expected to fail first. A prediction can even be made as to how many cycles it will take for this to happen, using fatigue results from beam tests completed and described in Chapters 3 and 4, or using the current design rules. However, it cannot be known what will happen after the first connector fails without the use of the FE program, informing how the shear stud forces will redistribute in the full girder and how long subsequent critical studs will remain intact before also experiencing fatigue failure.

The deterministic MLA simulation is a single simulation case where critical studs (those with the highest stress levels) fail after the expected number of cycles and are reprogrammed with a reduced stiffness. Two cases of reduced stiffness were considered: 50% reduction in stiffness, and 100% reduction in stiffness (complete failure of the studs). The latter was used for conservatism, assuming that fatigue failure completely disengaged a stud in transferring any longitudinal shear force. The 50% reduced stiffness case was meant to reflect the observations made during the beam testing at the University of Waterloo (UW), where studs were found to fail in a crack pattern that allowed them to transmit shear even after a large fatigue crack was present, or even propagated completely from one side of the stud to the other. Cracks

were found to move into the top flange of the steel section, resulting in a wedge capable of transmitting shear through mechanical bearing. On average, studs were found to lose only about 20% of their stiffness, long term, after a fatigue failure. A reduced stiffness value, termed the “post-failure stiffness” (PFS), of 50% was chosen as a conservative approximation (see Figure 6-8). In both cases, the conservative assumption is made that stiffness loss occurs immediately; in the tests, the studs were actually found to lose stiffness gradually as the fatigue cracks propagated. Results of this analysis will be shown for the 100% stud post-failure stiffness reduction assumption until near the end of this chapter, when the probabilistic simulation for code calibration is presented.

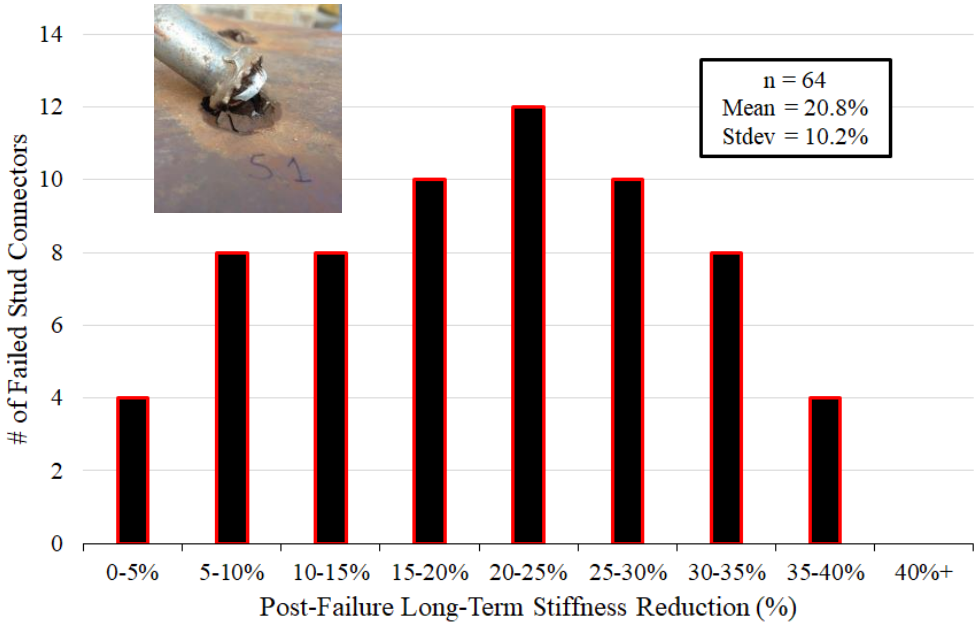

Figure 6-8: Post-failure long-term stiffness (PFS) reduction of CS and PS studs.

The fatigue endurance limit concept presents a challenge when conducting failure simulations. The current fatigue code provisions state that any shear stud experiencing a stress range of under 24 MPa with the passage of a fatigue code truck sustains no damage, and will not fail regardless of the number of loading cycles. As discussed previously, almost all highway bridges designed in Canada, including the bridge under discussion, are required to have studs designed at this endurance limit due to the high number of loading cycles expected. Furthermore, the design stress may be 24 MPa, but the actual maximum FE connector stress for this bridge is only 20 MPa, as shown in Figure 6-4. To avoid the complexities introduced by the endurance limit, the decision was made to conservatively ignore this limit, and assume the *S-N* curve to maintain a slope of m = 3 past the endurance limit. This is consistent with the assumption made in the probabilistic simulation, since statistically an endurance limit is arguably fictitious if the truck weight statistical distribution does not have a maximum value. The *S-N* curve used in the deterministic MLA simulation was the mean curve obtained from the UW beam test results shown in Figure 4-23.

Since the simulation is meant to capture the results of multiple stud fatigue failures, an overall failure definition for the girder shear connection was necessary. One obvious failure point is the violation of the ULS strength requirement; if the number of studs remaining on the girder was less than the number required to resist the factored moment on the girder, this simulation should certainly be terminated. For the example girder, this corresponds to a degree of shear connection of approximately 50%, or 78 studs. However, a more conservative approach was desired. Another approach could be to define failure when the bridge girder reaches a degree of shear connection of 100%, or 154 studs remaining. This would indicate that the margin between the studs required for strength and fatigue was depleted. This approach would be intuitive, but would still result in about 270 stud failures, or 64% of the studs initially installed on the bridge.

An investigation into the deflection of the example girder as studs failed progressively revealed that a sharp increase in deflection occurred after approximately 204 studs failed. This can be observed in Figure 6-9, where the deflection increase is plotted on the y-axis, and the number of studs failed (top), as well as the number of cycles (bottom) is shown on each x-axis. Points 1 through 4 shown in each plot correspond to points of interest during the progressive failure of the shear connection. Point 1 represents the undamaged girder, Point 2 represents the point of increase in deflection, Point 3 represents the point where a 100% degree shear connection remains, and Point 4 represents the point where only a 50% degree of shear connection remains (and M_r approximately equals M_f).

The definition of failure for the shear connection was conservatively chosen as Point 2, the start of the sharp increase in deflection when plotted with the number of cycles (N). A threshold of 15% deflection increase was chosen as the start of the sharper increase. For the example girder, this corresponds to a deflection increase from an initial 22.3 mm to approximately 25.6 mm, an increase of 3.3 mm. This is a conservative failure definition, and a convenient choice since the main output of the simulation, N, is not sensitive between Points 2 and 3 (and even Point 4 for the deterministic case, but this will not hold true probabilistically). The insensitivity to Points 2 through 4 is shown by the steep incline in the curve in Figure 6-11 (bottom).

With this failure definition, Figure 6-9 (bottom) reveals that the deterministic MLA simulation results in a fatigue life of approximately 350 million cycles for the girder, or 4 times the number of cycles expected. This is reassuring, but there can be no indication of the reliability of this system without considering the probabilistic nature of the input variables. In the following section the probabilistic parameters are discussed and a probabilistic MLA simulation is performed.

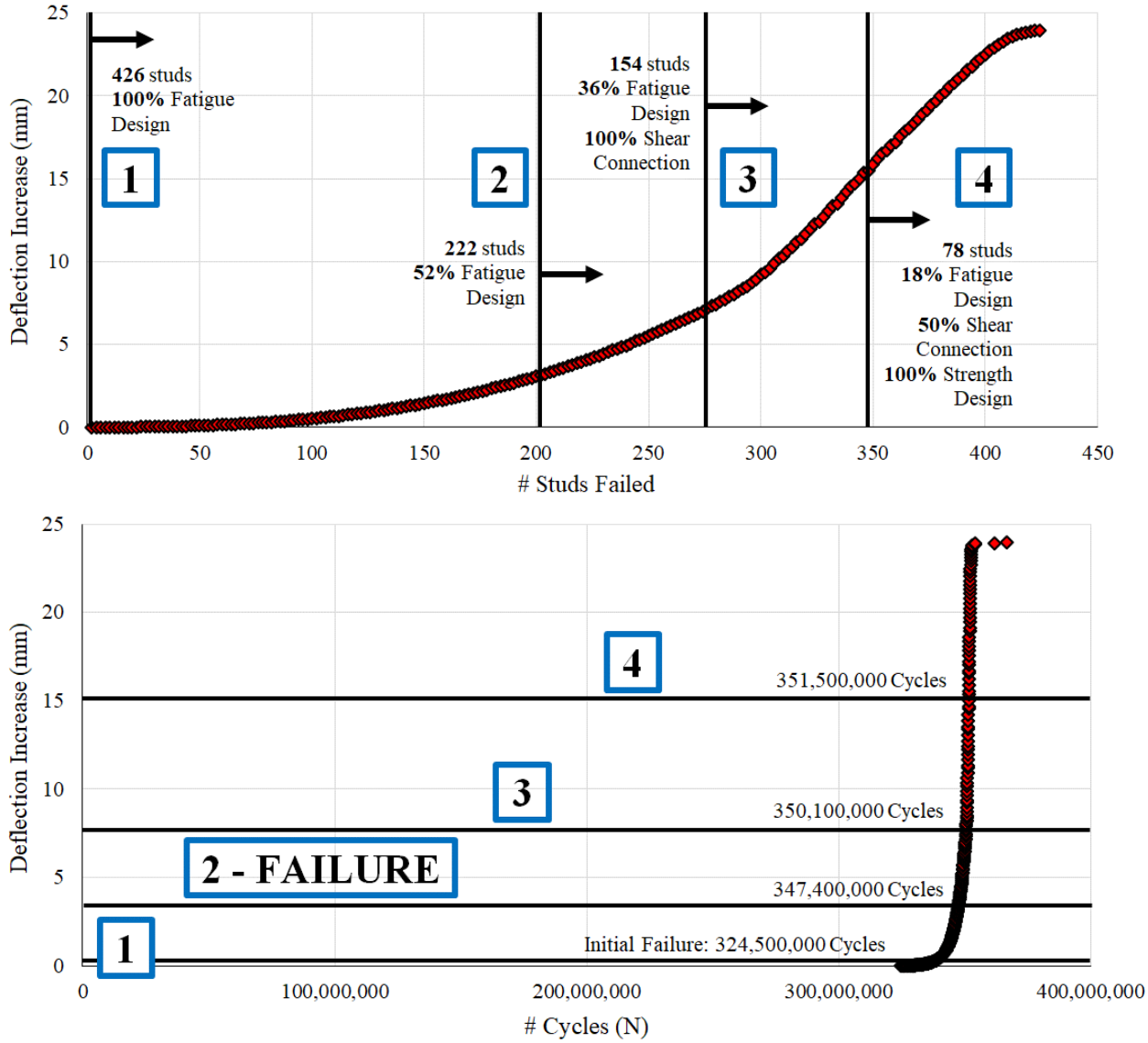

Figure 6-9: Deflection increase plotted with # studs failed (top) and # cycles (bottom).

6.5.2 Probabilistic MLA Simulation

To assess the reliability of the girder, statistical parameters were assigned to both the load (fatigue code truck weight) and resistance (stud connector strength). A procedure from the International Institute of Welding (Hobbacher, 2005) was used to assign a stud fatigue resistance curve to each connector in the model. These curves each have a slope of m = 3, and a vertical shift dictated by the failure distribution observed in n = 33 stud failures in the Waterloo beam testing program. The IIW procedure accounts for the uncertainty in estimating the mean and standard deviation of *log(C)* due to the small sample size, giving values associated with a two-sided confidence interval of p = 75% of each. In Equation 6-10, i represents the random variable corresponding to the logarithm of the y-intercept, C, for the *S-N* fatigue curve of a given stud. This is equal to the mean *log(C)* value of the sample data subtract the product of k and the standard deviation of *log(C)*. The factor k is given in Equation 6-11, and may be used to simplify the Equation 6-10

into Equation 6-12. Note that the inverse normal distribution function shown will give a random variate with a mean of zero and a standard deviation of one.

Equation 6-10 $$i = \bar{x} - k\left[s\right]$$

Equation 6-11 $$k = \frac{t_{(p,n-1)}}{\sqrt{n}} + \Phi^{-1}_{RAND(0,1)}\sqrt{\frac{n-1}{\chi^2_{\left(\frac{1+p}{2},n-1\right)}}}$$

Substituting p = 0.75 and n = 33 gives:

Equation 6-12 $$i = 12.33 - \Phi^{-1}_{RAND(0,1)}\left[0.500\right]$$

Equation 6-12 gives i, or $log(C)$, for a given stud by substituting the actual mean ($log(C)$ = 12.42) and standard deviation (0.424) of the sample data into Equation 6-10, along with k from Equation 6-11 for p = 0.75 and n = 33. The method in Equation 6-10 through Equation 6-12 contrasts with the simplified approach of ignoring the uncertainty in the estimation of the mean and variance, which is given in Equation 6-13 and Equation 6-14.

Equation 6-13 $$i = \bar{x} - \Phi^{-1}_{RAND(0,1)}\left[s\right]$$

Equation 6-14 $$i = 12.42 - \Phi^{-1}_{RAND(0,1)}\left[0.424\right]$$

By comparing Equation 6-12 and Equation 6-14 it can be noted that the effective mean is 0.7% lower, and the effective standard deviation is 18% higher with the more conservative IIW procedure. Figure 6-11 shows both the IIW curve and the simplified approach, plotted next to the test failures and the current CSA S6 design *SN* curve.

The probabilistic nature of the effective fatigue code truck weight was previously described in Section 6.1, and will not be further discussed. Details for the full MCS procedure may also be found there. The results of the analysis are now presented.

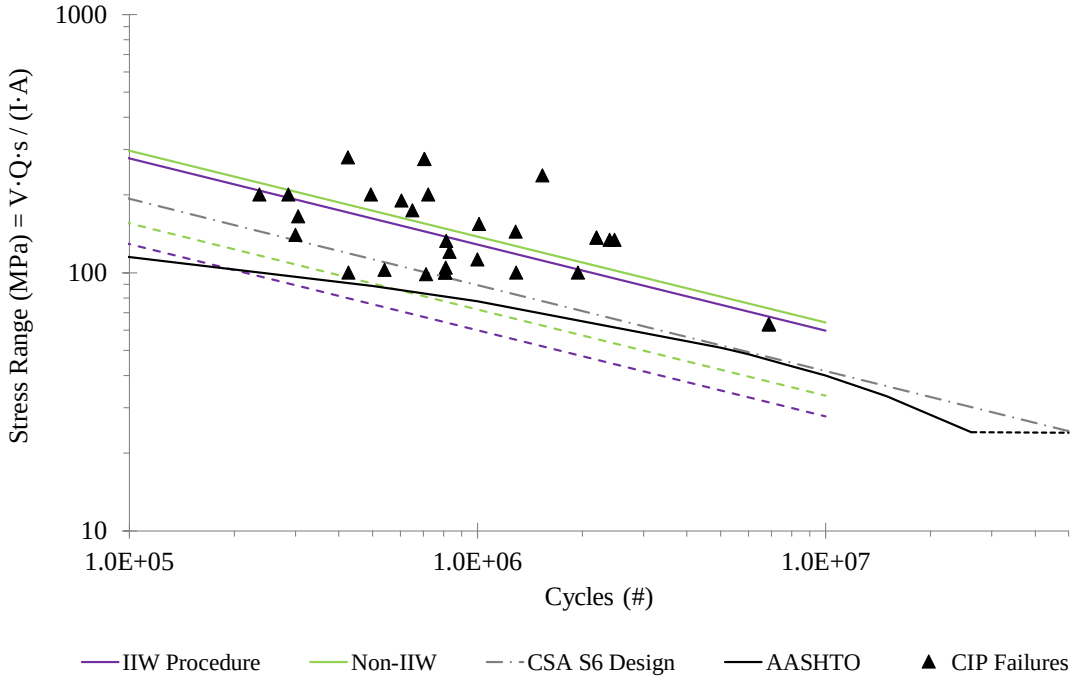

Figure 6-10: Mean *SN* (solid) and -2 standard deviation *SN* (dashed) used in analysis.

Results of three simulations (trials) of the probabilistic analysis are shown in Figure 6-11, two of which have been truncated based on the previously established failure definition. The deterministic simulation from Figure 6-9 is also shown for comparison purposes. Several observations can be made: the probabilistic results show a more gradual failure, with the initial stud failure happening earlier and with greater numbers of cycles between points of interest two, three, and four. In addition, the average number of cycles until failure in the probabilistic simulations is much lower on average than that of the deterministic simulation. No variability in stud strengths in the deterministic case represents the ideal situation for a long-lasting shear connection but does not provide the same length of warning time once the connection begins to fail. Evidently, the variability in stud strengths leads to early individual stud failures, which cause increased stress levels in the connection and shift the “unzipping” process to an earlier time frame.

In Figure 6-12, the failure patterns are shown for the same three simulations compared to the deterministic failure pattern. Studs remaining are shown on the y-axis, with stud locations on the x-axis; the graph should be read from top to bottom, as time passes, and studs fail. The deterministic pattern shows that after the stud with the highest stress fails, the closest neighbouring stud will fail next because it has taken over some shear from the adjacent, failed connector. The shear connection failure occurs from both outsides towards the centre of the bridge. However, in the probabilistic (stochastic) failure patterns it can be noted that initial and subsequent failures occur at random locations. Eventually an unzipping pattern similar to the deterministic pattern emerges, however, when a critical number of studs have failed in one area. All simulations shown in Figure 6-11 and Figure 6-12 were completed assuming no post-failure stiffness in the studs.

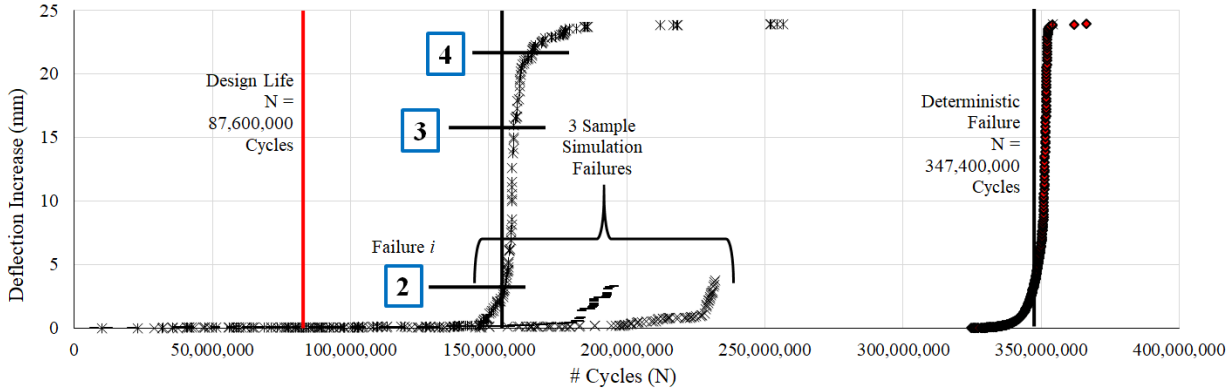

Figure 6-11: Deflection increase and # cycles, including sample simulation failures.

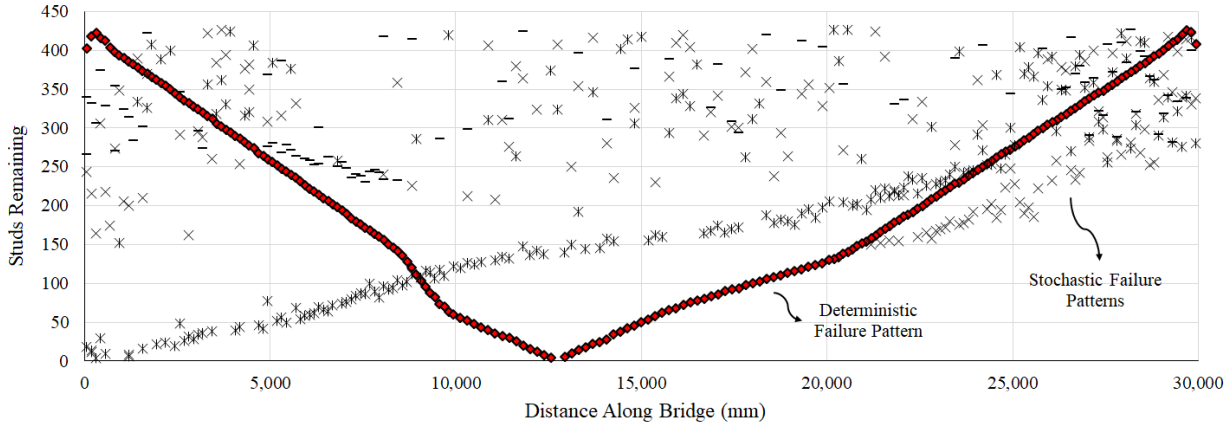

Figure 6-12: Comparison between deterministic and stochastic failure patterns.

To determine the reliability of the system, the probability distribution of the number of cycles until failure, *N*, must be estimated. A lognormal distribution was used to fit the data in a procedure that will now be demonstrated for 100 probabilistic simulations with studs having no post-failure stiffness. Three of the 100 simulations were already shown in Figure 6-11 and Figure 6-12. The factor of safety (*FS*) for each simulation is obtained by dividing *N* by the design life of 87.6 million cycles. The average *N* of all simulations was 199.8 million cycles (*FS* = 2.28) with a standard deviation of 37.1 million cycles (0.424·*FS*). On average, the first individual connector failure occurred after 23.2 million cycles.

Probability paper plots showing the goodness of fit for three distribution types are given in Figure 6-13. The upper left plot is for the normal distribution, and it shows a reasonable goodness of fit with a coefficient of determination (R^2) value of 95.5%. Equation 6-3 gives a β value of 2.99, or 3.02 when using the mean and standard deviation from the normal distribution probability paper plot. A normal distribution is generally not thought to fit fatigue data as well as a lognormal distribution, however, and will not be used further.

A lognormal distribution gives a better goodness of fit with R^2 = 98.7% (upper right plot in Figure 6-13). The lognormal parameters from Equation 6-4, λ and ζ, were calculated to be 0.808·ln(*FS*) and 0.180·ln(*FS*),

respectively, for the 100 simulations, which is close to the values estimated using the probability paper plot ($\lambda = 0.808 \cdot \ln(FS)$, $\zeta = 0.185 \cdot \ln(FS)$). Equation 6-4 yields a β value of 4.50, or 4.37 when using the mean and standard deviation from the probability paper plot.

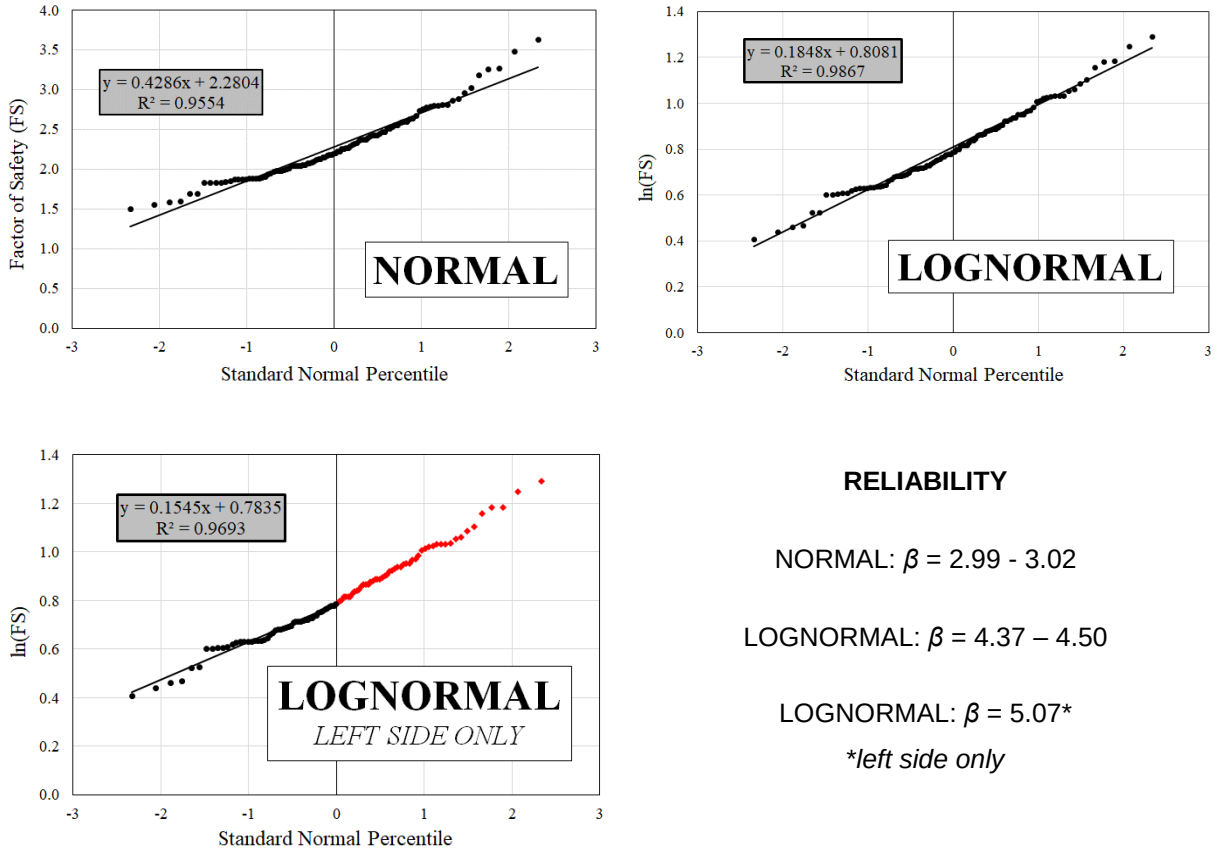

Figure 6-13: Probability paper plots for normal, lognormal, and modified lognormal distributions.

The lower left plot in Figure 6-13 shows a lognormal probability paper plot with only the left half of the data used to draw the line of best fit. This is done because the pattern of the failures falling below the mean is more important than those falling above the mean (a violation of the design fatigue life will always be from the weaker half of the failure data). It was thought that this method would be particularly useful when considering the helpful effects of the endurance limit; considering only the left half of the data ensures that simulation results from “runouts” (or very long-lasting simulation results) will not increase the level of scatter estimated by the probability paper plot. This avoids the problem of runouts causing an illogical downward shift of the design S-N curve (e.g. the 95% or 97.7% survival probability curve) because their negative effect on the scatter outweighs their positive effect on the mean. No endurance limit was used for the 100 probabilistic simulations being considered but the standard deviation estimated by the left side only probability paper plot was still lower at $0.154 \cdot \ln(FS)$. A reliability value of 5.07 resulted from the use of this method, and the probability plot goodness of fit fell in between the normal and lognormal values with R^2 = 96.7%.

The probability density function for the 100 simulations is shown in Figure 6-14, along with the lognormal distribution using the estimated population parameters. The results from the simulations presented so far indicate that current code practice for the design of shear studs is very conservative as it relates to the simple span geometry used in the analysis. Not only is the reliability of the system estimated at close to β = 4.5, but this analysis has assumed no consideration of the endurance limit, no post-failure stiffness of the studs, and neglects the redundancy effects of having multiple girders.

The level of reliability that should be present in the full shear connection could be a matter of debate but should probably be between β = 3 and 4 based on Figure 2-13 from the CSA S6 Commentary (2014). This considers the fact that degradation of the shear connection could result in the collapse of the girder if enough studs are cracked and a ULS event occurs. This depends on the post-failure stiffness assumed for each stud and the amount of over-design with respect to the critical moment; the bridge under consideration probably would not fail under ULS conditions even if all studs were assumed to have failed, yet maintained 50% of their initial stiffness as was present at minimum in the testing. However, not only could degradation result in collapse or catastrophic failure, but the connection is largely uninspectable. The only times that inspections can be made are if decks are being replaced, which may start to happen less as design lives for decks increase through the practice of waterproofing and the use of stainless-steel reinforcing. One aspect of the shear connection failure that would shift the target reliability index lower is the gradual nature of the failure and the accompanied increase in deflection, which may provide some warning.

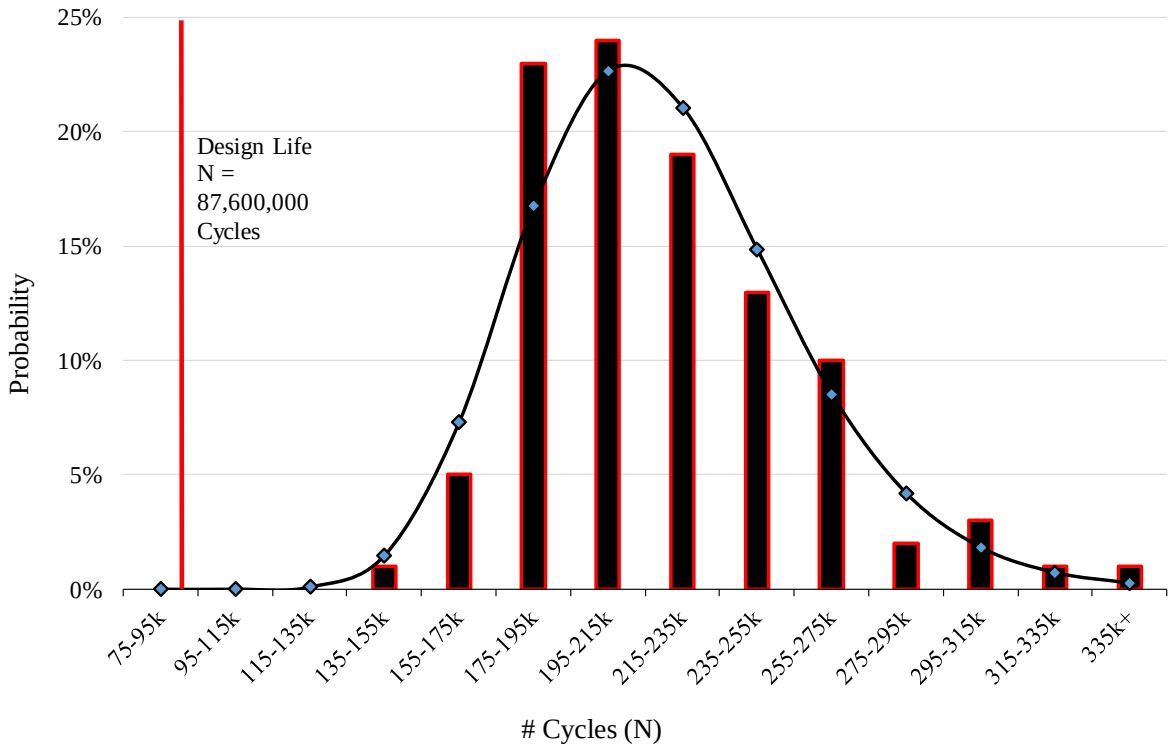

Figure 6-14: Probability density function of girder shear connection failures.

One hundred simulation was chosen as the number of trials necessary for this analysis based on Figure 6-15, where the reliability index is shown as the number of simulations is performed. There are diminishing returns for performing more than one hundred simulations.

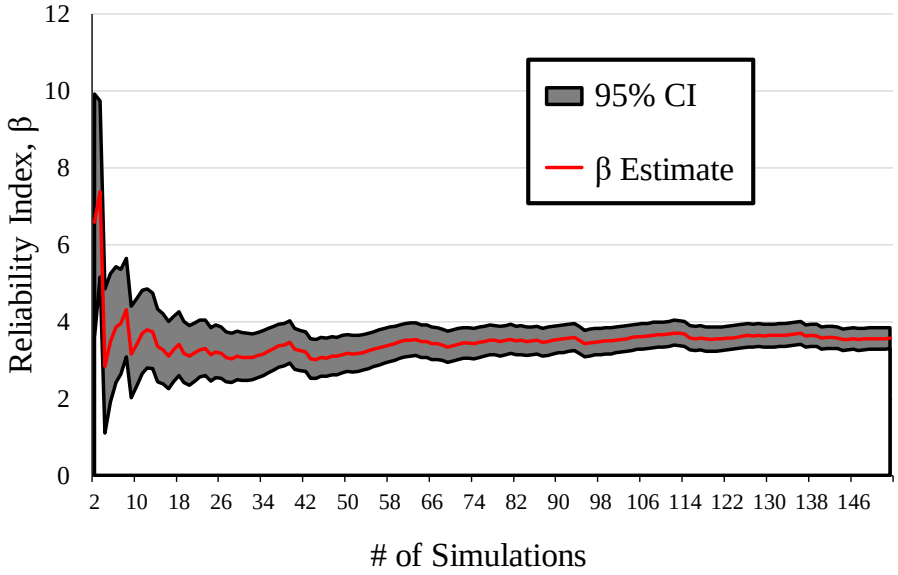

Figure 6-15: Reliability index with the number of Monte Carlo Simulations performed.

6.5.3 Probabilistic MLA Simulation for Code Calibration

A reliability level has been conservatively estimated for the shear connection system using the CSA S6 design geometry and loading. Since this level has been shown to be significantly above the code reliability target of β = 3.5 for ductile components (Hong, Goda, Lam, & Au, 2010), an analysis is now presented in which loading (and stud stress) is increased, until the reliability target is met. This analysis is easily possible using the same linear elastic model, by simply introducing a “load multiplier” to increase the truck loading (and proportionally increase stud stresses by the same multiplier).

In Figure 6-16 the results from this parametric analysis are shown for the 100% stud post-failure stiffness reduction assumption, with the data point at the x-axis (load multiplier) value of 1.00 corresponding to the results of the 100 simulations discussed in the previous subsection. Reliability index is on the y-axis, calculated with the lognormal distribution from Equation 6-4. It can be seen from the plot that an increase in loading of about 12% will result in a decrease in the reliability index from approximately 4.5 to 3.0, in an approximately linear manner. The target β value of 3.5 corresponds to a load multiplier of approximately 7.5%. This is not a large increase, because the analysis is based on a 100% stiffness reduction upon stud failure. As mention in Section 6.5.1 and shown in Figure 6-8, the long-term post-failure stiffness of each stud observed in testing was above 50%.

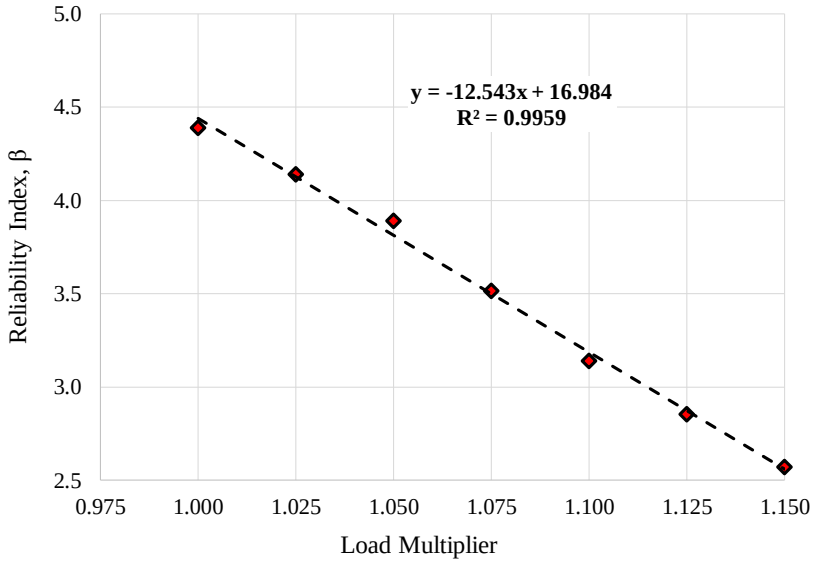

Figure 6-16: Reliability index as a function of load multiplier (100% stiffness reduction).

An analysis has also been performed considering a 50% post-failure stiffness reduction in the studs in accordance with the Chapter 4 test results. Figure 6-17 shows a widened x and y-axis and compares the results of simulations with varying load multipliers using both the 100% and 50% stud post-failure stud stiffness reduction assumptions. The post-failure stiffness affects the reliability of the connection in a significant way, shifting the linear relationship by more than 0.5 on the load-multiplier axis. The result is that a safe connection could be designed with a 50% loading increase or more over current design levels with the new post-failure stiffness assumption. However, the post-failure stud stiffness does not significantly affect the slope of the line of best fit, which maintains a value of approximately -12.6 in both cases.

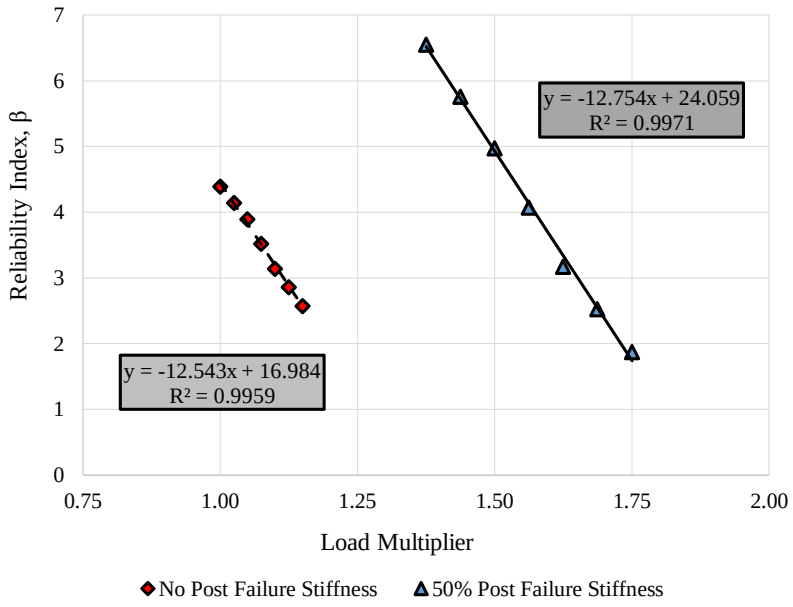

Figure 6-17: Reliability index as a function of load multiplier (50% and 100% stiffness reductions).

In NCHRP report number 299, Moses, Schilling, and Raju state that fatigue reliability is most sensitive to uncertainty in four factors including the lateral girder distribution ratio (also known as the amplification factor), the impact factor (also known as the DLA), the gross weight of the code truck, and lastly the fatigue curve (1987). In future work, it is recommended that sensitivity analysis be conducted for each of these four factors. The current model has demonstrated, using typical values for these parameters, that a relaxing of code provisions is warranted in order to meet a target β value of 3.5. However, the analysis is not comprehensive at this point. In the following sections, the effects of several other variables that were not considered in the analysis are discussed, including the number of traffic lanes, N_d, bridge class (i.e. design traffic volume), and *S-N* curve slopes.

6.6 System and Component Reliability

Now that a level of reliability has been estimated for the shear connection system as a whole, a comparison between it to the reliability of a single stud is of interest. Figure 6-18 compares the simulation results from the full system, assuming no PFS and 50% PFS, and the reliability of a stud designed according to the IIW design curve derived from the Waterloo tests (i.e., the curve used to define failure of individual studs in the full system analysis presented previously).

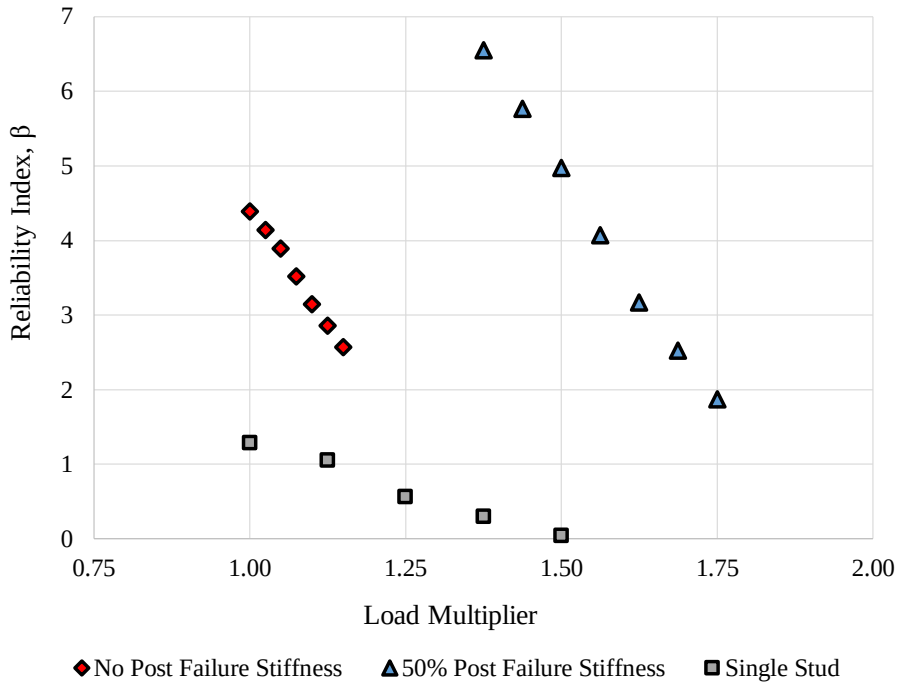

Figure 6-18: Comparison between system and component reliability.

The result is a very low level of reliability for the single stud in comparison to the full system. This level of reliability is not permissible for a component that is uninspectable and that could lead to a progressive failure, eventually resulting in collapse. Until now, the degree to which the underlying system was reliable

was not known. Figure 6-18 shows that system effects are not only beneficial, but necessary for the stud shear connection to be deemed reliable.

The consideration of individual studs is a necessary part of the design process, since complications associated with performing calculations on full shear connection systems are prohibitive. However, an acknowledgement should be in the design process that studs are not like other fatigue details. This analysis suggests that welded studs should be assigned a fatigue category applicable only to themselves, which takes system effects into account in the formulation of the category *S-N* curve and endurance limit. This is consistent with a change proposed for the 2019 CSA S6 code, currently on display for public consultation (CSA S6, 2018).

6.7 Discussion of Analysis Applicability

6.7.1 Consideration of Variable ADTT and N_d

To extend the applicability of the presented example bridge analysis to a more general highway bridge case, it is necessary to explore the effect of two more variables; the average daily truck traffic volume (ADTT), and the number of cycles caused by the passage of a truck over the bridge, N_d. These two variables determine the total cyclic demand on the bridge. Moses et al. observed that uncertainty in the traffic volume affects the bridge reliability to a lesser extent than other variables, because fatigue damage is linearly proportional to traffic volume, but is proportional to the cube of stress range due to the slope of the *S-N* curve (1987). However, the effects of ADTT and N_d on the analysis may still be significant, because the expected number of cycles (and the number of design cycles, as a result) can be quite different depending on the geometry of a bridge.

The example bridge presented has three lanes available to trucks, so a multiplier of $p = 0.80$ was applied to the ADTT to reflect the fact that not all traffic would be in the typical truck lane. Thus, the results of the analysis may apply to bridges with three or more design lanes available to trucks, but to extend the results to bridges with only one lane available to trucks, N_c should be altered from 87.6 million cycles to 109.5 million cycles ($p = 1$). When this is done for a simulation with a load multiplier of 1.5 and a 50% stud post-failure stiffness assumption, the reliability of the bridge decreases significantly from 4.97 to 3.30. The latter β value of 3.30 is below the target β value of 3.5 and near the low end of what may be considered acceptable (between 3 and 4, see Figure 2-13 and Hong, Goda, Lam, & Au, 2010). In Figure 6-19 (top) this shift in reliability index is shown graphically, and in Figure 6-19 (bottom), the shift in N_c (or the demand variable, Q) is shown superimposed on a sample PDF of girder shear connection failures.

It is apparent that a rise in expected traffic volume will have a significant and detrimental effect on the reliability of the system. This sensitivity is pronounced because the model ignores any increase in expected fatigue life of studs as the endurance limit is approached or exceeded, for conservatism (recall that a slope of $m = 3$ is maintained past the endurance limit). It is expected that better fatigue data at lower stresses

would allow the model to account for this increase in expected fatigue life, and the model would give higher levels of reliability when considering bridges with a single lane available to trucks, or when considering bridges with ADTT greater than 4,000 trucks per day.

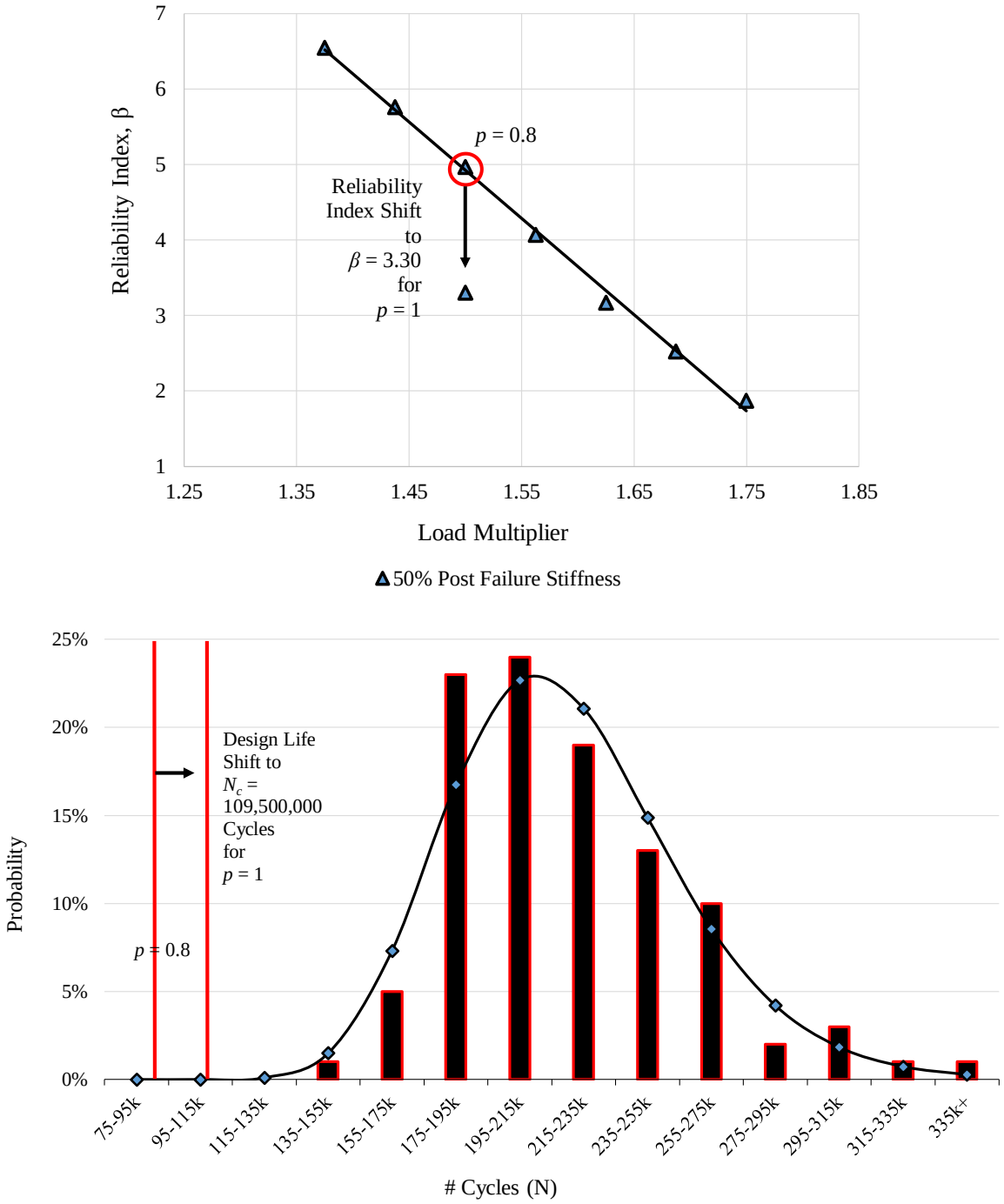

Figure 6-19: The effect of design lanes and resulting traffic multiplier (*p*) on reliability.

Not only will the number of truck lanes affect the design ADTT, but the bridge length and configuration type are also of interest. In some configurations, the passage of a truck over the bridge may induce more than

one load cycle. Figure 6-20 is taken from CSA S6, and shows values of N_d for several types of longitudinal members and spans. The example bridge girder is a 30 m long simple-span member, and therefore every truck passage converts to one cycle of loading for design purposes. However, shear connectors in bridges with spans less than 12 m will experience two cycles of loading per truck passage according to Figure 6-20, because individual axles provide these cycles independently. Short spans may also necessitate the use of a DLA greater than 1.25, since it is likely that less than three axles may be on the bridge at once. However, a composite bridge with a span less than 12 m is quite rare, since concrete girder bridges become more economical at short span lengths.

Similar to short spans, continuous and cantilevered members are also affected by multiple cycles per truck passage. However, this effect is confined to negative moment regions near interior supports or along cantilevers, where the design of shear connectors is entirely different. In these regions the connectors are not strictly necessary, and so the fatigue reliability analysis findings still apply. The end result of the effect of bridge length and configuration type on the conclusions made in this chapter is that these conclusions do not apply to rare composite bridges with spans shorter than 12 m, but they do apply for shear stud design in all other situations.

Longitudinal members	**Span length, *L*, ≥ 12 m**	**Span length, *L*, < 12 m**
Simple-span girders	1.0	2.0
Continuous girders		
Near interior support (within 0.1*L* on either side)	1.5	2.0
All other locations	1.0	2.0
Cantilever girders	5.0	5.0
Trusses	1.0	1.0
Transverse members	**Spacing ≥ 6 m**	**Spacing < 6 m**
All cases	1	2

Figure 6-20: Values of N_d depending on bridge configuration (see CSA S6 Cl. 10.17.2.3.1, 2014).

6.7.2 Consideration of Bridge Class

The example bridge presented is a Class A highway bridge with three lanes available to trucks, with a total number of 87.6 million design cycles. As discussed in the previous subsection, depending on the number of lanes available to trucks, this number could be increased to 109.5 million cycles (one truck lane), or 93.1 million cycles (two lanes available to trucks). Each of these volumes are above the number of cycles at which point the endurance limit governs (50.2 million cycles), signalling that every Class A bridge must be designed for this endurance limit.

During the shear connection fatigue design procedure in Section 6.2.2, the spacing and number of studs were determined from the 24 MPa endurance limit, but the subsequent probabilistic analysis ignored this

limit, assuming instead that the *S-N* fatigue curve continued past the limit with the slope of $m = 3$. This was done because the reliability of current designs was being evaluated, and the design procedure needed to be followed, complete with observance of the endurance limit. However, this inconsistency would not have occurred if the bridge was not a Class A bridge. For example, a Class B bridge design would have resulted in a stud design stress range of 36 MPa, on the finite life portion of the *S-N* curve, and a design fatigue life of 21.9 million cycles.

Under the probabilistic analysis assumption of ignoring the endurance limit, studs are designed to last for 50.2 million cycles (an allowable stress of 24 MPa), despite a fatigue demand of 87.6 million cycles. This difference is compensated for by multiple stud failures and the gradual "unzipping" of the shear connection. However, a Class B bridge design would have studs designed to last for 21.9 million cycles (an allowable stress of 36 MPa), which would be equal to the fatigue demand. The result of this is that non-Class A bridges would have higher levels of reliability if analysed using the same method. A thorough analysis of such bridges could demonstrate an allowable shift in the design *logC* value for the stud connector *S-N* curve (the finite life portion of the curve). However, since CSA S6 mandates that all new bridges be designed as Class A bridges except with permission otherwise, this result would not impact the economy of most bridges (CSA, 2014). Nevertheless, if resources permit, it is recommended that future analysis be conducted on non-Class A bridges.

6.7.3 Consideration of *S-N* Curve Slopes

At present the model used for analysis does not consider any change in slope of the *S-N* curve for low stress levels. However, this is not consistent with the current Canadian design code in effect, CSA S6 (2014), which assumes a horizontal line for stud stress ranges below 24 MPa. Additionally, the proposed design code under public review for publication in 2019, CSA S6 (2018), includes a line of slope $m = 5$ as a transition between the current $m = 3$ finite life region line and the horizontal line for the infinite life region (endurance limit). This new curve is proposed as "Category S" and has an endurance limit of 35 MPa. Both curves, present and proposed, are shown graphically in Figure 6-21.

As mentioned, a horizontal line signifying infinite life does not work in a statistical model. However, if $m = 5$ is being considered for the region closer to infinite life, where most cycles are known to take place in Class A bridges, then the present model should explore the effect of using a curve with $m = 5$. It is not necessary to take a piecewise curve with both $m = 3$ and 5, since the low cycle region of the curve will not have a large impact. Figure 6-22 shows the *S-N* curve current used in the model, and a curve proposed for future investigation with a slope of $m = 5$. It is interesting to note that the European code currently uses a slope of $m = 8$ (CEN, 2005); this adds further motivation to consider other *S-N* curve slopes in the reliability analysis.

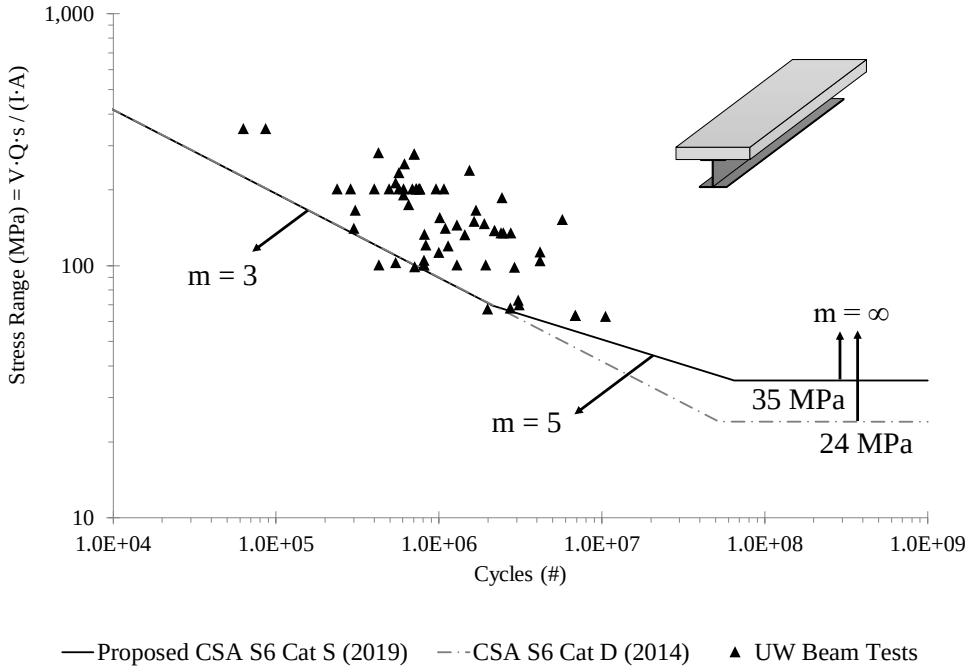

Figure 6-21: Current CSA *S-N* curve (Cat D) and proposed curve (Cat S).

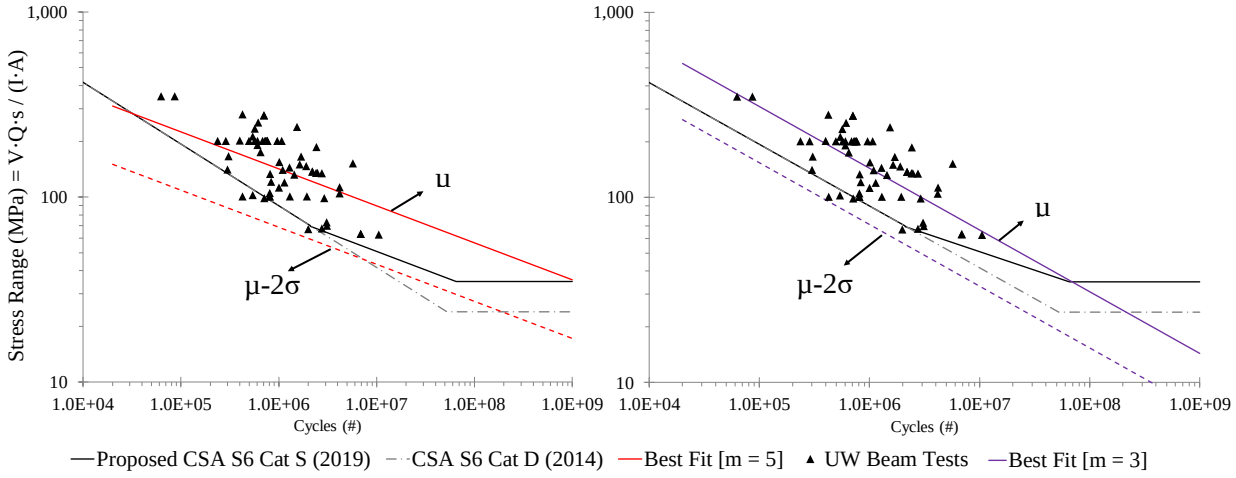

Figure 6-22: *S-N* curve in use in the model (*m* = 3) and proposed for investigation (*m* = 5).

6.7.4 Summary of Assumptions

An attempt was made to err on the side of conservative throughout the reliability analysis procedure. The following assumptions were made during the analysis, and are believed to be conservative, to varying degrees:

- Immediate loss of stud stiffness upon fatigue failure
- 100% and 50% stud post-failure long term stiffness reduction

- Single girder analysis (no consideration of redistribution to non-truck lane girders)
- No consideration of endurance limit

These sources of conservatism may explain the fact that no fatigue failures have ever been observed in the field, despite the SAP2000 model indicating an average initial stud failure after 15 million cycles. The following quote from Moses et al. (1987), puts uncertainty in the overall reliability analysis in perspective:

"One of the most important benefits of a reliability analysis is that it shows the interrelationship of the various conservative assumptions that are made at each step in a design procedure. Such an analysis helps to put into proper perspective the consequences of exceeding a conservative design value in a single step; usually this detrimental effect will be counteracted at some other step so that the overall safety parameter will not be violated. Many of the input variables may be uncertainly known, but the overall result can be known to a higher degree of certainty because of the combination."

The conclusion of this reliability analysis on welded stud shear connectors is that the current design procedure is very conservative, and out of step with the code reliability target for all bridge classes and configurations with the exception of Class A bridges with short spans (less than 12 m). An increase in the current endurance limit by a factor of 1.5 times is suggested, resulting in an increase from 24 MPa to 36 MPa. This value may be increased further in the future, should analysis methods or input data be of sufficient quality to narrow the list of conservative assumptions outlined above. This future analysis should include a consideration of statistical traffic volumes, various bridge classes, various bridge configurations, and different *S-N* curve slopes.

7 SYNTHESIS, CONCLUSIONS, AND RECOMMENDATIONS

In this chapter, a synthesis of the thesis work described in the preceding chapters is provided. The major conclusions are summarized, and areas of future work are recommended. The synthesis portion presented herein is organized by the preceding chapters, while the conclusions portion is organized by the thesis objectives laid out in Section 1.3.

7.1 Synthesis of Contributions

In Chapter 1, the case for an enhanced and updated understanding of the fatigue behaviour of welded shear studs in composite bridges is made. The current design rules for welded shear studs in the Canadian code for bridges, CSA S6 (2014), are created based on results from non-representative push tests, and lead to great numbers of studs in new designs. High strength bolt shear connectors are presented as potentially viable alternatives to studs, given their fatigue resistance and disassembly benefits. Table 1-1 lists the attributes of the ideal shear connection, and high strength through-bolts are noted for their grout-free requirements in precast applications, but durability, construction tolerances, and bottom access install are all issues of concern. High strength bolts embedded in grouted shear pockets do not have the same concerns, but they lack the important grout-free advantage needed to advance accelerated bridge construction.

In Chapter 2, a review of the literature on the state-of-the-art in shear connection research and shear connection design provisions is presented, along with a review of fundamentals of reliability analysis of components and systems subjected to repeated loading. It is established that the degree of composite interaction is the proper measure of composite performance, while the degree of shear connection only applies at the ultimate limit state (ULS), and only refers to one location along a composite beam. Although the calculation for the degree of composite interaction is not simple, it is made easier through the use of FE models, such as the one described subsequently in Chapter 5. The literature review found that welded shear studs are a unique fatigue-critical detail, in that they are uninspectable and highly redundant in the shear connection system, but they are treated the same as other details in current design processes. Questions regarding the applicability of push test results used to form current stud design criteria, the consequence of failure of a single stud compared to a system of redundant studs, and the implications of a shear connector that is not fatigue-critical are all unanswered in the literature at this time.

As a consequence of these research gaps and pertinent questions, the aims of this thesis are:

1. *to obtain S-N fatigue data for stud shear connectors in beams;*
2. *to investigate the fatigue behaviour of studs in precast slabs with grouted shear pockets;*
3. *to conduct fatigue tests on two high strength bolt connector types in beams;*
4. *to investigate bolted shear connector fatigue behaviour in beams and full bridges; and*
5. *to assess and calibrate the fatigue design of studs considering the risk of system failure.*

In Chapter 3, an experimental program is described, which is designed to address Objectives 1 through 3, and provide input data for an FE mechanistic model that will address Objectives 4 and 5. The fabrication and assembly of eighteen composite beams is discussed, including six beams shear connected with cast-in-place studs (CS), six with studs in grouted shear pockets (PS), three with high strength through-bolts (TB), and three with high strength bolts embedded in grouted shear pockets (EB). The simplest of the beams to construct were the CS specimens. The PS and EB specimens offered a comparable amount of effort to assemble; the EB beams required the added step of drilling holes in the top flange of each beam, but the precast slab grouting procedure was identical in both cases. The TB specimens were the most effort to build, given the added complexity of creating the formwork for the slabs, aligning holes in the slabs to holes in the beams for the through-bolts to pass through, and ensuring that the bolt pretension did not crack the slabs.

In Chapter 4 the fatigue testing results from these specimens is presented, including over 60 fatigue failures in the CS and PS specimens, and four in the EB specimens. Fatigue failures in welded shear studs were successfully detected through local distortion strain gauges, and a failure definition was validated by specimen autopsy observations. The failure definition corresponds to the onset of stiffness loss in stud connectors, as it was found that few connectors lost stiffness altogether, with most exhibiting a long-term stiffness reduction between 10 and 30%. The test results provide evidence of the effects of redundancy, seen in the long fatigue lives of the beams after the first stud failures, and the value of beam tests for allowing effects, such as those resulting from concrete shrinkage and load redistribution following stud failure, to be observed. It is shown that the use of pocketed shear studs in precast deck slabs leads to a different fatigue cracking behaviour in the shear studs and the flange base metal, and it is hypothesized that this trend can be explained by concrete shrinkage in the CIP slabs (Porter, 2016, develops this analytically). For the investigated loading, geometry, and sample size, the PS specimens exhibited slightly better fatigue performance than the CS specimens. This result would appear to support the notion that pocketed shear studs in precast deck slabs can be designed using the detail category for shear studs in CIP slabs. The mean *S-N* curves based on the test results obtained fell above the existing design curves, but the curves for mean minus two standard deviations were all on or slightly below the existing design curves (Figure 4-23).

The fatigue performance of high strength bolt specimens was substantially better compared to the stud specimens, even when cycled at multiple times the equivalent loading. The only bolts to fail were the critical bolts in the EB1 specimen, and this at an elastically estimated shear stress level of over 580 MPa (higher when considering the reduced bolt area due to threads). A statistical *S-N* analysis was not conducted on the bolt failures due to the small sample size. However, it is thought to be unlikely that fatigue considerations would govern the design of high strength bolt shear connectors given the test results.

With the use of profile strain gauges, slab forces were calculated for all specimen types. Partial composite interaction was confirmed to exist in the beams, lowering the stress of each connector type compared to elastically calculated stresses currently used in design. Initial static tests served to provide load-slip, or

"force-displacement" curves for each connector type. These curves are then used in Chapter 5 along with comparable curves from push tests as input properties for link elements representing shear connectors in an FE composite beam mechanistic model.

Chapter 5 describes this parametric FE model, built in SAP2000 and run with the aid of an API script. The model is verified with test data from slip gauges and profile strain gauges, as well as results from a composite beam model made with solid elements in Abaqus (Porter, 2016). The model shows that shear connector load-slip curves from beam tests are better indicators of beam behaviour than results from push tests. It is shown that bolt slip in through-bolt connectors significantly increases interfacial slip and decreases the degree of composite interaction in a beam. However, it influences maximum material stresses to a lesser degree because maximum stresses do not occur in beam regions of high shear and slip (Table 5-1). High strength bolts embedded in grouted shear pockets are more successful at inducing composite interaction than through-bolts, but neither form as stiff a connection as welded shear studs. As load levels increase, the gap between the performance of the three connector types increases, however, the fatigue-critical nature of studs does not allow for this high load level performance to be exploited.

In Chapter 6, the SAP2000 composite beam FE model is modified for the recursive analysis of a full bridge girder, with a shear connection designed with welded studs using current code rules. These rules result in 426 studs for the 30 m span, governed by FLS, while ULS design only requires 154 studs for a 100% shear connection (only half of which are required to ensure adequate strength). Static and moving load analyses are performed to investigate the consequence of failure of single studs in succession. One important ancillary analysis result shows that partial composite interaction effects translate to 15-30% lower connector stresses than currently assumed in design (Figure 6-3). A failure definition for the shear connection system is defined according to an observed sharp increase in deflection after approximately 25-50% of the studs are programmed to be failed. The assumption of deterministic stud strength in moving load analysis with multiple simulated stud connector failures is shown to be an ideal case in terms of fatigue life for the system, but the worst case in terms of failure warning. An attempt was made to err on the side of conservativism in the reliability analysis procedure when creating the probabilistic model. Conservative assumptions include no consideration of endurance limit or multiple girder redundancy, and the use of 100% and 50% post-failure stiffness (PFS) assumptions for the studs (while an average of 20% was observed during testing).

The conclusion of the reliability analysis considering system effects is that the current design procedure is very conservative for all bridge classes and configurations with the exception of Class A bridge spans less than 12 m in length. An increase in the current endurance limit is advised to 1.5 times the current limit, resulting in an increase from 24 MPa to 36 MPa. This increase is recommended based on results from the 50% PFS analysis assumption, and results in a reliability level of $\beta = 3.30$ for the highest ADTT expected when only one lane is available to trucks.

7.2 Summary of Conclusions and Recommendations

7.2.1 Conclusions and Recommendations Related to Objective #1

Based on the work conducted to address Objective #1 (obtaining S-N fatigue data for stud shear connectors in beams) the following conclusions and recommendations are made:

- Based on over 60 stud failures observe through the testing of 12 stud-connected composite beams, the mean *S-N* curves for studs was seen to fall above the existing design curves, but the resulting 97.7% survival probability curves fall below these design curves.
- Based on the lack of observed fatigue failures at high applied cyclic load levels, it is concluded that fatigue is unlikely to be a design concern for bolted shear connectors.
- The presented test results provide evidence of the effects of redundancy and the value of beam tests, rather than push tests, for assessing and designing shear connectors.

7.2.2 Conclusions and Recommendations Related to Objective #2

Based on the work conducted to address Objective #2 (investigating the fatigue behaviour of studs in precast slabs with grouted pockets) the following conclusions and recommendations are made:

- The difference in fatigue performance of shear studs in CIP vs. precast slabs with grouted shear pockets is small. In this investigation, specimens with precast slabs actually exhibited better fatigue performance.
- The use of pocketed, as opposed to CIP, shear studs in precast deck slabs can lead to different fatigue cracking patterns in the studs and the girder flange base metal. This may be explained by the concrete shrinkage in CIP slabs.

7.2.3 Conclusions and Recommendations Related to Objective #3

Based on the work conducted to address Objective #3 (conducting fatigue tests on two high strength bolt connector types in beams) the following conclusions and recommendations are made:

- No fatigue failures were observed in the through-bolt tests.
- Four embedded bolt failures occurred in a specimen where the cyclic stud forces were so high that they exceeded the design bearing strength of the concrete next to the bolts.
- Limited bolt slip was observed in both bolt-connected specimens.
- Force-deformation (load-slip) curves were generated from profile strain gauges for use in a composite beam FE model to further investigate composite performance. These curves are recommended for such use in lieu of load-slip curves from push tests because they lead to more accurate modelling.

7.2.4 Conclusions and Recommendations Related to Objective #4

Based on the work conducted to address Objective #4 (investigating bolted shear connector fatigue behaviour in beams and full bridges) the following conclusions and recommendations are made:

- Shear connector load-slip curves obtained from beam tests were shown to be better indicators of beam behaviour than similar results obtained from push tests.
- Slip in bolted connections may significantly increase interfacial slip and decrease the degree of composite interaction in a bridge, particularly in regions of high shear. The consequence of this slip increase on maximum material stresses is mitigated because maximum stresses occur in regions of low shear.
- High strength bolts embedded in grouted shear pockets are more successful at inducing composite interaction than through-bolts, but neither is as stiff as welded shear studs.

7.2.5 Conclusions and Recommendations Related to Objective #5

Based on the work conducted to address Objective #5 (assessing and calibrating the design provisions for studs considering the risk of system failure) the following conclusions and recommendations are made:

- When system effects are considered, the current design procedure for welded shear studs is found to be overly conservative. This finding is demonstrated for an example bridge. It is then shown to be generally applicable for all bridge classes and for configurations not including short spans less than 12 m long.
- It is recommended that welded studs be assigned their own fatigue category, in recognition of their uniqueness in redundancy and the fact that they are uninspectable. This notion was first suggested by the relevant committee for the 2019 CSA S6 update (CSA, 2018).
- The effective endurance limit is suggested to be set at 36 MPa for the new fatigue category, an increase of 50% over the current limit of 24 MPa. Further reliability analysis and laboratory testing should be conducted to confirm this result. In particular, consideration should be given to statistical traffic volumes, various bridge classes and bridge configurations, and different *S-N* curve slopes. High cycle fatigue data near the proposed endurance limit region is also recommended.
- The finite-life region of the *S-N* curve may be shifted upwards in light of the findings of this thesis, but this is unlikely to affect many designs since all Class A bridges are governed by the fatigue endurance limit at this time, and all new highway bridges are required to be designed as Class A unless permission is obtained otherwise.

7.3 Recommendations for Future Work

7.3.1 Welded Stud Shear Connectors

Although the beam tests conducted as part of this research program represent a significant improvement on the prior use of push tests to establish the design *S-N* curve in the finite-life region, the final endurance limit recommendation was based on a simple reliability analysis ignoring infinite life considerations. It is recommended that longer life fatigue testing be conducted with varying stud diameters and flange thicknesses to further improve our understanding of stud fatigue behaviour in this domain. The results from such tests will not only serve to confirm and further supplement the *S-N* fatigue results presented in this work, but will also confirm the fatigue crack patterns assumed to exist in establishing the connection post-failure stiffness. These recommended tests could be completed on small-scale specimens, provided that beam test boundary conditions are simulated.

Additional sensitivity analysis should be carried out on the reliability analyses presented in Chapter 6. This

7.3.2 Shear Connectors in Grouted Shear Pockets

Welded stud shear connectors are shown to perform as well in grouted shear pockets as in conventional CIP applications through this work. However, as higher ratios of precast deck surface to grouted surface areas are desired in precast bridges, and as progress is made in limiting the amount of grout necessary for panel-to-panel connections in the future, fatigue resistant high strength bolt connections may become a more economical alternative. With this in mind, it is recommended that a cost-analysis be completed comparing welded studs to embedded high strength bolt shear connectors, in both CIP and precast applications. This comparison must estimate the installation and material costs per connector type and weigh the increased cost per bolted connector with the drastic (estimated 4-6 times) decrease in the number of connectors required. Consideration of deconstruction costs may also be beneficial.

7.3.3 High Strength Bolt Shear Connectors

It is recommended that further testing on bolted connections be conducted, both on the embedded bolt detail and the through-bolt detail. Tests including cyclic load reversals are necessary to ensure that the integrity of each connection remains intact, and further ultimate limit state tests are also recommended to verify that the full capacity of a composite cross-section can be developed using fewer high strength bolt shear connectors compared to welded studs. The through-bolt connection concept would also require the investigation of steps for preventing installation cracks in the deck and loss of bolt prestressing due to creep and shrinkage effects, prior to widespread implementation in practice.

REFERENCES

2017 Infrastructure Report Card. (2017). American Society of Civil Engineers. Federal Highway Administration.

A Toolkit for Accelerated Bridge Construction. (2013). Transportation Research Board Strategic Highway Research Program, Washington, DC, USA.

AASHTO (American Association of State Highway and Transportation Officials). (2014). AASHTO LRFD bridge design specifications, 4th Ed., Washington, D.C., USA.

Au, A., Lam, C., & Tharmabala, B. (2010). Development of bolted deck slab system to expedite bridge construction. *International Conference on Short and Medium Span Bridges,* Niagara Falls, ON, CAN.

Badie, S. S. & Tadros, M. K. (2008). *National Cooperative Highway Research Program – Full-Depth Precast Concrete Bridge Deck Panel Systems.* (No. 584). Transportation Research Board, Washington, D.C., USA.

Badie, S. S., Morgan Girgis, A. F., Tadros, M. K., & Nguyen, N. T. (2010). Relaxing the stud spacing limit for full-depth precast concrete deck panels supported on steel girders (phase I). *Journal of Bridge Engineering, 15*(5), 482-492.

Balkos, K. D. (2018). *The Static and Fatigue Behaviour of Through-Bolt Shear Connectors in Steel-Precast Composite Bridge Girders.* (Unpublished Master of Applied Science in Civil Engineering). University of Waterloo.

Balkos, K.D., Sjaarda, M., West, J. S., & Walbridge, S. (2018). Static and fatigue tests of steel-precast composite beam specimens with through-bolt shear connectors. *Journal of Bridge Engineering (Submitted)*.

Baptista, C., Antonio, R., & Nussbaumer, A. (2017). Probabilistic S-N curves for constant and variable amplitude. *International Journal of Fatigue, 101*, 312-317.

Bowser, M., Walbridge, S., & West, J. (2012). Discrete shear connection for a portable composite bridge. *Transportation Research Record,* Washington, DC, USA.

Burak, R., & Seraderian, R. (2010). *Accelerated Bridge Construction - On the Fast Track to Success.* Transportation Association of Canada, Halifax, NS, CAN.

Canadian Infrastructure Report Card. (2016). The Federation of Canadian Municipalities.

Chen, Y. (2013). *Innovative Shear Connections for the Accelerated Construction of Composite Bridges.* (Unpublished Master of Applied Science in Civil Engineering). University of Waterloo.

CISC (Canadian Institute of Steel Construction) (2014). CISC Commentary on CSA S16-09. Mississauga, ON, CAN.

CSA (Canadian Standards Association) (2013). CAN/CSA-W59-13, Welded Steel Construction (Metal Arc Welding). Mississauga, ON, CAN.

CSA (Canadian Standards Association) (2014). CAN/CSA-S16-14, Design of Steel Structures. Mississauga, ON, CAN.

CSA (Canadian Standards Association) (2014). CAN/CSA-S6-14, Canadian Highway Bridge Design Code. Mississauga, ON, CAN.

CSA (Canadian Standards Association) (2010). S6.1S1-10 Commentary on CAN/CSA-S6-06. Mississauga, ON, CAN.

CSA (Canadian Standards Association) (2018). CAN/CSA-S6-19, Canadian Highway Bridge Design Code (Public Review Period Prior to Publication). Mississauga, ON, CAN.

CEN. (2005). Eurocode 4, ENV 1994: Design of composite steel and concrete structures. European Committee for Standardisation (CEN). Brussels, Belgium, EU.

Dedic, D. J., & Klaiber, W. F. (1984). *High-Strength Bolts as Shear Connectors in Rehabilitation Work.* Concrete International, ACI, Farmington Hills, MI. USA.

Dorton, R. A., Holowka, M., & King, J. P. C. (1977). Conestogo river bridge - design and testing. *Canadian Journal of Civil Engineering, 4*(1), 18-39.

Eryilmaz, Serkan. (2019). (k1, k2, …, km)-out-of-n system and its reliability. *Journal of Computational and Applied Mathematics*, 346, 591-598.

Gattesco, N., & Giuriani, E. (1996). Experimental Study on Stud Shear Connectors Subjected to Cyclic Loading. *Journal of Constructional Steel Research, 38*(1), 1-21.

Hobbacher, A. (2005) *Recommendations for fatigue design of welded joints and components*. International Institute of Welding. Wilhelmshaven, Germany, EU.

Hong, H. P., Goda, K., Lam, C., & Au, A., (2010). Assessment of fatigue reliability of steel girder bridges. *International Conference on Short and Medium Span Bridges,* Niagara Falls, ON, CAN.

Huh, B., Lam, C., & Tharmabala, B. (2010). Effect of shear stud clusters in composite girder design. *International Conference on Short and Medium Span Bridges,* Niagara Falls, ON, CAN.

Issa, M. A., Patton, T. A., Abdalla, H. A., & Yousif, A. A. (2003). Composite behavior of shear connections in full-depth precast concrete bridge deck panels on steel stringers. *PCI Journal, 48*(5), 76-89.

Issa, M. A., Idriss, A., Kaspar, I. I., & Khayyat, S. Y. (1995). Full depth precast and precast, prestressed concrete bridge deck panels. *PCI Journal, 40*(1), 59-80.

Johnson, R. P. (2000). Resistance of stud shear connectors to fatigue. *Journal of Constructional Steel Research, 56*(2), 101-116.

King, D. C., Slutter, R. G., & Driscoll, G. C. (1965). *Fatigue Strength of ½ Inch Diameter Stud Shear Connectors.* (No. 285.6A). Lehigh University Institute of Research. Bethlehem, PA, USA.

Kwon, G., Engelhardt, M. D., & Klingner, R. E. (2009). Strengthening bridges by developing composite action in existing non-composite bridge girders. *Structural Engineering International: Journal of the International Association for Bridge and Structural Engineering (IABSE), 19*(4), 432-437.

Kwon, G., Engelhardt, M. D., & Klingner, R. E. (2010). Behavior of post-installed shear connectors under static and fatigue loading. *Journal of Constructional Steel Research, 66*(4), 532-541.

LaRose, K. E. (2006). *Performance of Shear Stud Clusters for Precast Concrete Bridge Deck Panels.* (Unpublished Master of Applied Science). University of British Columbia. Vancouver, BC, CAN.

Meeting the Customers' Needs for Safer, Smoother Roads. (1999). *FOCUS Accelerating Infrastructure Innovations,* (April/May 1999). Retrieved from http://www.fhwa.dot.gov/publications/focus/99apr/needs.cfm

Mirza, S. (2007). *Danger Ahead: The Coming Collapse of Canada's Municipal Infrastructure.* The Federation of Canadian Municipalities. Ottawa, ON, CAN.

Moses, F., Schilling, C. G., & Raju, K. S. (1987). *NCHRP Report 299: Fatigue evaluation procedures for steel bridges.* Transportation Research Board, Washington, D.C., USA.

MTO Carling Avenue Eastbound Bridge Rapid Replacement Project. (2013). Retrieved November/11, 2013, from http://www.mto.gov.on.ca/english/bridges/carling-avenue.shtml

MTO. (2013). Rapid Bridge Replacement Keeps Commuters Moving. Retrieved November/11, 2013, from http://www.newswire.ca/en/story/269433/rapid-bridge-replacement-keeps-commuters-moving#

MTO Quality and Standards Division. (1991). Ontario Highway Bridge Design Code. Downsview, ON, CAN.

Newmark, N. M., Siess, C. P., and Viest, I. M. 1951. Tests and analysis of composite beams with incomplete interaction. *Proceedings of the Society for Experimental Stress Analysis, 9*(1): 75-92.

Nyman, W. E., & Moses, F. (1985). Calibration of bridge fatigue design model. *Journal of Structural Engineering, 11(6)*, 1251-1266.

Nowak, A. S., & Collins, K. R. (2012) *Reliability of structures*, 2nd Edition. Boca Raton, FL, USA. CRC Press.

Oehlers, D. J., & Foley, L. (1985). Fatigue strength of stud shear connections in composite beams. *Proceedings of the Institution of Civil Engineers (London), 79* (pt 2), 349-364.

Oehlers, D. J., Nguyen, N. T., Ahmed, M., & Bradford, M. A. (1997). Partial interaction in composite steel and concrete beams with full shear connection. *Journal of Constructional Steel Research, 41*(2/3): 235-248.

Oehlers, D. J., & Seracino, R. (2002). A tiered approach to the fatigue assessment of composite steel and concrete bridge beams. *Proceedings of the Institution of Civil Engineers – Structures & Buildings, 152*(3): 249-257.

Ollgaard, J. G., Slutter, R. G., & Fisher, J. W. (1971). Shear strength of stud connectors in lightweight and normal weight concrete. *AISC Engineering Journal*, 71-10.

Ovuoba, B., & Prinz, G. S. (2015). *On the Fatigue Capacity of Headed Shear Studs in Composite Bridge Girders*. University of Arkansas. Fayetteville, AR, USA.

Porter, T. K. (2016). *The Fatigue Resistance of Headed Shear Stud Connectors in Steel-Precast Composite Girders.* (Unpublished Master of Applied Science in Civil Engineering). University of Waterloo.

SAP 2000 Version 17. (2014). Computers and Structures, Inc. Berkeley, California USA.

Slutter, R. G., & Fisher, J. W. (1966). *Fatigue Strength of Shear Connectors.* (No. 316.2). Lehigh University Institute of Research. Bethlehem, PA, USA.

Sjaarda, M., Porter, T., West, J. S., & Walbridge, S. (2016). Fatigue of Stud Shear Connectors in Steel-Precast Composite Bridges. *CSCE Conference Proceedings.* London, ON, CAN.

Sjaarda, M., Porter, T., West, J. S., & Walbridge, S. (2017). Fatigue Behavior of Welded Shear Studs in Precast Composite Beams. *Journal of Bridge Engineering, 22(11)*, 04017089.

Sjaarda, M., West, J. S., & Walbridge, S. (2014). Shear connectors for steel-precast composite bridges. *American Institute for Steel Construction NASCC Publications*. Toronto, ON, CAN.

Sjaarda, M., West, J. S., & Walbridge, S. (2018). Assessment of shear connections through composite beam modelling. *Transportation Research Record*, Washington, D.C, USA.

Tadros, M. K., & Baishya, M. C. (1998). *National Cooperative Highway Research Program - Rapid Replacement of Bridge Decks.* (No. 407). Transportation Research Board. Washington, D.C., USA.

Thomann, M., & Lebet, J. (2008). A mechanical model for connections by adherence for steel-concrete composite beams. *Engineering Structures, 30*(1), 163-173.

Yura, J. A., Methvin, E. R., & Engelhardt, M. D. (2008). *Design of Composite Steel Beams for Bridges.* Center for Transportation Research, The University of Texas at Austin, Report No. FHWA/TX-08/0-4811-1.

Zhang, Q. (2007). *Fatigue Resistance of Shear Stud Connectors.* (Unpublished Master of Engineering in Structural Engineering). University of Alberta. Calgary, AB, CAN.